



National Library
of Canada

Canadian Theses Service

Ottawa, Canada
K1A 0N4

Bibliothèque nationale
du Canada

Services des thèses canadiennes

CANADIAN THESES

THÈSES CANADIENNES

NOTICE

The quality of this microfiche is heavily dependent upon the quality of the original thesis submitted for microfilming. Every effort has been made to ensure the highest quality of reproduction possible.

If pages are missing, contact the university which granted the degree.

Some pages may have indistinct print especially if the original pages were typed with a poor typewriter ribbon or if the university sent us an inferior photocopy.

Previously copyrighted materials (journal articles, published tests, etc.) are not filmed.

Reproduction in full or in part of this film is governed by the Canadian Copyright Act, R.S.C. 1970, c. C-30. Please read the authorization forms which accompany this thesis.

AVIS

La qualité de cette microfiche dépend grandement de la qualité de la thèse soumise au microfilmage. Nous avons tout fait pour assurer une qualité supérieure de reproduction.

S'il manque des pages, veuillez communiquer avec l'université qui a conféré le grade.

La qualité d'impression de certaines pages peut laisser à désirer, surtout si les pages originales ont été dactylographiées à l'aide d'un ruban usé ou si l'université nous a fait parvenir une photocopie de qualité inférieure.

Les documents qui font déjà l'objet d'un droit d'auteur (articles de revue, examens publiés, etc.) ne sont pas microfilmés.

La reproduction, même partielle, de ce microfilm est soumise à la Loi canadienne sur le droit d'auteur, SRC 1970, c. C-30. Veuillez prendre connaissance des formules d'autorisation qui accompagnent cette thèse.

THIS DISSERTATION
HAS BEEN MICROFILMED
EXACTLY AS RECEIVED

LA THÈSE A ÉTÉ
MICROFILMÉE TELLE QUE
NOUS L'AVONS REÇUE

Tests and Strength Evaluation of Asbestos-Cement
Housing Structure

Antonio Perinayegon

A Thesis
in
The Department
of
Civil Engineering

Presented in Partial Fulfilment of the Requirements
for the degree of Master of Engineering at,
Concordia University
Montréal, Québec, Canada

March 1984

© Antonio Perinayegon, 1984

ABSTRACT

Tests and Strength Evaluation of Asbestos-Cement Housing Structure

Antonio Perinayegon

Full scale tests were performed on new asbestos-cement building system (ACEX System) utilizing panels in form of 's' and 'v' elements. The main purpose of those tests was to study the overall behaviour as well as the capacities of panels working as walls, roof and floors leading to a definition of safe loading limits and practical design criteria.

A new method of designing asbestos-cement in flexure has been presented and the application of the empirical ACI formula for concrete walls has been verified.

ACKNOWLEDGEMENTS

ACKNOWLEDGEMENTS

The research was carried out based on a contract agreement with Mr. Guy Blain, Architect and special thanks go to him for the preparation of the test panels. The asbestos-cement used in this project was produced by Atlas Turner Inc.

The author wishes to express his gratitude to Dr. Z.A. Zielinski, Project Director, for his guidance, cooperation and encouragement throughout all stages of this research program and the preparation of this thesis.

A special acknowledgement is extended to my colleague Mr. Rohadi Mas Alimin for his participation and help during the experimental program.

The author is also indebted to Concordia University for the use of the structural laboratory facilities and to technicians D. Roy, A. Osadca and L. Stankevicius for their assistance.

Miss Ida Eva Zielinska helped during the various stages of the experimental program and the preparation of the research notebook.

Thanks are also due to Mrs. Ilana Crawford for typing the thesis.

Finally, my studies could not have been done without the infinite patience and understanding of my wife Norah.

TABLE OF CONTENTS

TABLE OF CONTENTS

	<u>Page</u>
ABSTRACT	i
ACKNOWLEDGEMENTS	ii
LIST OF TABLES	v
LIST OF FIGURES	vi
NOMENCLATURE	x
CHAPTER 1	
INTRODUCTION	1
CHAPTER 2	
DESCRIPTION OF SYSTEM	2
2.1 Description of System (based on design information)	2
2.2 's' Component	7
2.3 'v' Component	7
2.4 Material	10
2.5 Testing Arrangement	11
2.6 Testing Procedure	11
2.7 Loading Measurements	12
CHAPTER 3	
TESTING PROGRAM, OBSERVATIONS AND RESULTS	15
3.1 First Stage-Roof Panels Made of 's' Element	15
3.2 Second Stage-Wall Panels Made of 's' Element	29
3.3 Third Stage-Beams Made of Single 'v' Elements and Double 'v' Elements	39
3.4 Fourth Stage-Single 'v' Beam and Double 'v' Beam Assemblies with Attached Top Plates	57
3.5 Fifth Stage-Beams Made of Single 'v' Elements and Double 'v' Elements Loaded in Floor Plane	74

	<u>Page</u>
3.6 Sixth Stage-Columns Made of 'v' Elements	91
3.7 Supplemental Tests - Properties of Asbestos-Cement	93
CHAPTER 4	
CONCLUSIONS	100
4.1 Safe Loading Definition	100
4.2 Proposed Design Procedure	100
4.2.1 Flexural Members	100
4.2.2 Compression Members	101
CHAPTER 5	
PROPOSED DESIGN PROCEDURE FOR ASBESTOS-CEMENT STRUCTURES	103
5.1 Flexural Strength	103
5.2 Compression Strength	109
5.3 Determination of Safe Service Load	110
REFERENCES	112
APPENDIX A: Design Calculations	113

LIST OF TABLES

LIST OF TABLES

<u>Table</u>	<u>Title</u>	<u>Page</u>
3.1.1	Comparative results and equivalent uniform distributed loads (1st stage)	20
3.2.1	Comparison of tested and calculated results	33
3.3.1	Comparative results and equivalent uniform distributed loads (3rd stage)	46
3.3.2	Comparative results and equivalent uniform distributed loads (3rd stage)	47
3.4.1	Comparative results and equivalent uniform distributed loads (4th stage)	64
3.5.1	Comparative results and equivalent uniform distributed loads (5th stage)	80
3.5.2	Comparative results and equivalent uniform distributed loads (5th stage)	81
3.6.1	Comparison of tested and calculated results	92
3.7.1	Rupture strength evaluation	96
3.7.2.a	Compressive strength evaluation	97
3.7.2.b	Compressive strength evaluation	98
3.7.3	Strength of angle connector	99
4.1	Comparison of tested and calculated results and allowable loads	102
4.2	Comparison of tested and calculated results and allowable loads	102
5.1	Coefficients A and B	108

LIST OF FIGURES

LIST OF FIGURES

<u>Figure</u>	<u>Description</u>	<u>Page</u>
2.1.1	Plan of a single-family house	4
2.1.2	View of single-family houses	5
2.1.3	View of individual cottage	6
2.2.1	"S" elements, wall & roof assemblies	8
2.3.1	Types of "V" elements	9
2.3.2	Types of beams	9
2.5.1	Arrangement of floor & beam panels tests	13
2.5.2	Arrangement of wall panel & column tests	14
3.1.1	Dimensions of roof assemblies	19
3.1.2	Stress distribution - roof panel 1-SR6	21
3.1.3	Time-deflection curve (creep test panel 2-SR6)	22
3.1.4	Load-deflection curve	23
3.1.5	Load-deflection curve	23
3.1.6	View of testing set-up of roof panel 2-SR6	24
3.1.7	View of Testing set-up of roof panel 1-SR5	25
3.1.8	View of roof panel 1-SR5 (at failure)	26
3.1.9	Top view of testing set-up of roof panel 2-SR5	27
3.1.10	View of roof panel 2-SR5 (at failure)	28
3.2.1	Dimensions of wall assemblies	32
3.2.2	Dimensions of short wall assemblies	33
3.2.3	Overall views of wall panels	35
3.2.4	Overall view of wall panel 7SW5	36
3.2.5	Overall view of wall panel 7SW5 (at failure)	36

<u>Figure</u>	<u>Description</u>	<u>Page</u>
3.2.6	Side view of wall panel 8SW5 (at failure)	37
3.2.7	Front view of wall panel 8SW5 (at failure)	37
3.2.8	Back view of wall panel 8SW5 (at failure)	38
3.3.1	Dimensions of single "v" beams	43
3.3.2	Dimensions of single "v" beam with steel reinforcement (2 bars of 3/8" dia. and area of 0.22 in ²)	44
3.3.3	Dimensions of double "v" beams	45
3.3.4	Load-deflection curve	48
3.3.5	Load-deflection curve	48
3.3.6	Load-deflection curve	49
3.3.7	Load-deflection curve	49
3.3.8	Load-deflection curve	50
3.3.9	View of beam 2FV4b (at failure)	51
3.3.10	View of testing set-up of beam 3FV3a	52
3.3.11	View of beam 3FV3a (at failure)	52
3.3.12	View of testing set-up of beam 10FV3a	53
3.3.13	View of beam 10FV3a (at failure of left V-section)	54
3.3.14	View of beam 10FV3a (after complete failure)	54
3.3.15	View of testing set-up of beam 10FV3b	55
3.3.16	View of beam 10FV3b (at failure of left v-section)	55
3.3.17	View of testing set-up of beam 11FV4b	56
3.3.18	View of beam 11FV4b (at failure of left v-section)	56

<u>Figure</u>	<u>Description</u>	<u>Page</u>
3.4.1	Dimensions of single "v" beams with top plates	61
3.4.2	Dimensions of single "v" beams with top plates and steel reinforcement (2 bars of 3/8" dia. and area of 0.22 in ²)	62
3.4.3	Dimensions of double "v" beams with top plates	63
3.4.4	Load-deflection curve	65
3.4.5	Load-deflection curve	65
3.4.6	Load-deflection curve	66
3.4.7	Load-deflection curve	67
3.4.8	Load-deflection curve	67
3.4.9	View of testing set-up of beam 5FV3	68
3.4.10	View of beam 5FV3 (at failure)	68
3.4.11	View of testing set-up of beam 5aFV3	69
3.4.12	View of beam 5aFV3 (at failure)	69
3.4.13	View of testing set-up of beam 6FV4	70
3.4.14	View of beam 6FV4 (at failure)	70
3.4.15	View of testing set-up of beam 7FV4	71
3.4.16	View of beam 7FV4 (at failure)	71
3.4.17	View of testing set-up of beam 12aFV3	72
3.4.18	View of beam 12aFV3 (at failure)	72
3.4.19	View of testing set-up of beam 13aFV4	73
3.4.20	View of beam 13aFV4 (at failure)	73
3.5.1	Dimensions of single "v" beams	77
3.5.2	Dimensions of double "v" beams	78
3.5.3	Horizontal loading arrangement for single "v" element	79

<u>Figure</u>	<u>Description</u>	<u>Page</u>
3.5.4	Horizontal loading arrangement for double "v" element	79
3.5.5	Load-deflection curve	82
3.5.6	Load-deflection curve	82
3.5.7	Load-deflection curve	83
3.5.8	Load-deflection curve	83
3.5.9	View of testing set-up of beam 8FV3a	84
3.5.10	View of beam 8FV3a (at failure)	84
3.5.11	View of beam 9FV4a (twisting under load)	85
3.5.12	View of beam 9FV4a (at failure)	85
3.5.13	View of testing set-up of beam 9FV4b	86
3.5.14	View of beam 9FV4b (at failure)	86
3.5.15	View of testing set-up of beam 14FV3	87
3.5.16	View of beam 14FV3 (at failure)	87
3.5.17	Views of testing set-up of beam 15FV4a	88
3.5.18	Views of beam 15FV4a (at failure)	89
3.5.19	View of testing set-up of beam 15FV4b	90
3.5.20	View of beam 15FV4b (at failure)	90
3.6.1	Dimensions of columns	92
3.7.1	Stress-strain curve for asbestos-cement in tension along the fibers	95
5.1	Stresses at failure	103
5.2	Strains and stresses at failure	104
5.3	Equivalent section	107

NOMENCLATURE

NOMENCLATURE

A_g	cross-sectional area
A'_s	area of steel in compression zone
A_s	area of steel in tension zone
b	width of section
E_{cc}	modulus of elasticity of asbestos-cement in compression
E_{ct}	modulus of elasticity of asbestos-cement in tension
f'_c	specified compressive strength of asbestos- cement
f_{cc}	compressive stress of top fibers
f_r	approximate rupture strength
f'_s	strength in steel in the compression zone
f_s	4350 psi, assuming that strain in tension is 0.00015
f_{to}	ultimate tensile strength of asbestos-cement
h	total height of section
l_c	vertical distance between supports
M_{cr}	flexural cracking moment
n	modular ratio (E_s/E_c)
P_u	failure load of test panels
x	height of compression zone
$\Delta A'_c$	area of concrete in compression in excess of basic rectangular bh
ΔA_c	area of concrete in tension in excess of basic rectangular bh
ϕ	capacity reduction factor

ψ_c coefficient of strengthening of section in compression in excess of basic rectangular bh.

ψ_t coefficient of strengthening of section in tension in excess of basic rectangular bh.

CHAPTER 1
INTRODUCTION

CHAPTER 1

INTRODUCTION

The ACEX System has been developed by Guy Blain, architect in collaboration with Atlas Turner Inc., IRDA (Institut de Recherche et de Developpement sur l'Amiante), and Z.A. Zielinski (in the final stage) for low cost housing. The system introduces new asbestos-cement elements, whose forms resemble the 's' and 'v' shape.

The subject of this report concerns the strength of the two elements and the evaluation of their behaviour when used as walls, roofs and beams.

In order to ascertain the validity of elaborate theories, tests were carried out at the Concordia University structures laboratory during the period of December 1983 to March 1984. The performance of these tests was in accordance with contractual agreements between the University and Mr. Guy Blain, as part of a project sponsored by IRDA.

CHAPTER 2

DESCRIPTION OF SYSTEM

CHAPTER 2

DESCRIPTION OF SYSTEM

2.1 Description of System (based on design information)

The development of this building system was undertaken based on the conviction that asbestos-cement components could form the basis of new ways of building single family low cost houses on a massive scale.

The objective was to come up with a solution suitable for housing needs encountered in the developing world and utilizing 100% of asbestos-cement as structural materials. Even though this building system can be adopted for multi-storey (midrise) building construction, commercialization is directed towards one and two storey houses as shown in Figures 2.1.1, 2.1.2 and 2.1.3. The main feature of the building system is its low cost, which is achieved by producing profiled asbestos-cement sheets at the factory and assembled on site without the use of structural frame, wood or metal studs.

The load bearing walls and partitions utilize the cavity principle, where natural ventilation, insulation or other local filler materials can be used to provide heat and sound insulation where required. The same basic asbestos-cement element (with a cavity) is used for the construction of walls and roofs. Connections and assembly are simple and can be done by non-professionals. Buildings constructed of

asbestos-cement components are rigid and able to withstand abnormal loads, such as earthquake, hurricanes and floods.

Door frames, window frames, base boards and connection angles made of asbestos-cement are easily pieced and assembled by one or two men. The exterior skin of the roof and wall panels which is waterproof due to a special configuration at the joint, do not need the use of any batten or coverstrip, and at the same time the assembly provides a flat face on both sides.

Mechanical and electrical services are easily installed in the cavity of interior partitions and exterior walls. Electrical outlets, switches, junction boxes also fit in the cavity. Electrical wires and pipes are run inside the walls.

A building constructed of asbestos-cement requires only concrete footing and since the components are light in weight, no crane or other mechanical handling equipment is required. The components may be stored and transported in stacks, thus reducing transportation costs. Its flexibility to satisfy various designs for housing projects makes this building system superior to other prefabricated and pre-assembled housing systems.

The building system introduces two new asbestos-cement elements. They are the 's' elements and the 'v' elements. The roof and wall panels are made of 's' elements whereas floor panels are made partly or wholly of 'v' elements.

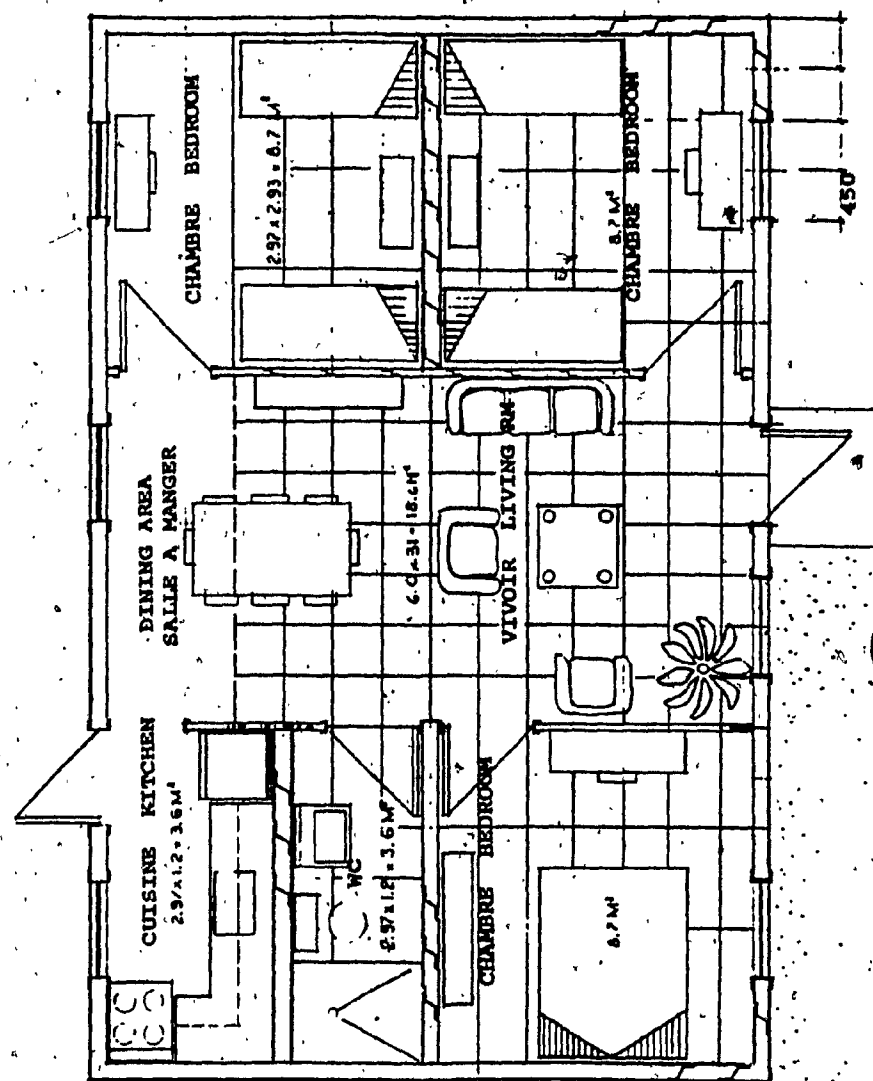


Figure 2.I. Plan view of a single-
Family House

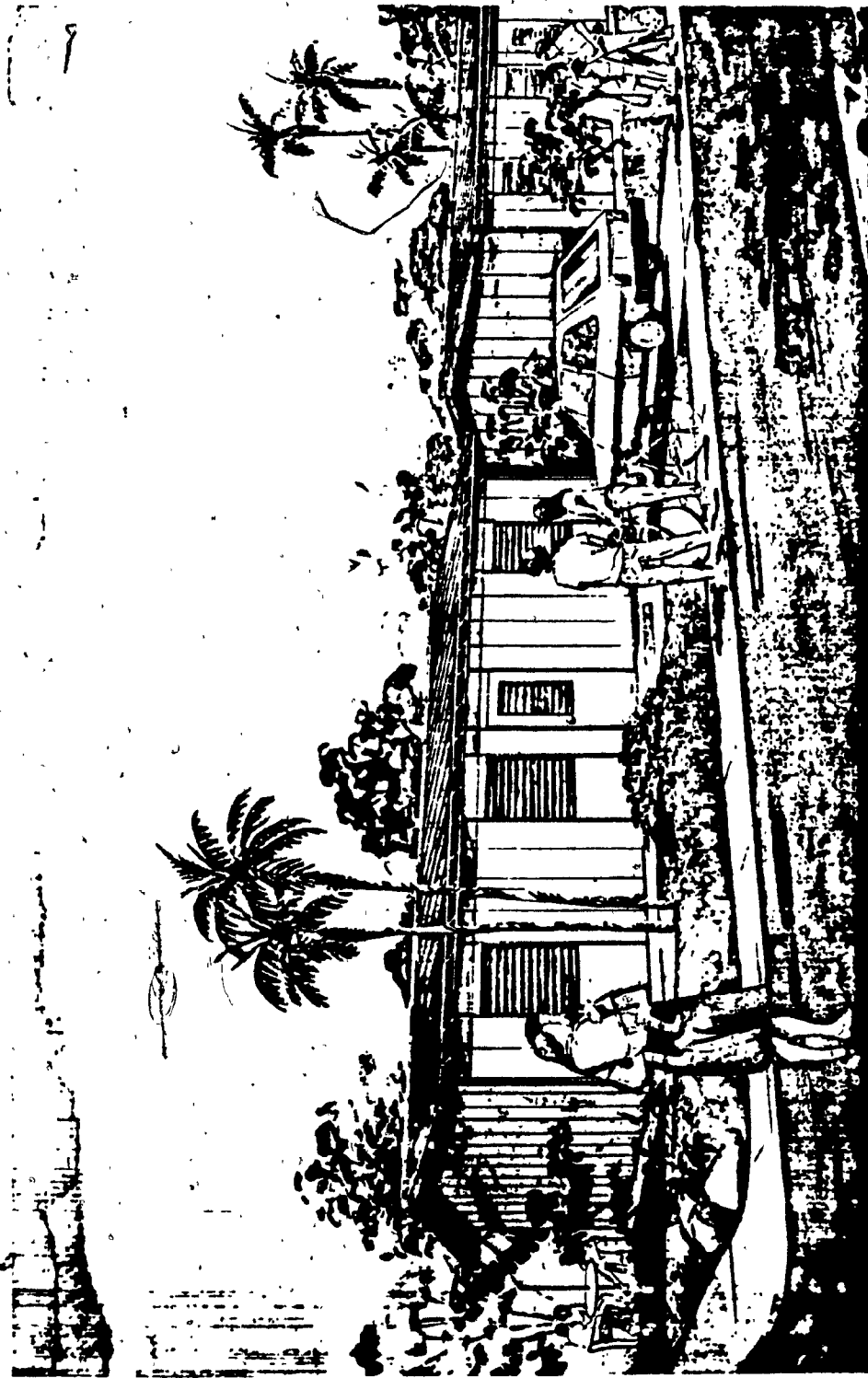


Figure 2.1.2 View of Single-Family Houses.

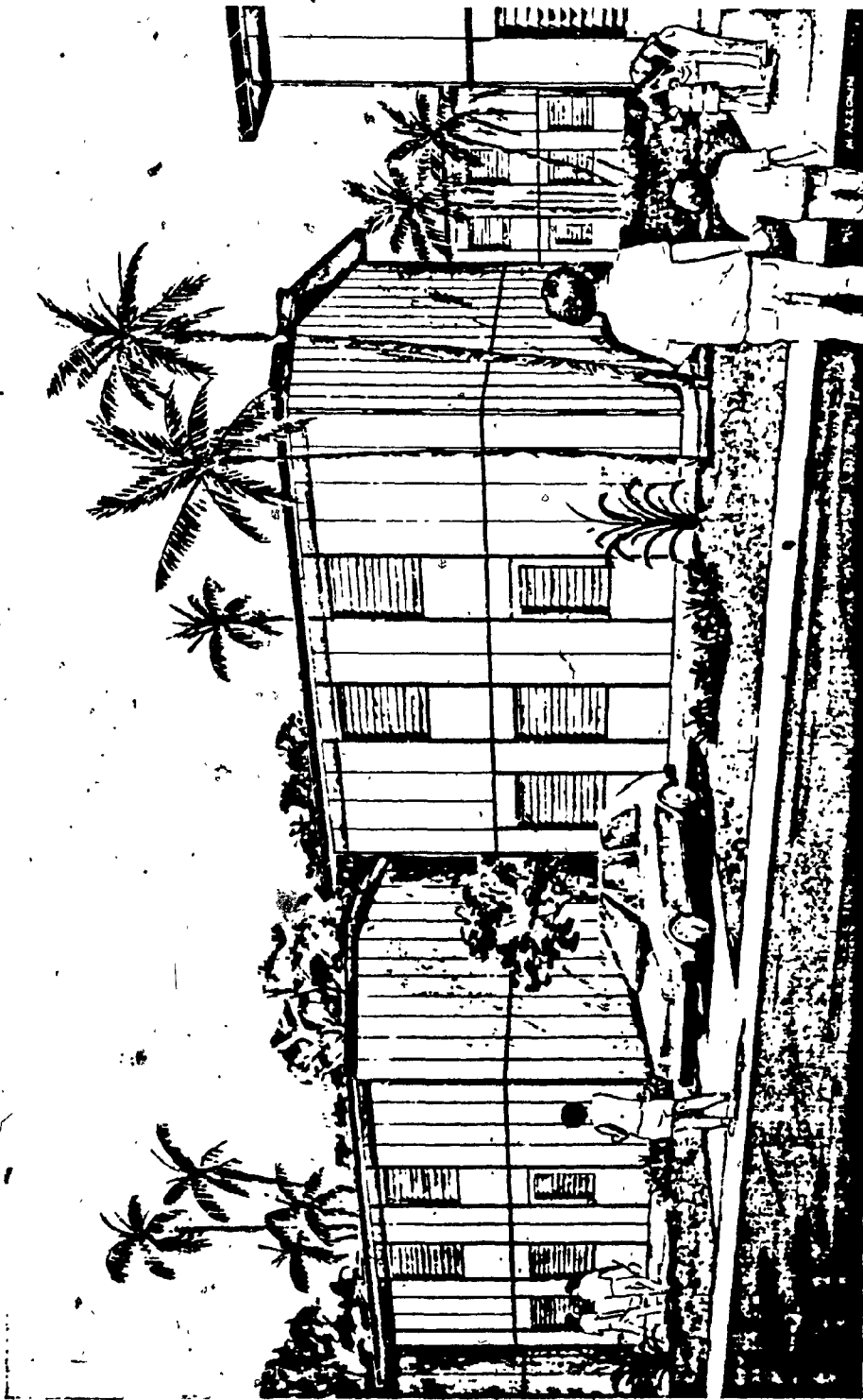


Figure 2.1.3. View of individual cottage

2.2 's' Component

Only one type of 's' element is used for roof and wall assemblies. It consists of a symmetrical element as shown in Figure 2.2.1(c). Its overall dimensions are 12'-0" long by 3'-11" wide and 5" or 6" thick. The thickness of the asbestos sheet is 3/8 of an inch.

For testing purposes, the roof panel consisted of a full width uncut 's' element and two reduced width 's' elements as shown in Figure 2.2.1(a) and a cut-off element from a full width flat unit. The overlapping edges were secured with 10-24 x 1" steel screws and expansion chills every 24 inches. A typical roof assembly is shown in Figure 2.2.1(d).

Also for testing purposes, the wall panel consisted of a combination of two reduced width 's' elements as shown in Figure 2.2.1(b). The two elements were attached at overlapping edges with 10-24 x 1" steel screws and expansion chills every 24 inches.

2.3 'v' Component

The 'v' element is basically used for floor structures. Floor assemblies can be made using either single or double 'v' elements which are produced in two different slab thicknesses: 3/8" for type 'v1' and $\frac{1}{2}$ of an inch for type 'v2' as shown in Figures 2.3.1(a) and 2.3.1(b) respectively.

The floor panels consisted of different combinations of

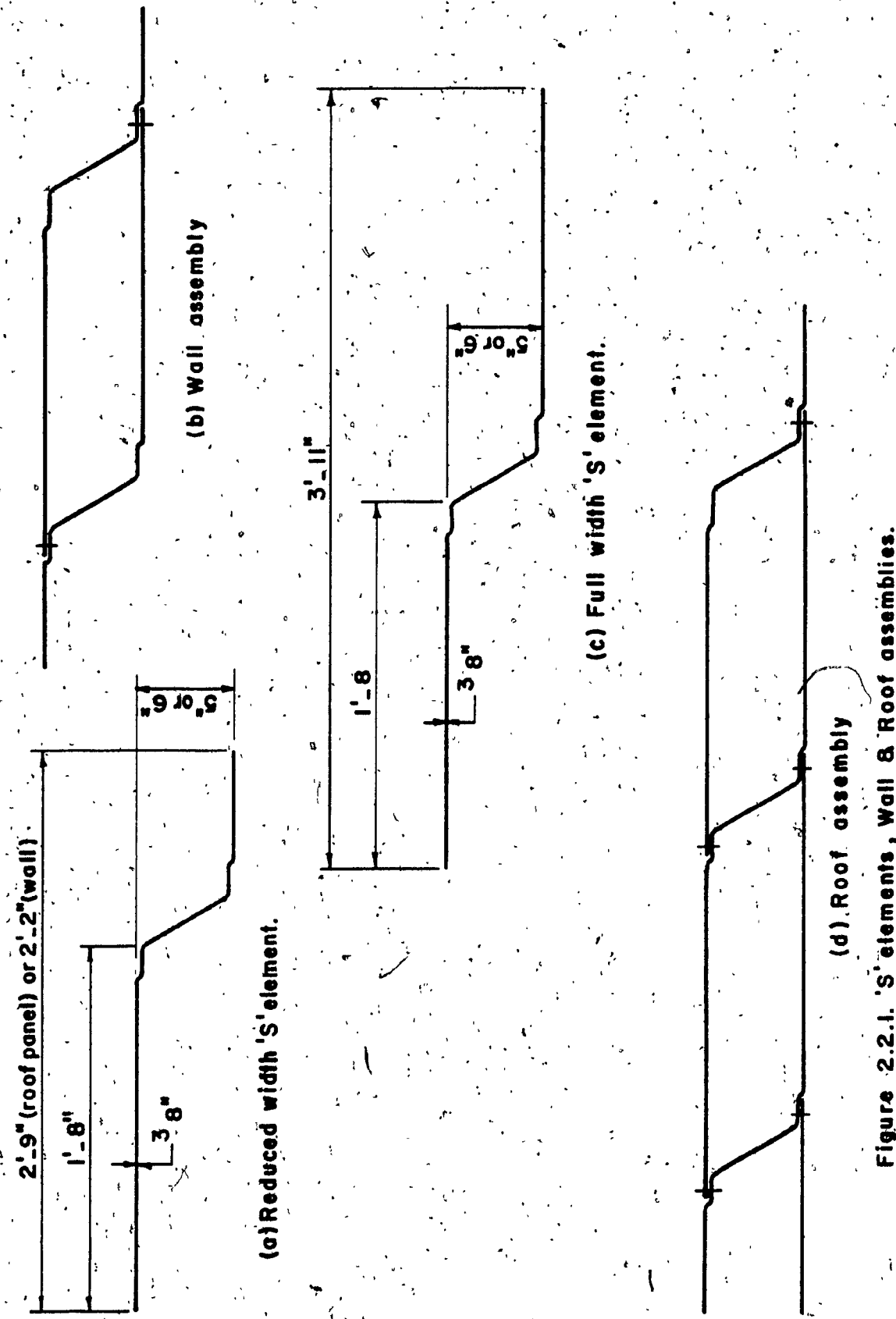
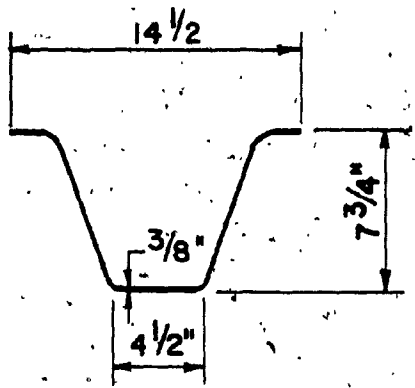
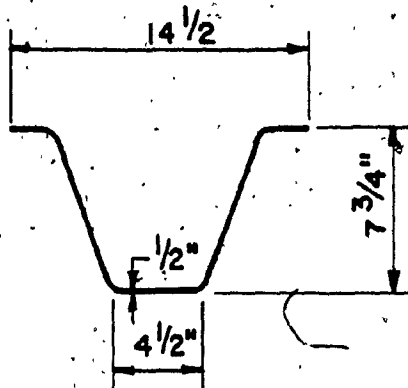


Figure 2.2.1. 'S' elements , Wall & Roof assemblies.

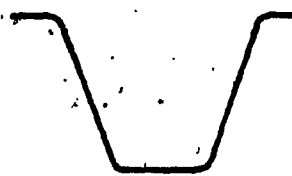


(a) 'V' element Type 'VI'

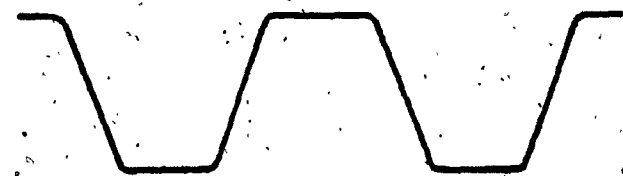


(b) 'V' element Type 'V2'

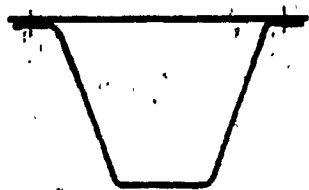
Figure 2.3.1 Types of 'V' elements



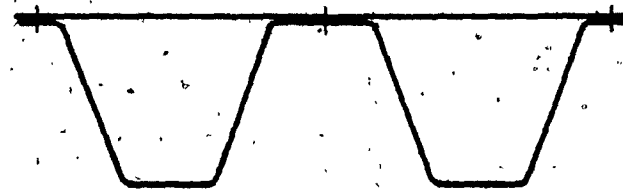
(a) Single 'V' Beam.



(b) Double 'V' Beam



(c) Single 'V' Beam
with top plate



(d) Double 'V' Beam
with top plate

Figure 2.3.2 Types of Beams.

'v' elements and in certain cases are combined with flat top plates. The different types of beam panel produced for testing purposes are shown in Figure 2.3.2. Attachments where necessary, were made with 10-24 x 1" steel screws and expansion chills.

2.4 Material

'S' elements and 'y' elements are made of apac and flat plates of densite. The properties of these two materials as specified by Atlas Turner Inc., who produced the elements described above, are shown in the following Table.

			APAC	DENSITE
Modulus of elasticity (lb/in ²)	E		1.8×10^6	1.8×10^6
Modulus of rupture (lb/in ²)	along length	f _t	3100	4500
	along width	f _{tc}	2400	3700
Tensile strength (lb/in ²)	along length	f _{to}	1800	2220
	along width	f _{toc}	1200	1450
Compressive strength (lb/in ²)	f _c		8600	12500

2.5 Testing Arrangement

All floor, roof and beam panels were tested as simply supported. The arrangement of this test is shown in Figure 2.5.1. Roller support or supports, as required, were provided on one side, while the other side was pin-connected. The panels rested on bearing pads made of $\frac{1}{2}$ " thick softwood. The load was applied at the midspan of the samples so that half the load was supported at each end.

Compression tests were performed on wall panels and column samples in a special frame as shown in Figure 2.5.2. The set-up consisted of an overhead mounted hydraulic jack with a calibrated loading cell, resting on a rigid steel beam. Necessary precautions were taken against sudden sidesway by bracing the test elements on the front and back faces.

2.6 Testing Procedure

The panels were statically loaded to failure. To facilitate observations, the centre lines of panels were drawn along the two principal axes, and the location of screws was marked with circles. Each panel was then carefully surveyed, and the dimensions and age recorded.

Once a panel was installed and ready for testing, the dial gauges were placed and adjusted; loads were then gradually applied by means of a hydraulic jack, in equal increments of 0.24 kips to 0.48 kips. Deflection and load readings were taken after each increment. The panel was first allowed

to stabilize and after which readings were made and recorded. This loading procedure was continued until the ultimate capacity was reached. At failure, crack patterns as well as failure load were marked on the panel and photographs were taken.

2.7 Loading Measurements

For floor, roof and beam assemblies, dial gauges were used to measure the vertical displacements. Electric strain gauges were also used on panels 1-SR6 and 11FV4(b). The electric strain gauges were placed on the top and bottom surfaces of roof panel 1-SR6 whereas only two strain gauges were placed on the bottom surface of beam 11FV4(b).

Corresponding to the load applied, the reading of all strain gauges and dial gauges were recorded. Recorded measurements were plotted for each panel.

The cut-out sections were tested on a Tinus Olsen machine in order to verify the properties of the material. The loading measurements were read directly from the machine gauge.

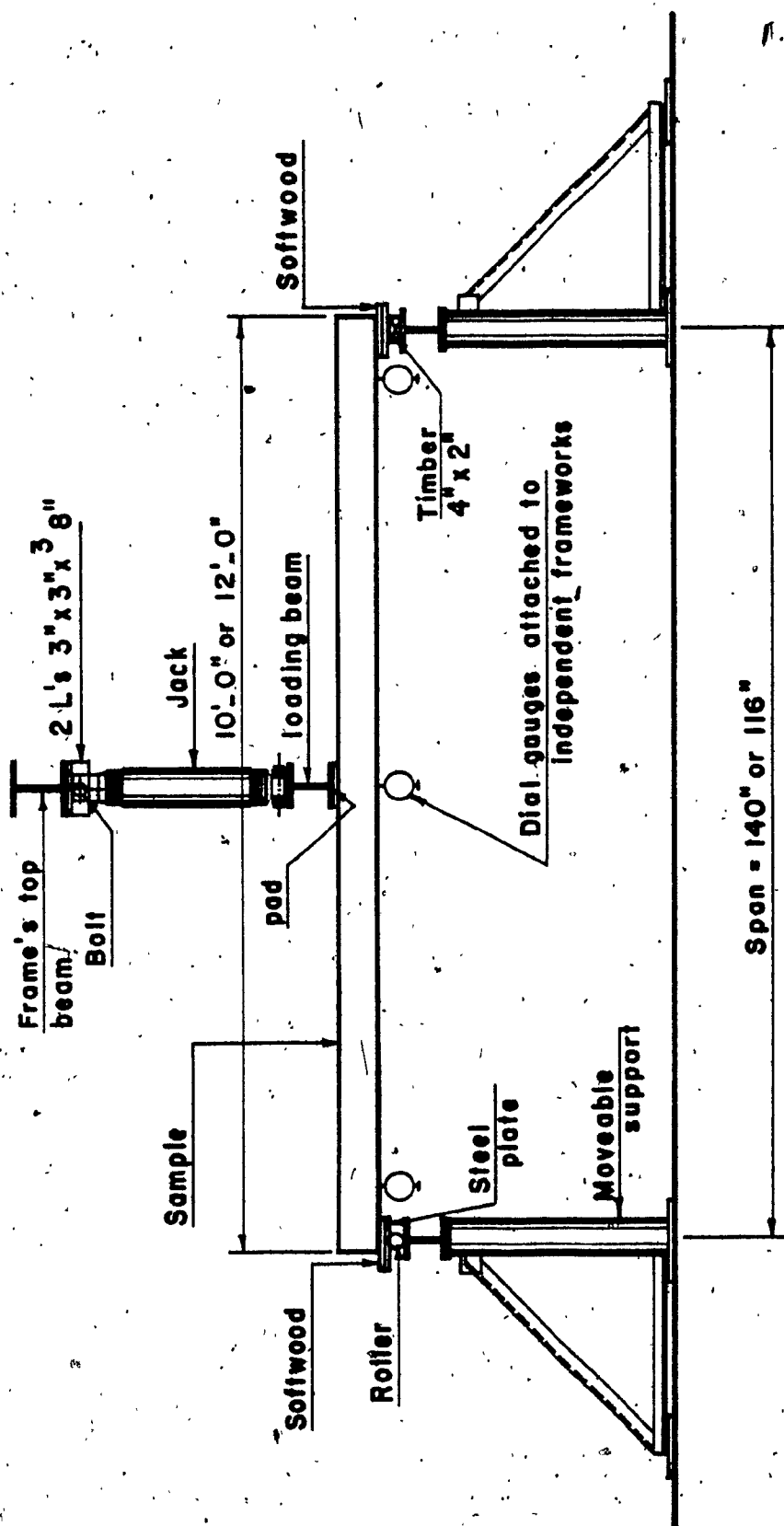


Figure 2.5.1. Arrangement of floor & beam panels tests.

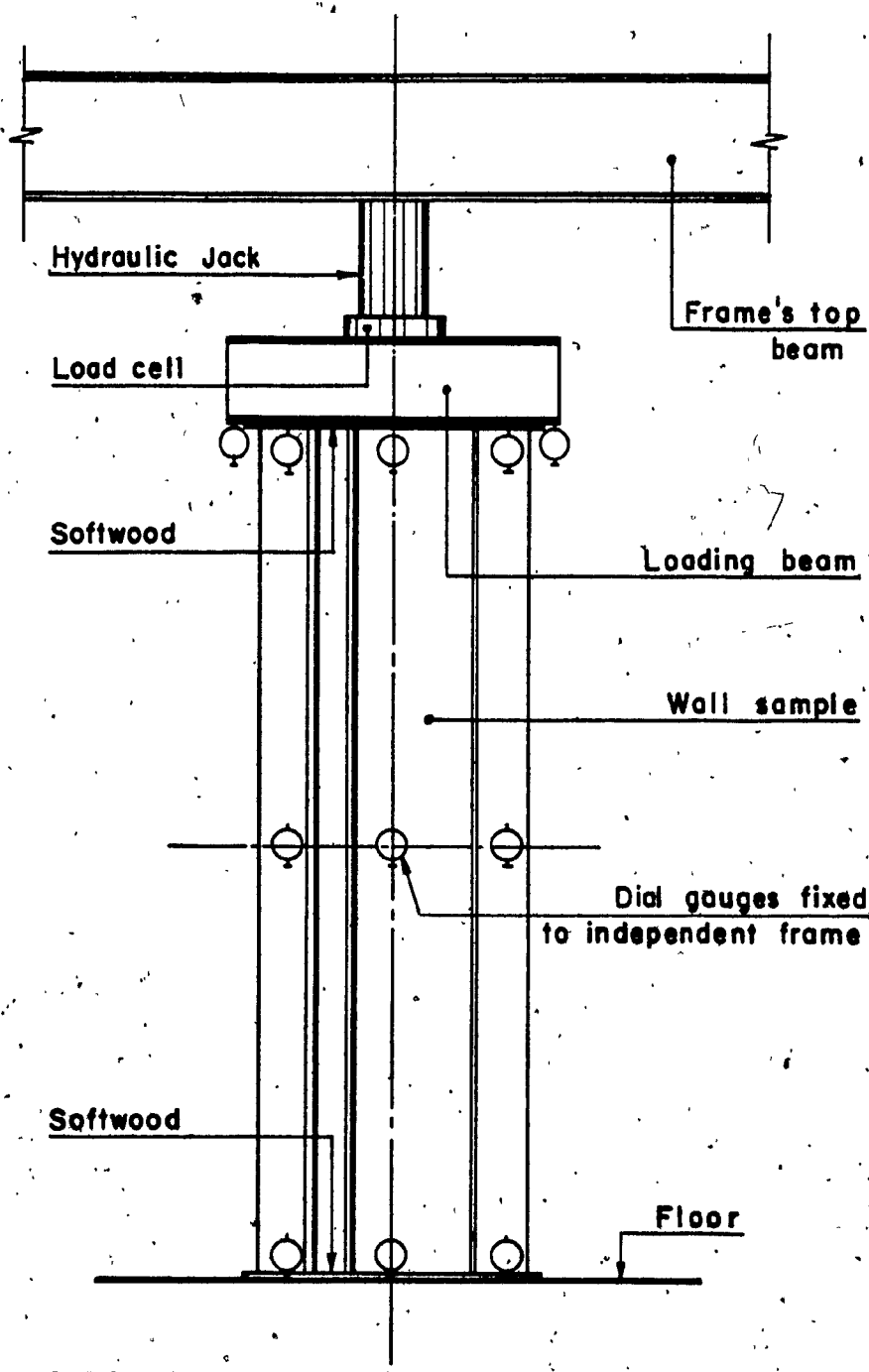


Figure 2.5.2 Arrangement of Wall panel & Column tests.

CHAPTER 3

TESTING PROGRAM, OBSERVATIONS AND RESULTS

CHAPTER 3

TESTING PROGRAM, OBSERVATIONS AND RESULTS

3.1 First Stage-Roof Panels Made of 's' Element

In the first stage, the behaviour as well as the capacity of roof elements as shown in Figure 3.1.1 were investigated in order to establish applicable criteria for roof structures.

Test samples were made in four series S1, S2, S3 and S4. Series S1 and S2 represented the testing of two roof panels denoted by 1-SR6 and 2-SR6 respectively (number 6 denotes overall depth of 6"). The dimensions of each panel were 4'-11" x 6" in cross-section and 12'-0" in length. Test series S3 and S4 were carried out on panels 1-SR5 and 2-SR5 (number 5 denotes overall depth of 5"), each measuring 12'-0" x 4'-11" x 5" thick as shown in Figure 3.1.1.

Test series S1 - roof panel 1-SR6 - Roof panel 1-SR6 was loaded as a simply supported beam in an upside down position. The panel failed under a load of 4.15 kips as shown in Table 3.1.1. Failure occurred when the left side of the bottom sheet cracked in tension, directly under the applied load. There were no cracks around the screws and no noticeable damage of the holes were observed. None of the screws were pulled out or bent. Although failure occurred at the bottom, this panel was still capable of carrying some loads until it cracked on the right side.

Figure 3.1.2 illustrates the nature of the stress

distribution in the roof assembly. The highest tensile stresses occurred at Points 6 and 8 and the highest compressive stresses at Point 3. Under initial loadings, Points 5, 6, 7 and 8 at the bottom of the panel were all in tension; with load increments, the tensile stresses increased at Points 6 and 8 and decreased at Points 5 and 7. Prior to failure, Points 6 and 8 reached the maximum tensile stress while Points 5 and 7 were subjected to compressive stresses.

Equivalent uniform distributed load corresponding to the tested failure load is shown in Table 3.1.1, as well as the calculated equivalent uniform distributed loads for 10'-0" span. Figure 3.1.5 shows the load-deflection curve, with the load in kips as the ordinate, and the deflection in inches as the abscissa.

Test series S2 - roof panel 2-SR6 - This test series was carried out in two phases. In the first phase, a creep test under sustained load was performed on roof panel 2-SR6. It was loaded as simply supported in an upside down position, with a uniform distributed load of $20 \text{ lb}/\text{ft}^2$ and measurements of deflection at the centre and at both ends were made every 12 hours for a period of 30 days. Once the panel was unloaded after 30 days, measurements of deflection were carried out immediately and again one hour later. The recovery was 80%. The deflection-time curve for the creep test is shown in Figure 3.1.3. As it may be noted, creep was almost finished after 20 days.

In the second phase, the panel in an upside down position was then loaded as in test series S1. Failure of this sample was due to the breaking of its bottom sheets in the middle directly under the load. The crack was about $1\frac{1}{2}$ inches away from the middle screws. The failure load was 2.975 kips as shown in Table 3.1.1. The load-deflection curve of 2-SR6 under midspan loading is shown in Figure 3.1.5.

Test series S3 - roof panel 1-SR5 - Contrary to test series S1 and S2, roof panel 1-SR5 was loaded in the normal (not upside down) position. As the load reached 2.88 kips, overall failure of the bottom flanges occurred in the vicinity of the middle screws, directly under the applied load. As in previous cases, despite the failure of the bottom flanges, the panel was still capable of sustaining additional loads, and no tearing of asbestos around the screws was observed.

Test series S4 - roof panel 2-SR5 - Roof panel 2-SR5 was identical to 1-SR5. The same test was carried out except that this panel was tested in an upside down position as in test series S1 and S2. The existing crack at the bottom right flange close to the roller support was marked. Failure occurred when the asbestos cracked at the bottom right side, and the existing crack opened $1/8$ of an inch. The failure load was 3.12 kips as indicated in Table 3.1.1. As for panel 1-SR5, the cracking of asbestos-cement occurred in tension under the applied load. Figure 3.1.4 shows the load-deflection curve.

Cut-out sections - Three samples each measuring 6" long by
6" wide by 3/8" thick were cut-out from each panel of test
series S1, S2, S3 and S4 and similar tests were conducted.
Results are tabulated in Table 3.7.1.

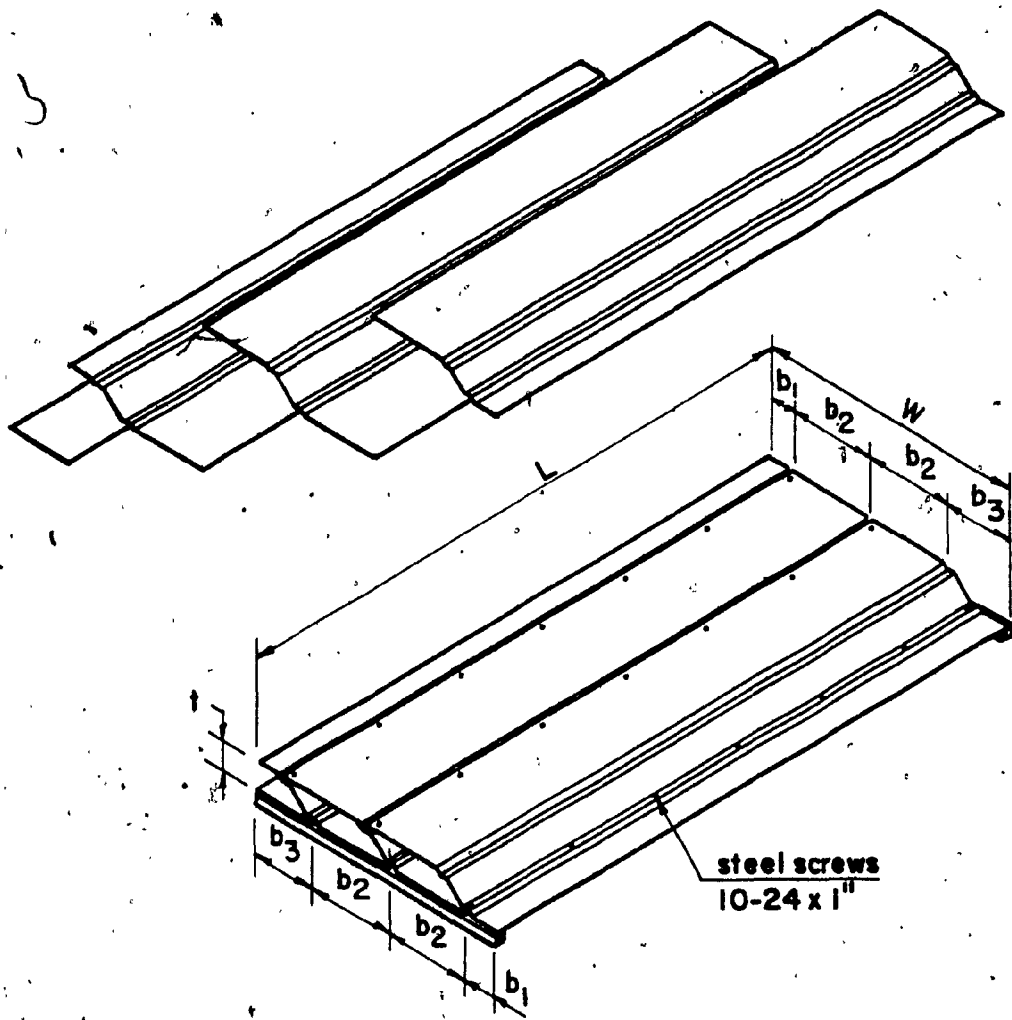
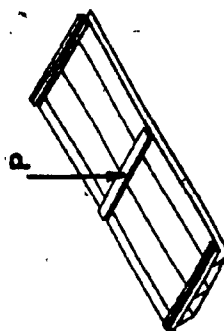
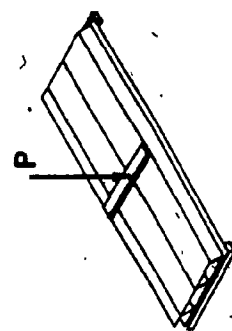


Figure 3.1.1. Dimensions of Roof assemblies.

Test Series	Sample No.	L	W	t	b ₁	b ₂	b ₃
S1	1-SR6	12'-0"	4'-11"	6"	6"	1'-8"	1'-1"
S2	2-SR6	12'-0"	4'-11"	6"	6"	1'-8"	1'-1"
S3	1-SR5	12'-0"	4'-11"	5"	6"	1'-8"	1'-1"
S4	2-SR5	12'-0"	4'-11"	5"	6"	1'-8"	1'-1"

Table 3.1.1. Comparative results and equivalent uniform distributed loads. (1st. stage)

Sample No.	Failure load P (kips)	Calculated load P (kips)	Equivalent uniform distributed load for 12'-0" span (tested)	Equiv. uniform load for 10'-0" span (calculated)
		k/ft	kN/m	kN/m
I-SR5	2.88	3.32	0.494	7.20
				0.129
				6.170
				0.719
				10.493
I-SR6	4.15	3.98	0.711	10.38
				0.183
				8.880
				1.036
				15.119
2-SR6	2.975	3.98	0.510	7.44
				0.133
				6.370
				0.743
				10.843
2-SR5	3.12	3.35	0.535	7.81
				0.139
				6.682
				0.779
				11.368



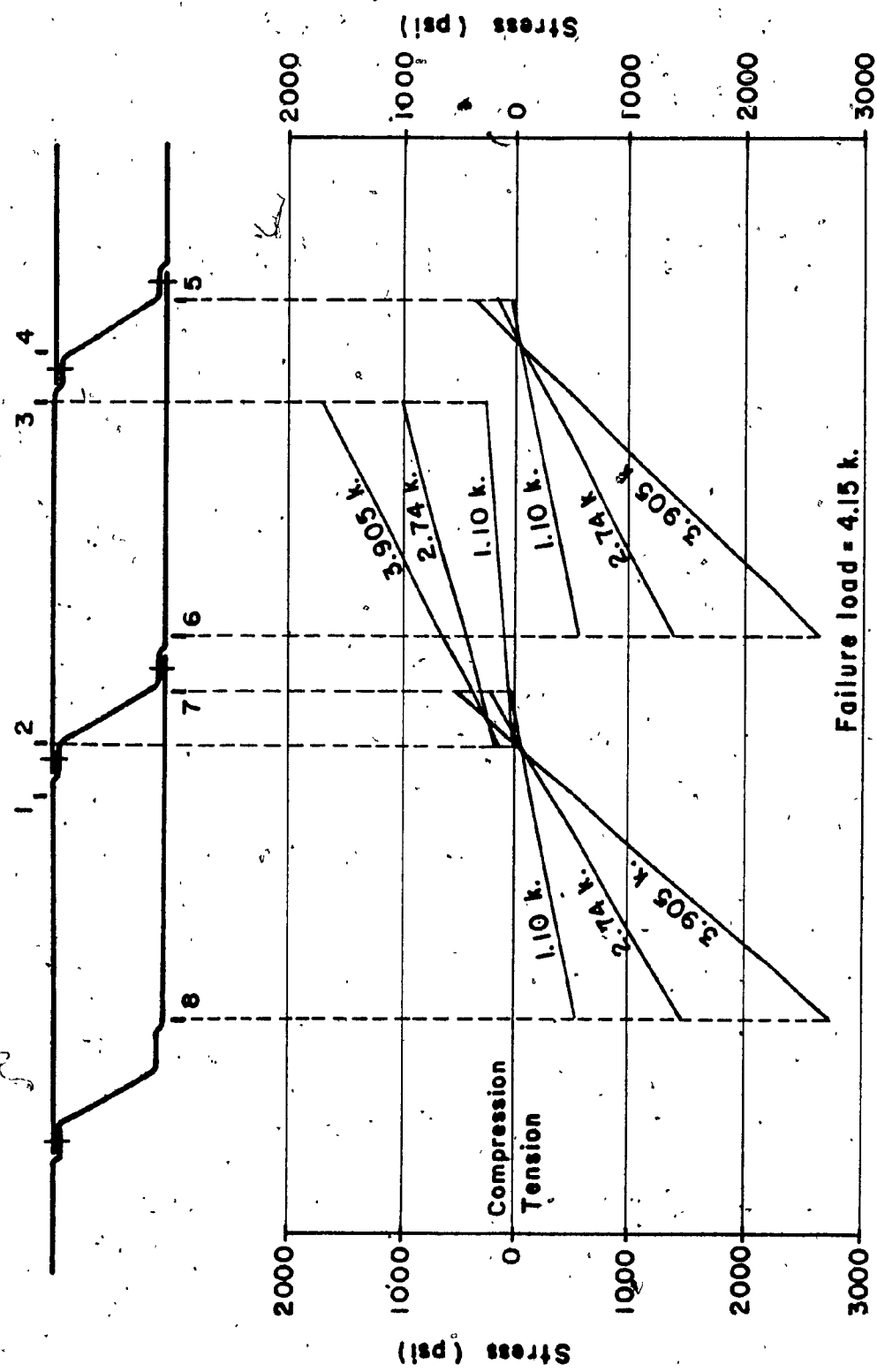


Figure 3.1.2. Stress distribution - Root panel I-SRG

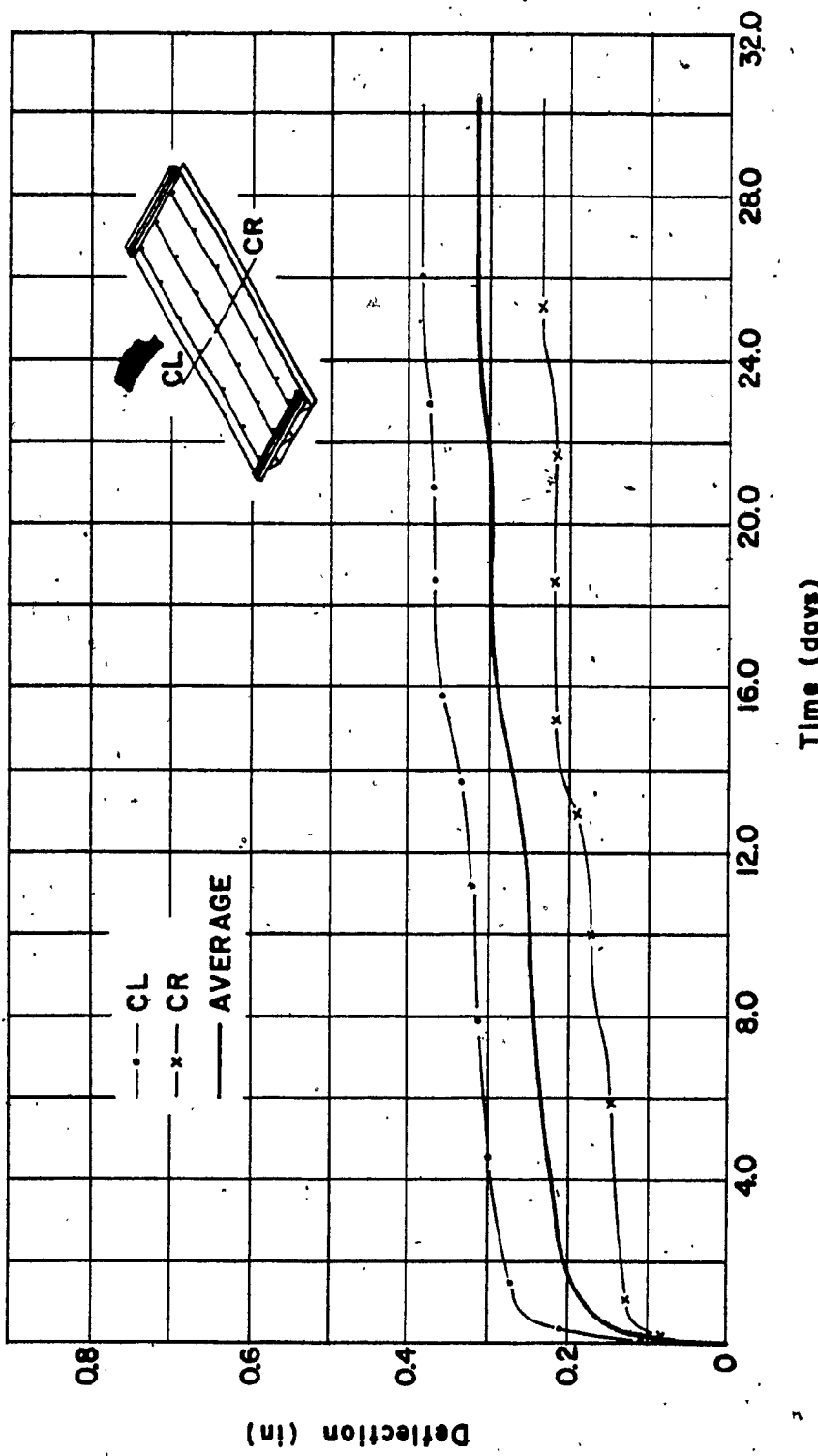


Figure 3.1.3. Time-Deflection curve (creep test - Panel 2-SR6)

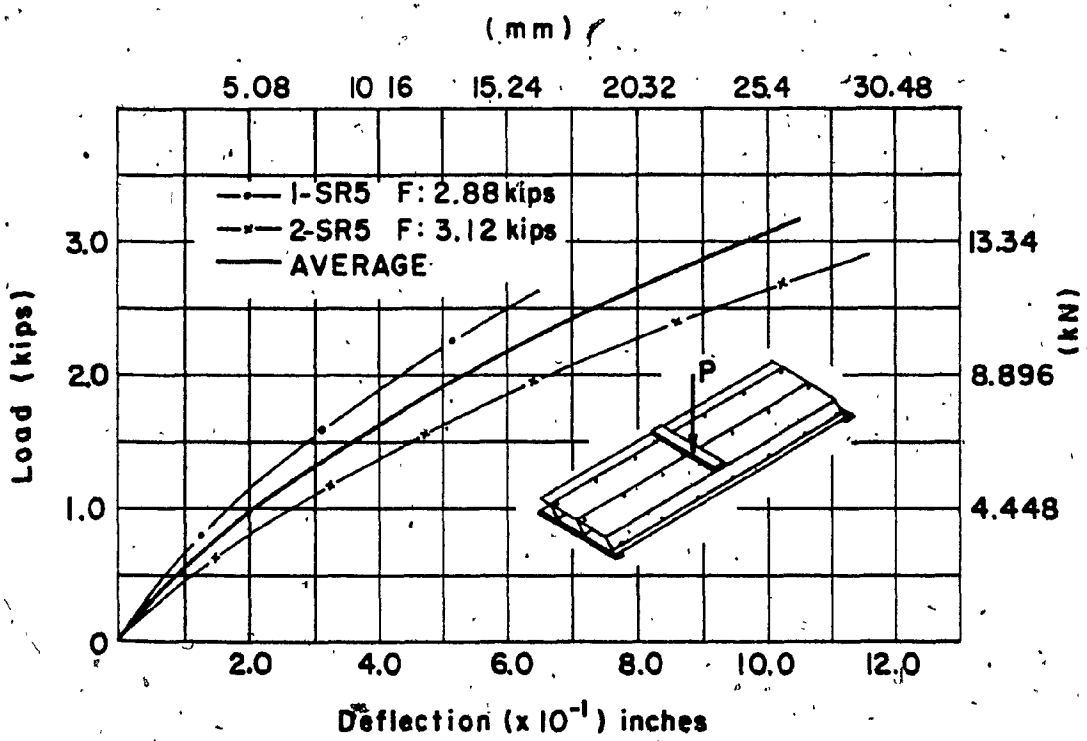


Figure 3.1.4. Load-Deflection curve.

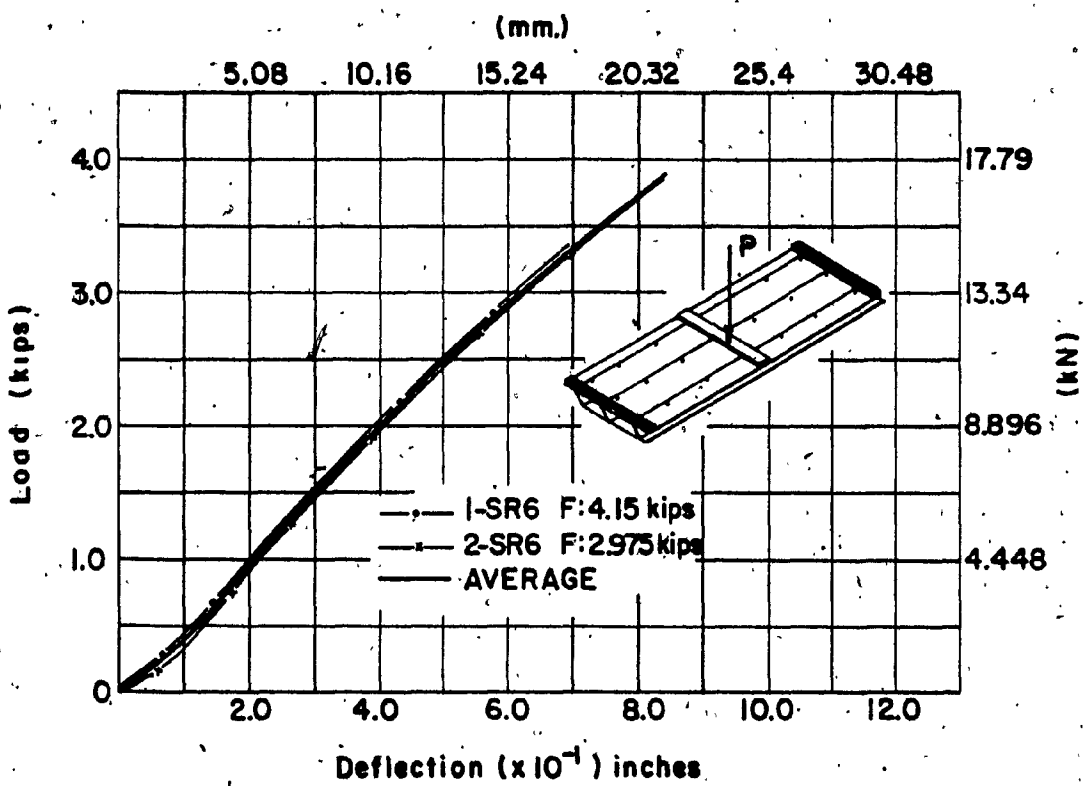


Figure 3.1.5. Load-Deflection curve.

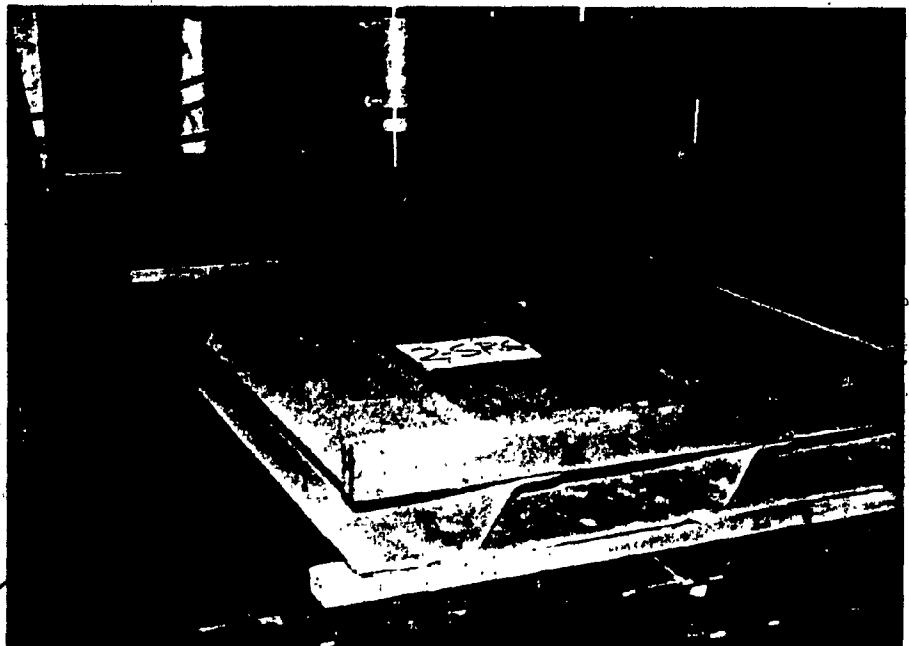
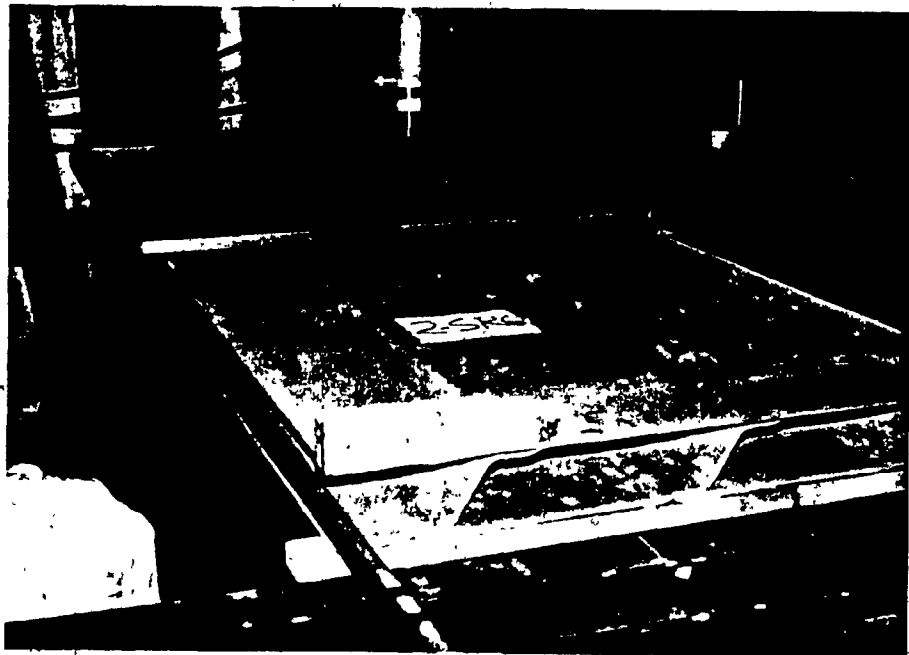


Figure 3.1.6. View of testing set-up of Roof panel 2-SR6.

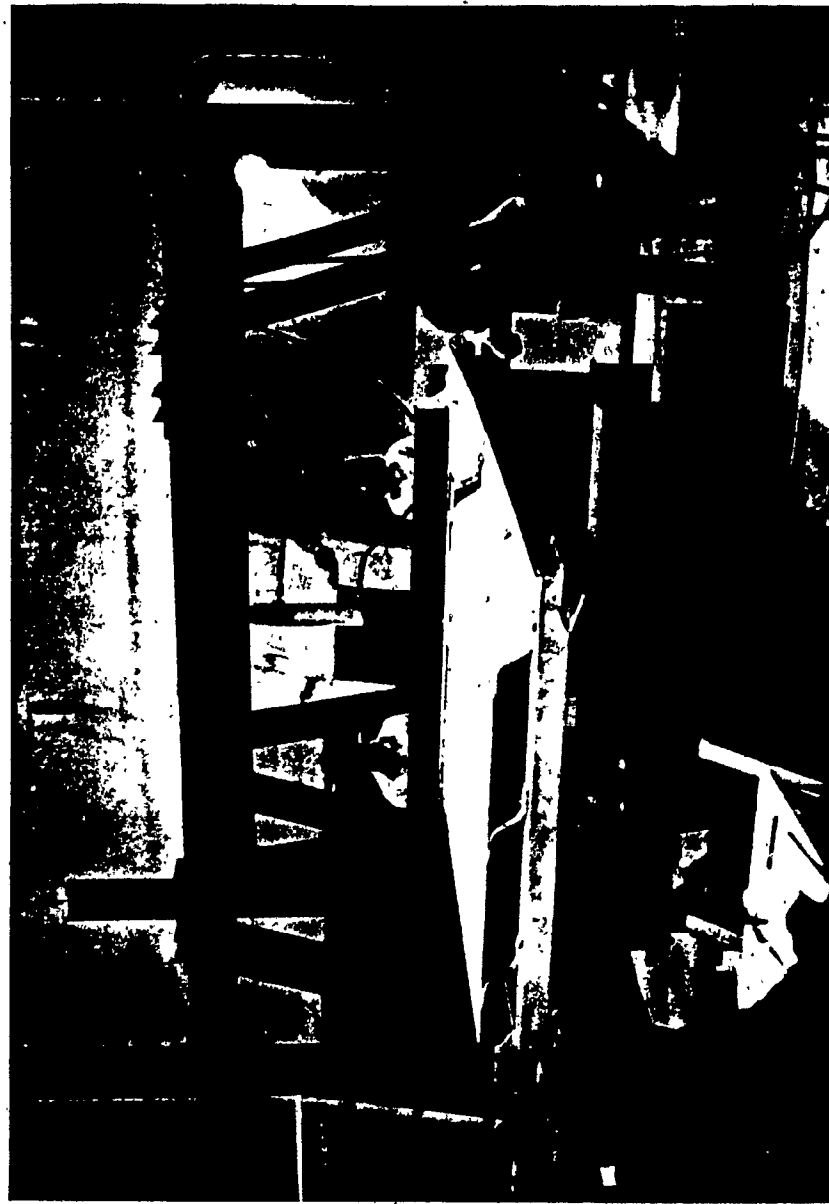


Figure 3.1.7. View of testing set-up of Roof panel I-SR5.



Figure 3.1.8. View of Roof panel I-SR5 (At failure).



Figure 3.1. 9. Top view of testing set-up of Roof panel 2-SR5



Figure 3.1.10. View of Roof panel 2-SR5 (At failure).

3.2 Second Stage - Wall Panels Made of 's' Elements

This stage consisted of two parts. The first part dealt with the behavior and capacity of walls leading to a consideration of safe loading limits and practical design criteria. In the second part, the maximum capacity for short walls (with no buckling influence) was found. This capacity was compared with corresponding walls of regular heights as tested in the first stage.

In the first part, test series S5, S6, S7 and S8 were carried out on four wall panels. In test series S5 and S6, wall panels 5SW6 and 6SW6 (last number 6 denotes overall depth of 6") were tested. Each panel had dimensions 3'-3" x 6" in cross-section and 10'-0" in height as shown in Figure 3.2.1. Wall panels 7SW5 and 8SW5 (last number 5 denotes overall depth of 5") were tested in test series S7 and S8 respectively. They both measured 10'-0" high, 3'-3" wide and 5" thick as shown in Figure 3.2.1.

In the second part, test series S9, S10, S11 and S12 were run on four short wall panels. They were named 9SW6, 10SW6, 11SW5 and 12SW5. As shown in Figure 3.2.2, panels 9SW6 and 10SW6 each had a cross-section of 3'-3" x 6" and a height of 2'-0", while panels 11SW5 and 12SW5 were 3'-3" wide, 5" thick and 2'-0" high.

Test series S5 - (Compression) - wall panel 5SW6 - In order to apply compression loads on wall panels, the arrangement as shown in Figure 2.5.2 was used. Wall panel 5SW6 was loaded

concentrically, but because its top surface was not perpendicular to the top rigid steel beam during the test, failure occurred early. Therefore, this test was ignored and its results were not used for comparisons. Failure occurred when the bottom part of the wall twisted out from its original position and broke. The failure load was 25 kips as indicated in Table 3.2.1.

Test series S6 - (Compression) - wall panel 6SW6 - Wall panel 6SW6 was identical to 5SW6, except for having additional screws so that the spacing was 12 inches instead of 24 inches. Care was taken to make sure that the load was uniformly applied on the whole surface at the top of the wall. Under a compressive load of 63 kips, the wall failed when the bottom part of one of the 's' sections crashed. No buckling of the wall between screws was observed.

Test series S7 - wall panel 7SW5 - Compressive test was also performed on wall panel 7SW5. The ultimate capacity was reached when the panel failed at the top by rapid splitting. During the test, buckling appeared the two last screws at the bottom of the panel and disappeared after the failure of the top part. The failure load was 35.68 kips.

Test series S8 - wall panel 8SW5 - A similar test to test series S8 was performed on wall panel 8SW5. Failure occurred when the bottom of the wider flange of one of 's'-sections cracked but did not chip off. Prior to failure, the asbestos-cement sheet buckled between the two last screws at the bottom of the wall, while no overall buckling of the assembly

was observed. The asbestos sheet cracked midway between the bottom screws and progressed towards the centre. The failure load was 37.5 kips and even though the bottom of the panel failed, it was capable of carrying more load until the wider flange of the front 's'-section cracked at the centre under a load lower than 37.5 kips.

Test series S9, S10, S11 and S12 - wall panels 9SW6, 10SW6, 11SW5 and 12SW5 - As mentioned earlier, these tests were done in order to evaluate the influence of buckling. Compression tests were carried out on short walls 9SW6, 10SW6, 11SW5 and 12SW5 which were parts of wall assemblies 5SW6, 6SW6, 7SW5 and 8SW5 respectively. More screws were added to panel 12SW5 to make them 12 inches apart instead of 24 inches, as were the cases for other panels. The height of each wall was 2'-0". The test results are shown in Table 3.2.1.

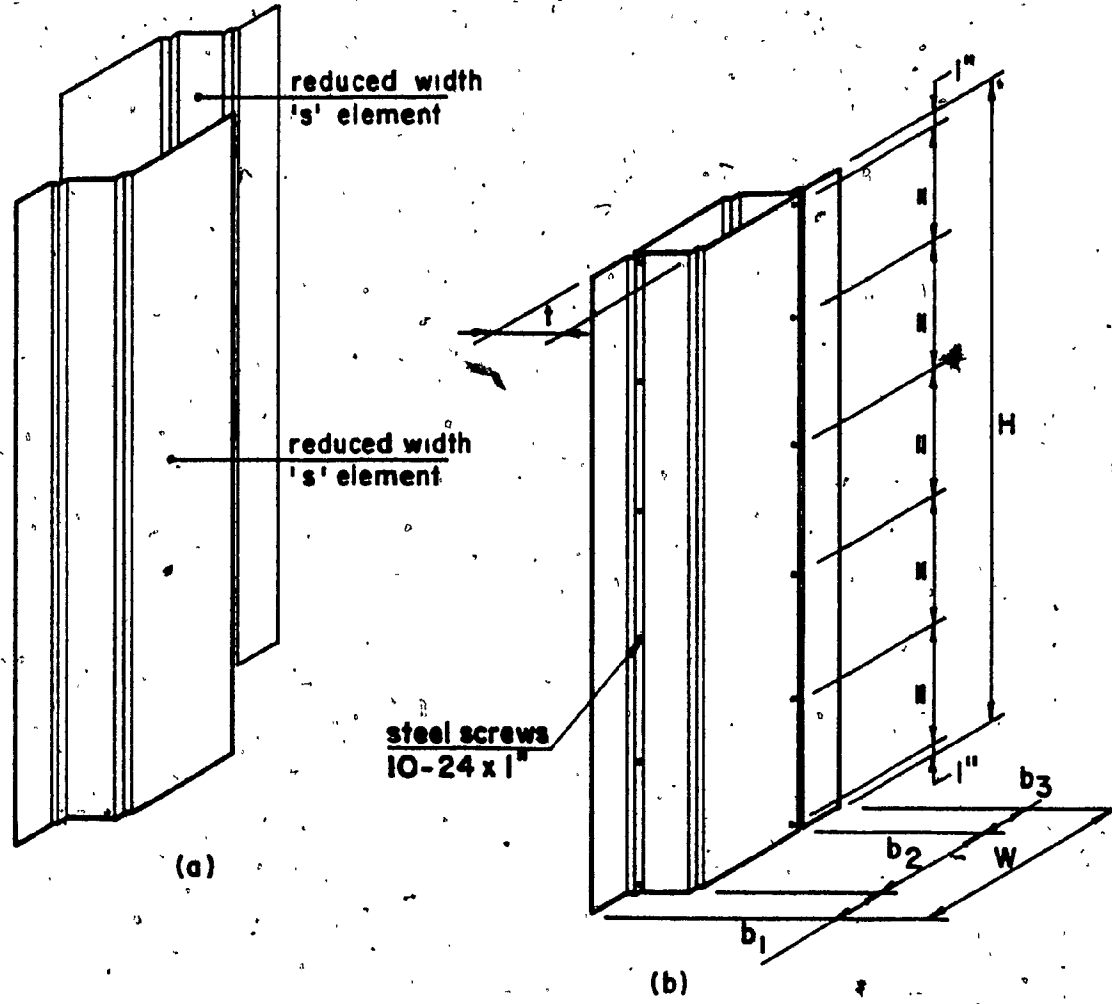


Figure 3.2.1. Dimensions of wall assemblies

Test Series	Sample No.	H	W	t	b_1	b_2	b_3
S5	5SW6	10'-0"	3'-3"	6"	6"	1'-8"	1'-1"
S6	6SW6	10'-0"	3'-3"	6"	6"	1'-8"	1'-1"
S7	7SW5	10'-0"	3'-3"	.5"	6"	1'-8"	1'-1"
S8	8SW5	10'-0"	3'-3"	5"	6"	1'-8"	1'-1"

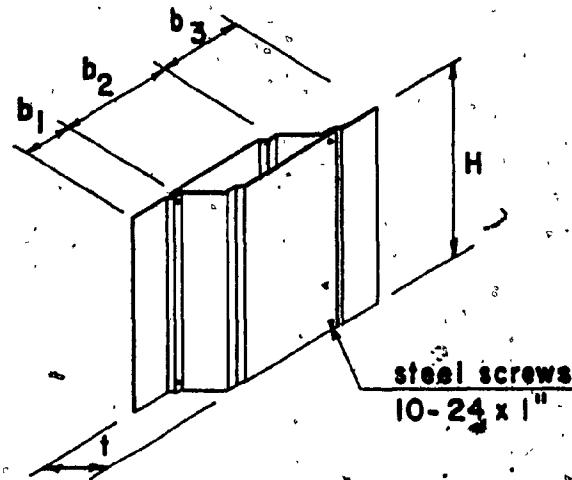
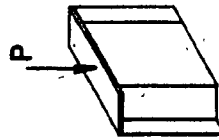
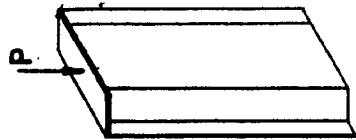


Figure 3.2.2 Dimensions of short wall assemblies

Test Series	Sample No.	H	W	t	b ₁	b ₂	b ₃
S9	9SW6	2'-0"	3'-3"	6"	6"	1'-8"	1'-1"
S10	10SW6	2'-0"	3'-3"	6"	6"	1'-8"	1'-1"
S11	11SW5	2'-0"	3'-3"	5"	6"	1'-8"	1'-1"
S12	12SW5	2'-0"	3'-3"	5"	6"	1'-8"	1'-1"

Table 3.2.1. Comparison of tested and calculated results.

Sample No.	Failure load 'P' (kips)	f_c (psi)	Calculated load 'P' (kips)
5SW6	25	6681	32.18
6SW6 *	63	7215 †	54.48
7SW5	35	9713	31.00
8SW5	375	10406	31.00
9SW6	42.7	11410	32.18
10SW6	68.0	6645 †	32.18
11SW5	40.1	11128	31.00
12SW5	*	59.9	6121 †
			84.15



* Screws at 12" c/c † - Overall stability governs

f_c - calculated uniform compression strength (ACI 318-83)

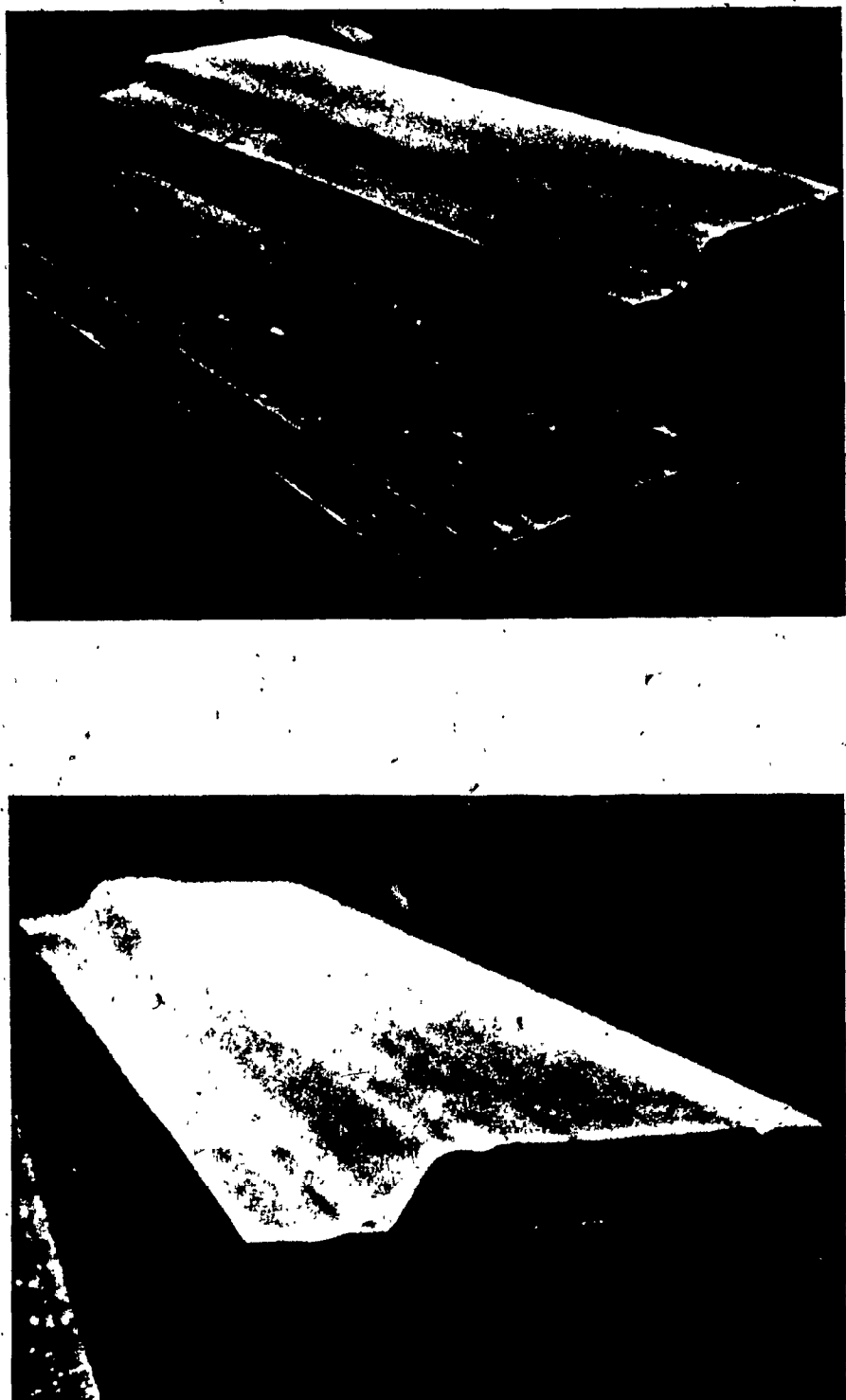


Figure 3.2.3. Overall views of Wall panels.



Figure 3.2.5. Overall view of Wall panel
7SW5 (At failure)



Figure 3.2.4. Overall view of Wall panel
7SW5.



Figure 3.2.6. Side view of Wall panel 8SW5 (At failure)

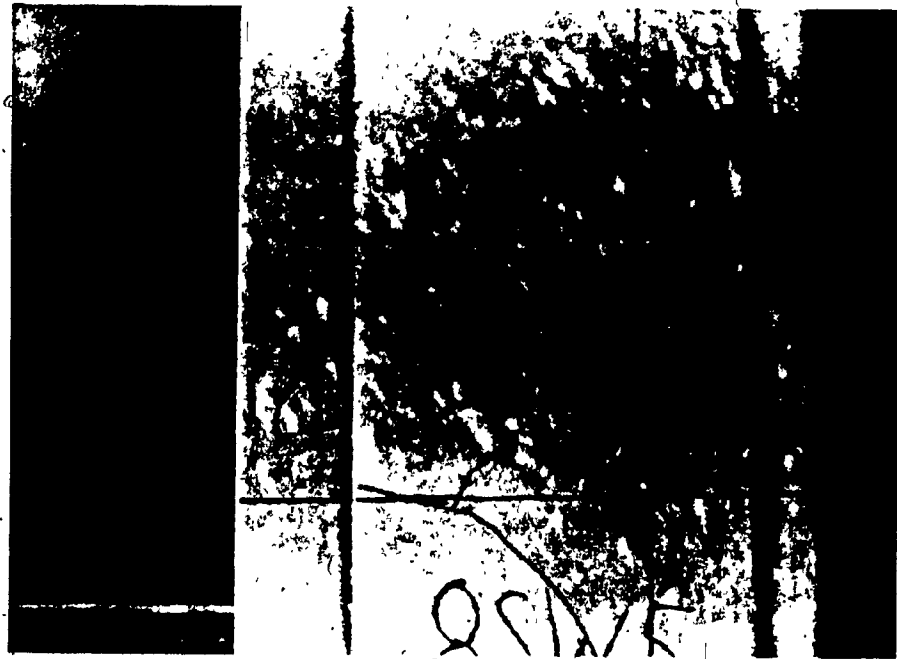


Figure 3.2.7. Front view of Wall panel 8SW5 (At failure)

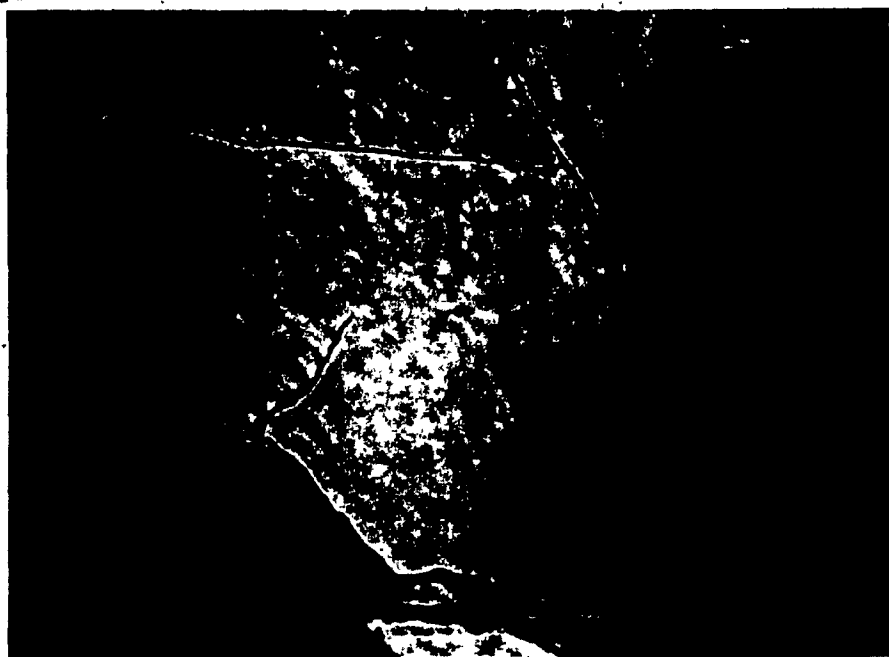


Figure 3.2.8. Back view of Wall panel BSW5 (At failure).

3.3 Third Stage - Beams Made of Single 'v' Elements and Double 'v' Elements

In the third stage, tests were performed on beams made of (a) single 'v' elements, (b) single 'v' elements with steel reinforcement at the bottom, and (c) double 'v' elements.

Single 'v' element beams were tested to establish their load capacities as beams in floor systems and compared with corresponding reinforced elements. These capacities were also compared with double 'v' elements.

This stage included test series V1, V2, V3, V4 and V5.

In test series V1, beams 1-FV3a and 1-FV3b, made of single 'v' elements, were tested. The overall dimensions of each beam were 10'-0" long and 7 $\frac{1}{4}$ " deep, as shown in Figure 3.3.1. Two other single 'v' beams, 2-FV4a and 2-FV4b, were tested in test series V2. They both were 12'-0" long and 7 $\frac{1}{4}$ " deep as illustrated in Figure 3.3.1. One single 'v' beam 3-FV3a was tested in test series V3. The bottom of this beam was reinforced with 2#3 bars embedded in early high strength portland cement as shown in Figure 3.3.2. The beam measured 10'-0" in length and 7 $\frac{1}{4}$ " deep, as indicated in Figure 3.3.2. Tests were conducted on beams 10-FV3a and 10-FV3b in test series V4, while test series V5 dealt with the testing of beams 11-FV4a and 11-FV4b. Beams 10-FV3a, 10-FV3b, 11-FV4a and 11-FV4b were all made of double 'v' elements glued together as shown in Figure 3.3.3. Both beams 10-FV3a and 10-FV3b were 10'-0" long

and $7\frac{1}{2}$ " deep, whereas beams 11-FV4a and 11-FV4b were 12'-0" long and $7\frac{1}{2}$ " deep.

The arrangement of a test on a typical v-section beam is shown in Figure 2.5.1.

Test series V1 - single 'v' element beams 1-FV3a and 1-FV3b -
Both beams failed by a sudden tension crack directly under the applied load. The ultimate loads reached for beam 1-FV3a and 1-FV3b were 1.55 and 1.31 kips respectively. Corresponding equivalent uniform distributed loads have been calculated and are shown in Table 3.3.1. Figure 3.3.4 shows the load-deflection curve.

Test series V2 - single 'v' element - beams 2-FV4a and 2-FV4b -
As in the previous test series, beam 2-FV4a and 2-FV4b failed by a sudden tension cracking at midspan under the applied load. Both beams failed in tension under a load of 1.55 kips, as indicated in Table 3.3.2. The load-deflection curves are shown in Figure 3.3.5.

Test series V3 - beam 3-FV3a strengthened with steel bars -
The left side of the bottom flange of beam 3-FV3a cracked in tension under a load of 2.74 kips and as a result, the pressure applied by the jack dropped suddenly. When the load was brought back to 1.31 kips, the whole bottom flange cracked.

The behavior of this beam under load can be clarified by the fact that after the failure of asbestos-cement, load was transmitted to steel which was subjected to a sudden increase of stress and began to yield. This explains the

sudden drop of pressure by the jack. This test also demonstrates that the tensile capacity of this beam is double that of a corresponding non-reinforced beam 1-FV3a. The load-deflection curve is shown in Figure 3.3.6.

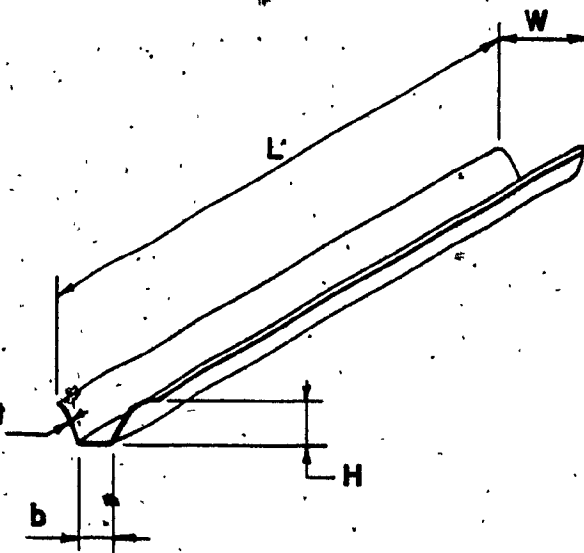
Test series V4 - double 'v' beams 10-FV3a and 10-FV3b - The sequence of failure of both beams was identical. The right v-section of both beams cracked close to the location of the applied load under a 3.78 kip load. The crack stopped at the joint between the two v-sections leaving the left v-section intact. The left v-section of each beam was then moved to the centre and loaded. They both failed under a load of 1.43 kips.

It was observed from this test that the tensile capacity of a double 'v' beam is two-and-a-half times higher than that of a comparable single 'v', non-reinforced beam, 1-FV3a, and one-and-a-half times higher than that of a single 'v' reinforced beam, 3-FV3a. The load-deflection curves are illustrated in Figure 3.3.7..

Test series V5 - double 'v' beams 11-FV4a and 11-FV4b - The entire right v-section of both beams 11-FV4a and 11-FV4b failed in tension under loads of 4.68 kips and 4.15 kips respectively. As in test series V4, the left section was shifted to the centre and loaded to failure.

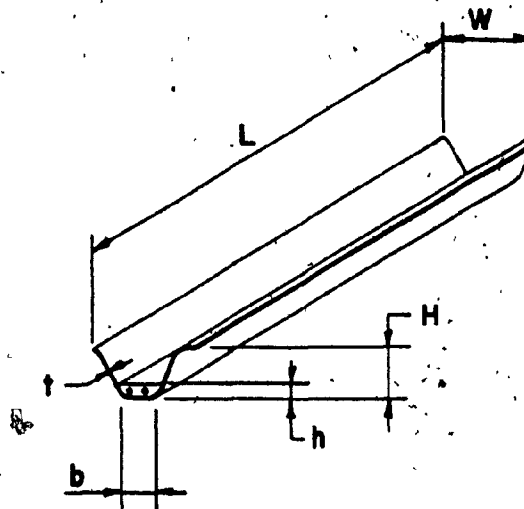
The results of this test series again revealed that double 'v' beams are much stronger than single 'v' beams. Comparing a double 'v' beam, 11-FV4a, to a single 'v' beam,

2-FV4a, shows a 67% difference in tensile strength. The load-deflection curves for both beams are shown in Figure 3.3.8.



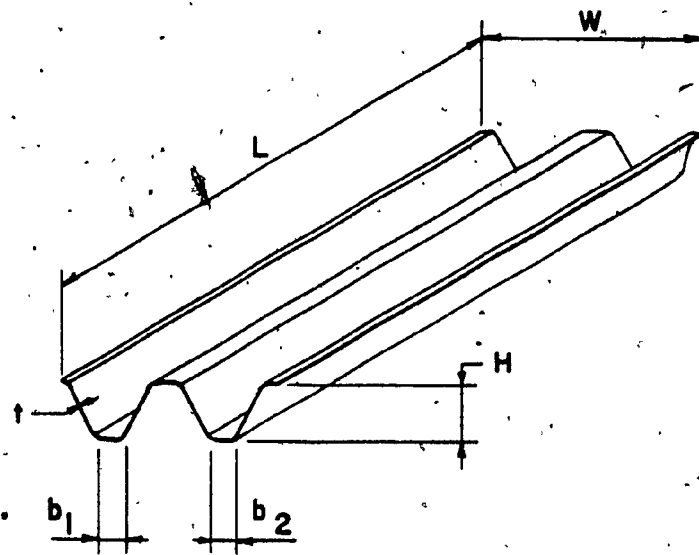
Test Series	Sample No.	L	W	b	H	t
VI	IFV3a.	10'-0"	14 1/2"	4 1/2"	7 3/4"	3/8"
VI	IFV3b.	10'-0"	14 1/2"	4 1/2"	7 3/4"	3/8"
V2	2FV4a.	12'-0"	14 1/2"	4 1/2"	7 3/4"	1/2"
V2	2FV4b.	12'-0"	14 1/2"	4 1/2"	7 3/4"	1/2"

Figure 3.3.1. Dimensions of single 'v' beams.



Test Series	Sample No.	L	W	b	H	h	t
V3	3FV3a.	10'-0"	14 $\frac{3}{4}$ "	4 $\frac{1}{2}$ "	7 $\frac{3}{4}$ "	2"	$\frac{3}{8}$ "

Figure 3.3.2. Dimensions of single 'V' beam with steel reinforcement
(2#3 bars - area = 0.22 in^2)



Test Series	Sample No.	L	W	H	b ₁	b ₂	t
V4	I0FV3a	10'-0"	30 1/2"	7 3/4"	4 1/2"	4 1/2"	3/8"
V4	I0FV3b.	10'- 0"	30 1/2"	7 3/4"	4 1/2"	4 1/2"	3/8"
V5	IIFV4a	12'- 0"	30 1/2"	7 1/2"	4 1/2"	4 1/2"	1/2"
V5	IIFV4b	12'- 0"	30 1/2"	7 1/2"	4 1/2"	4 1/2"	1/2"

Figure 3.3.3. Dimensions of double 'v' beams.

Table 3.3.1. Comparative results and equivalent uniform distributed loads (3rd stage)

Sample No.	Failure load P (kips)	Calculated load P (kips)	Equivalent uniform distributed load for 10'-0" span (tested)	
			γ_{f1}	kN/m
IFV3a.	1.55	1.68	0.32	4.68
IFV3b.	1.31	1.68	0.271	3.95
3FV3a	2.74	1.79	0.567	8.27
10FV3a	3.7825	3.40	0.782	11.42
10FV3b	3.75	3.40	0.774	11.35

Table 3.3.2. Comparative results and equivalent uniform distributed loads. (3rd stage)

Sample No.	Failure load P (kips)	Calculated load P (kips)	Equivalent uniform distributed load for 12' 0" span (tested)		Equivalent uniform load for 10'-0" span
			k/ft	kN/m	
2FV4a	1.555	1.79	0.266	3.89	0.388 5.662
2FV4b	1.555	1.79	0.266	3.89	0.388 5.662
IIFV4a	4.68	3.414	0.802	11.71	11.68 17.045
IIFV4b	4.15	3.414	0.711	10.38	11.036 15.119

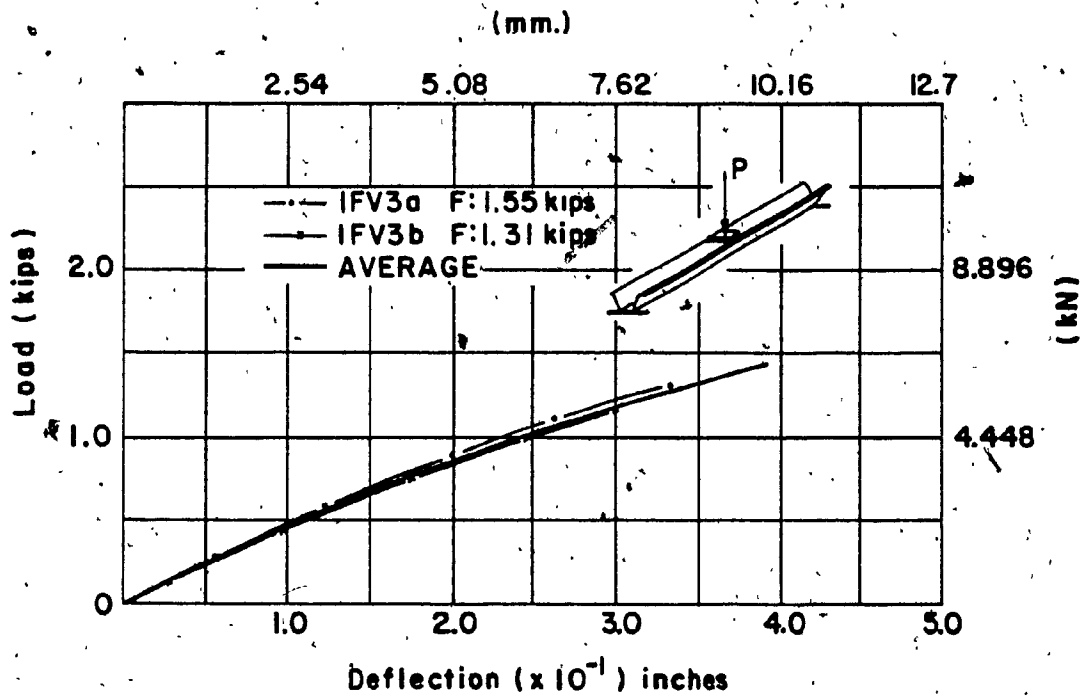


Figure 3.3.4 Load-Deflection curve

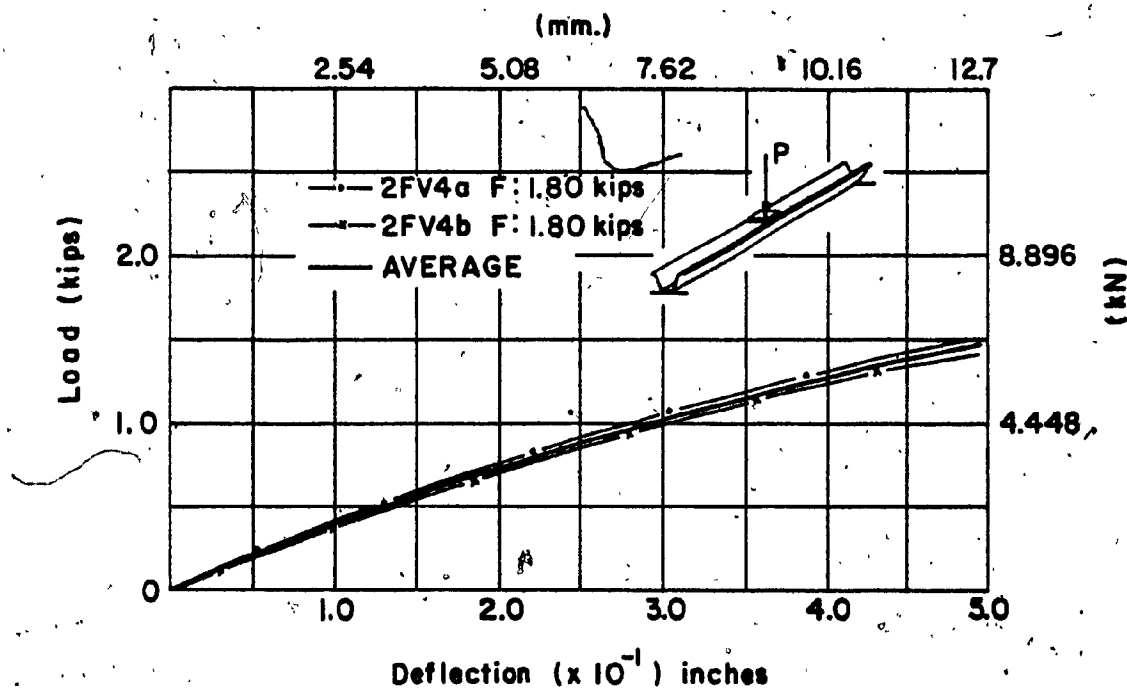


Figure 3.3.5. Load-Deflection curve.

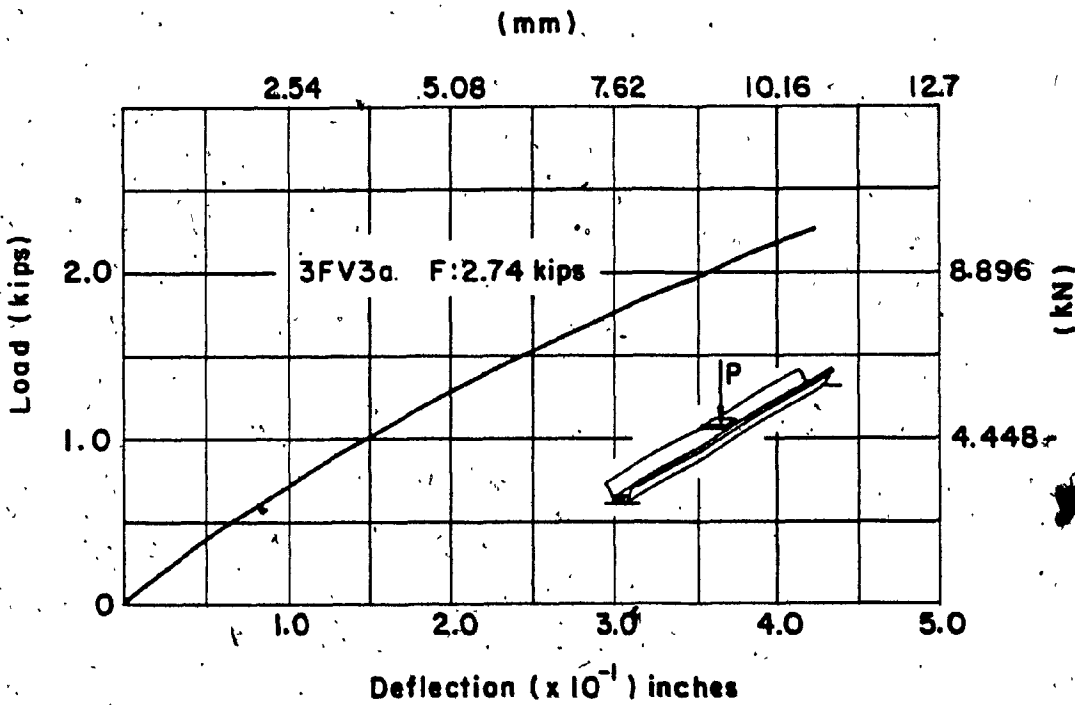


Figure 3.3.6. Load-Deflection curve.

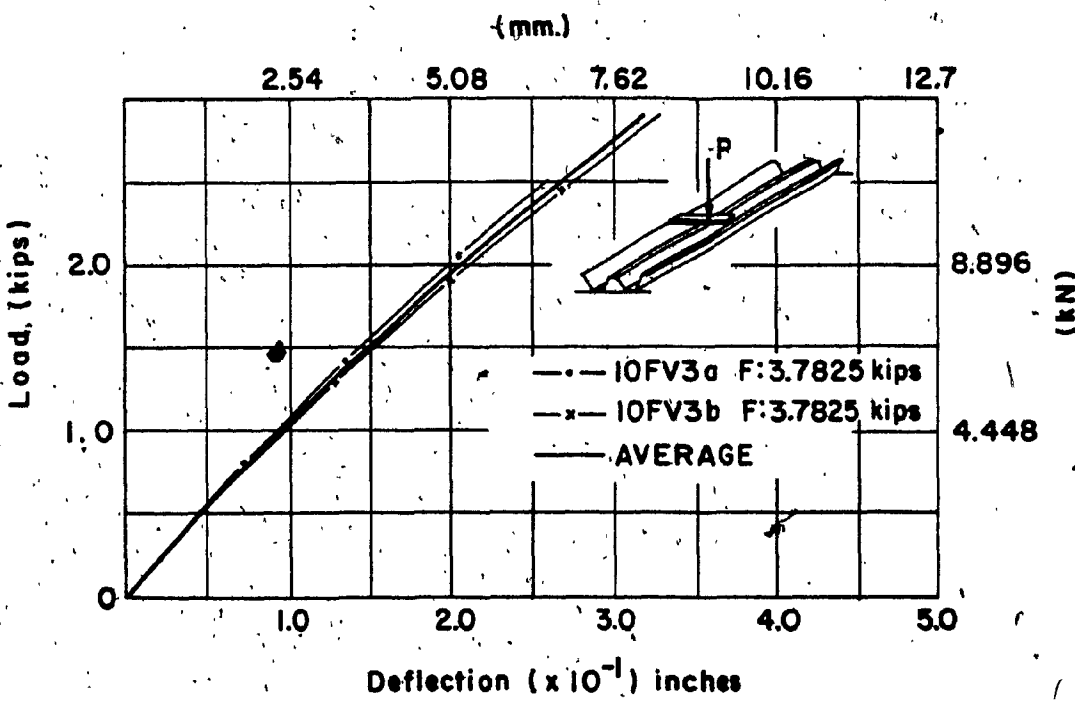


Figure 3.3.7. Load-Deflection curve.

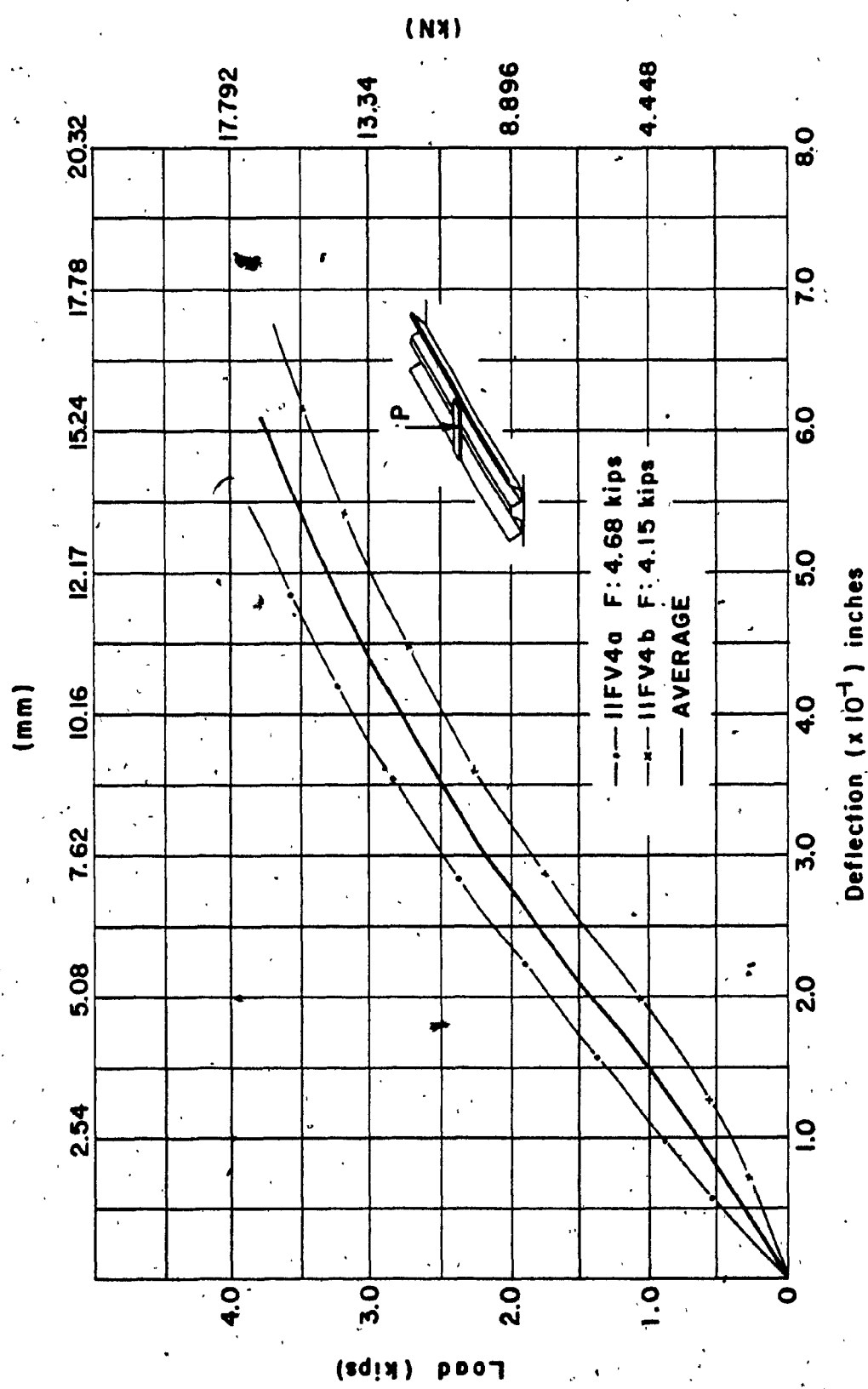


Figure. 3.3.8. Load-Deflection curve.

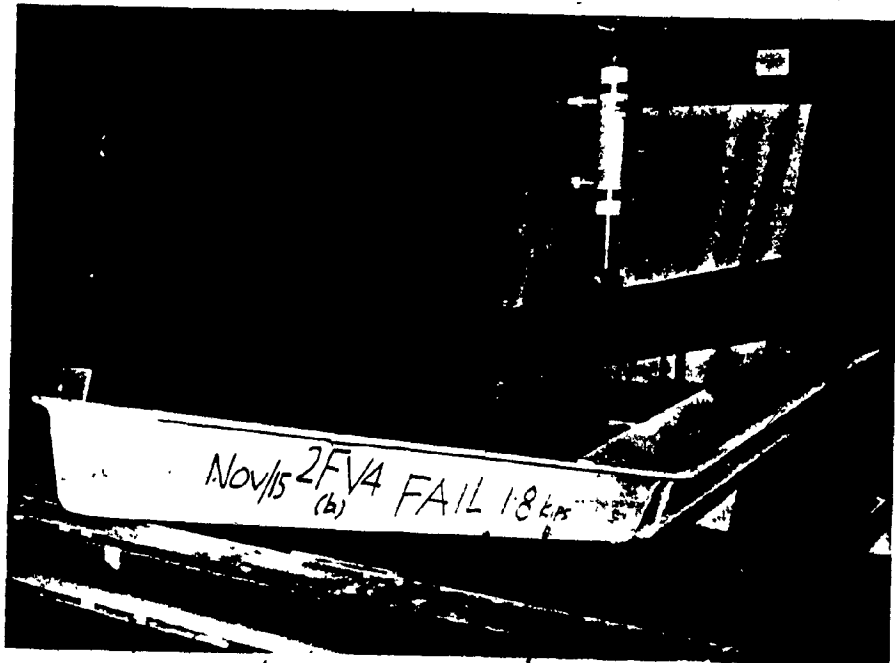


Figure 3.3.9. View of Beam 2FV4b (At failure).



Figure 3.3.10. View of testing set-up of Beam 3FV3a

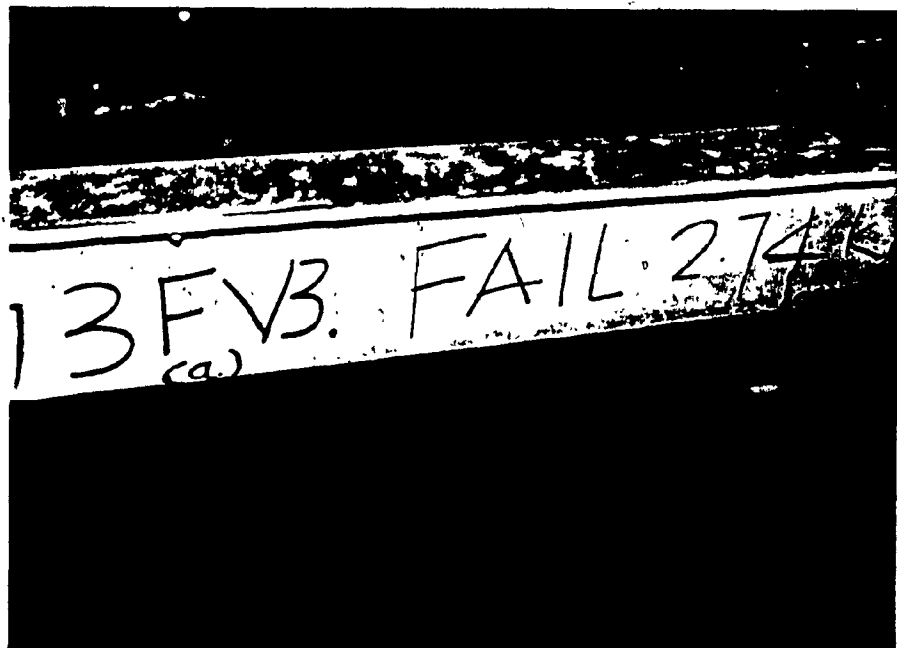


Figure 3.3.11. View of Beam 3FV3a (At failure)

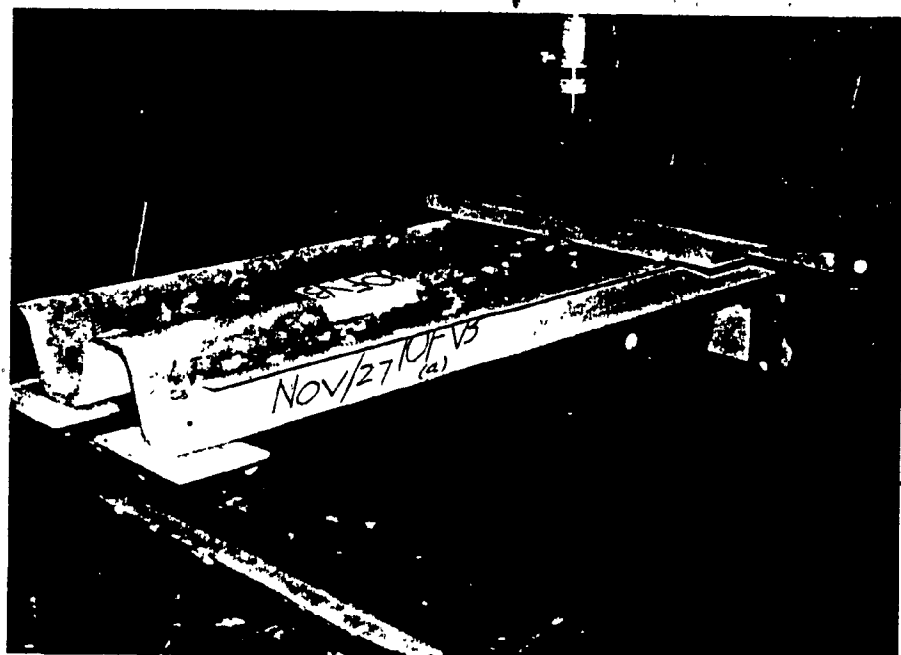


Figure 3.3.12. View of testing set-up of Beam 10FV3a

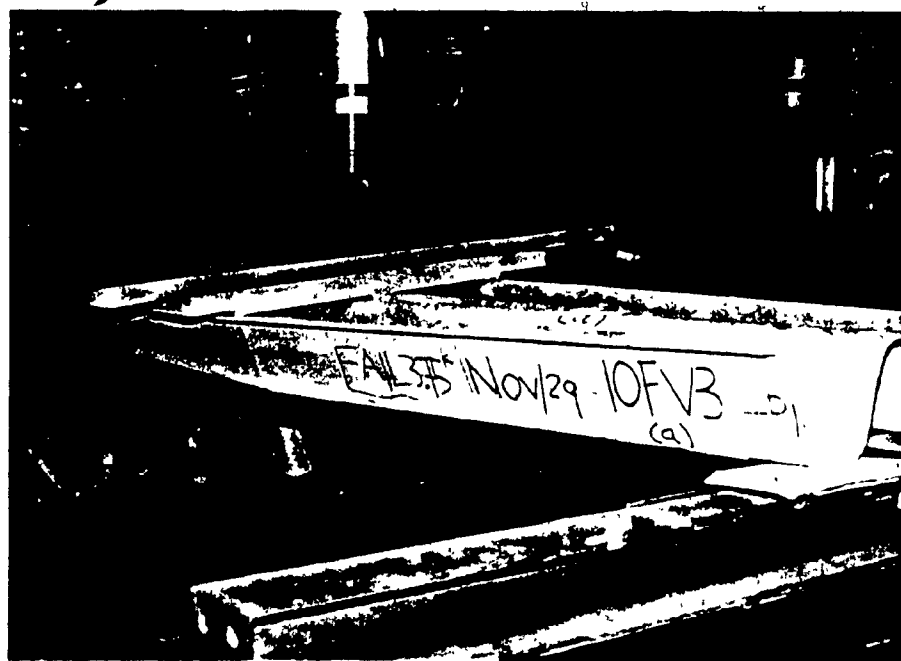


Figure 3.3.13. View of Beam IOFV3a (At failure of left V-Section).



Figure 3.3.14. View of Beam IOFV3a (After complete failure).

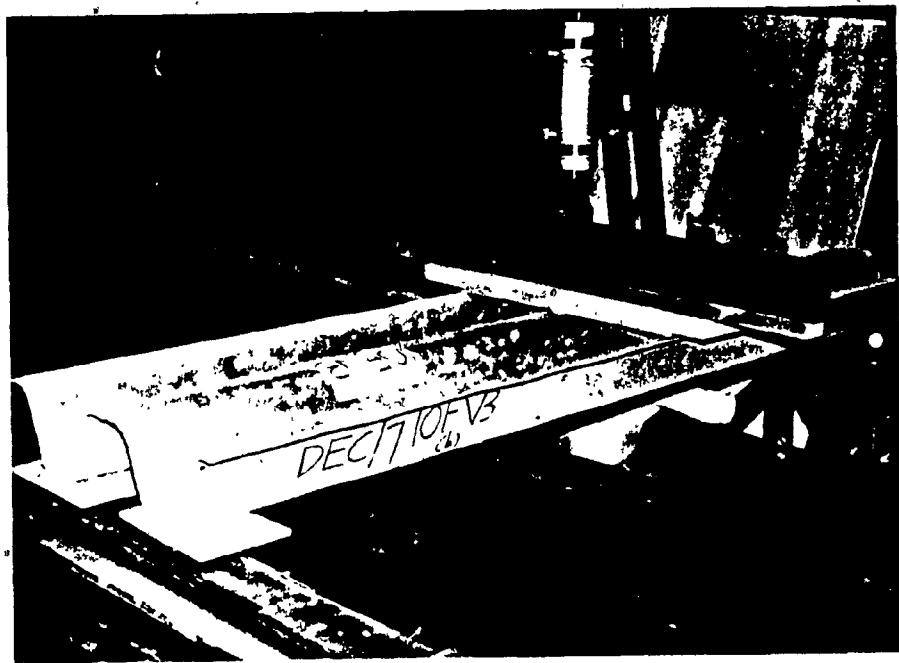


Figure 3.3.15. View of testing set-up of Beam IOFV3b.

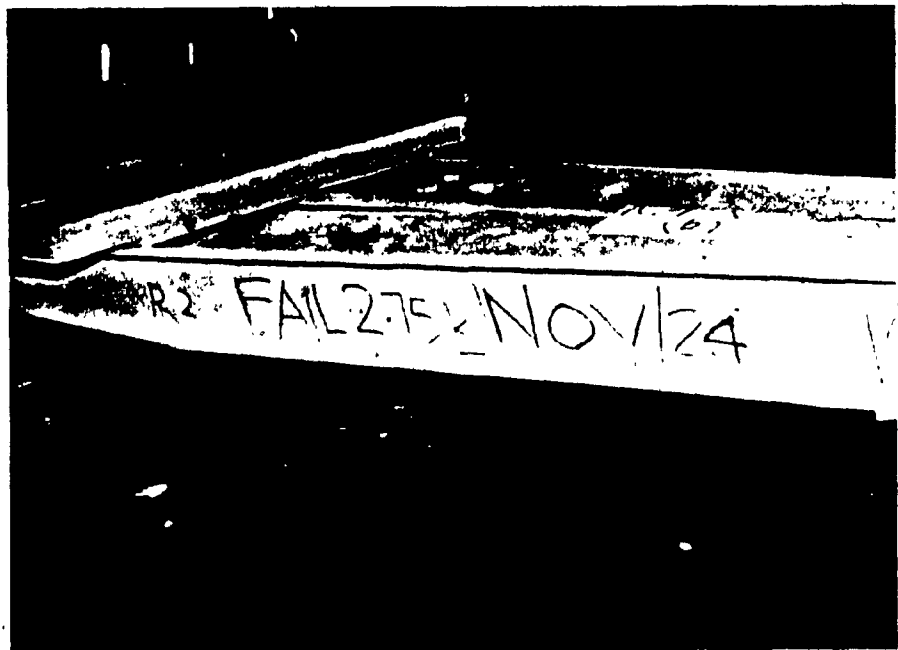


Figure 3.3.16. View of Beam IOFV3b (At failure of left V-Section)

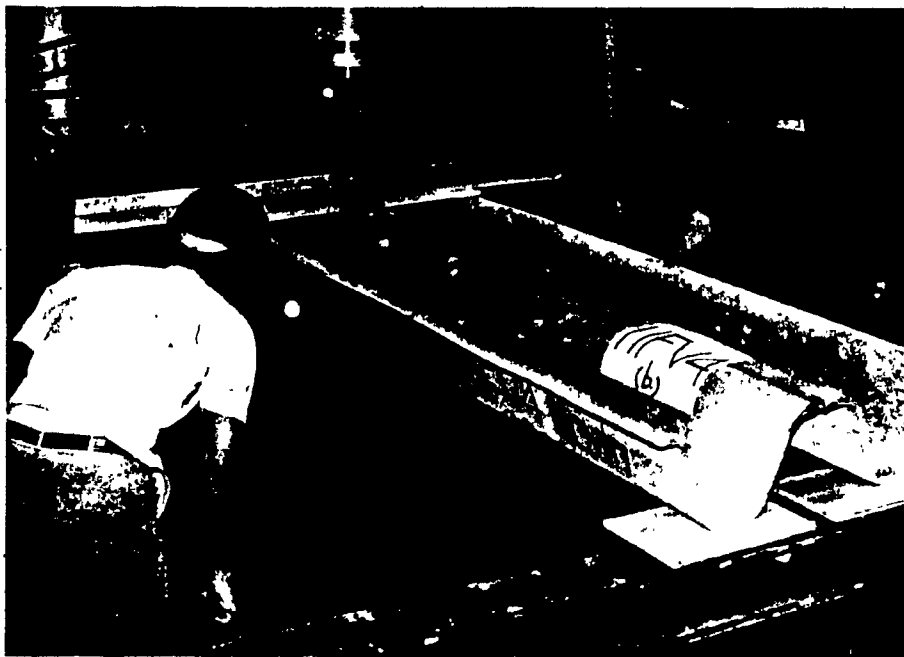


Figure 3.3.17. View of testing set-up of Beam II FV4 b.

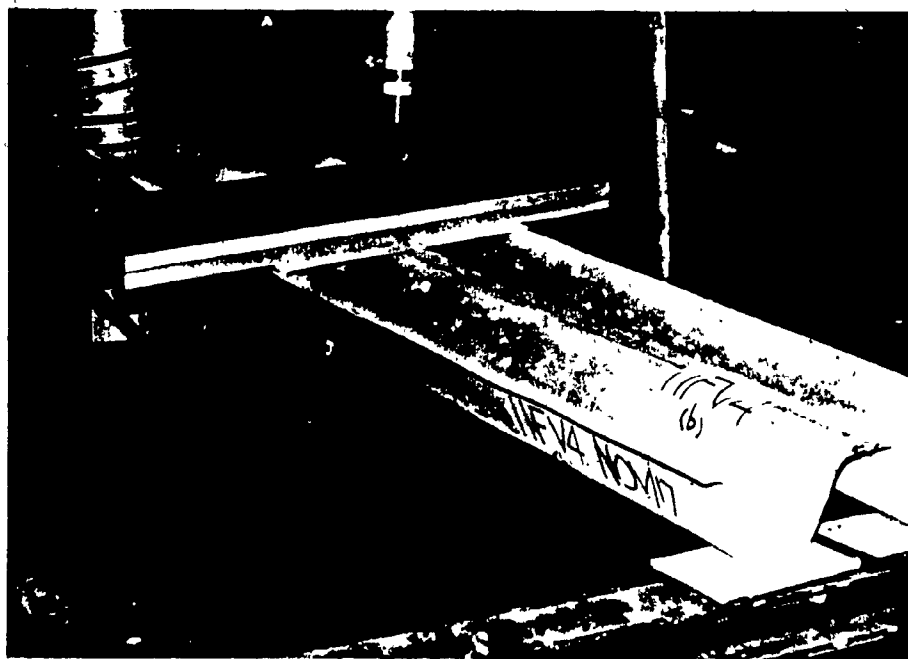


Figure 3.3.18. View of Beam II FV4 b (At failure of left V-Section)

3.4 Fourth Stage - Single 'v' Beam and Double 'v' Beam Assemblies with Attached Top Plates

The fourth stage consisted of testing beams made of (a) single 'v' element with attached top plate, (b) single 'v' element with top plate and steel reinforcement at the bottom, and (c) double 'v' elements with attached top plate. The top plates are made of densite, while the 'v' elements of apac.

The purpose of these tests was to establish the capacity of each beam assembly and to compare with beams made of 'v' elements with no top plates.

In this stage, test series V6, V7, V8, V9 and V10 were carried out. Test series V6 represented the testing of beams 5-FV3 and 5aFV3. Each beam consisted of a single 'v' element attached with a $\frac{1}{2}$ inch thick top densite plate as shown in Figure 3.4.1. Spots of epoxy were added, 4" apart to beam 5aFV3, in between the top plate and the top flanges of the v-section. The overall dimensions of both beams were 12'-0" long and 8" deep. The thickness of the asbestos-cement sheet of the v-section was 3/8 of an inch. Beams 6-FV4 and 6aFV4 of test series V7 were identical to beams 5-FV3 and 5aFV3 respectively with the exception that the thicknesses of the asbestos sheets of the v-sections were $\frac{1}{2}$ inch thick instead of 3/8" as shown in Figure 3.4.1. In test series V8, beams 7-FV4 and 7aFV4 as shown in Figure 3.4.2, were also identical to 5-FV3 and 5aFV3, but their bottom flanges were each strengthened with 2#3 bars embedded in early strength

portland cement. Only beam 12aFV3 was tested in test series V9. The beam consisted of two single 'v' elements glued together side by side and covered with a $\frac{1}{2}$ " thick densite plate as shown in Figure 3.4.3. Epoxy spots were also laid 7" apart in between the top flanges of the double 'v' beam and the top plate. Beam 13aFV4 of test series V10 was identical to beam 12aFV4 except that the thickness of the asbestos of the double 'v' section was $\frac{1}{2}$ " thick instead of 3/8" as was the case for the latter. Dimensions of beam 13aFV4 are shown in Figure 3.4.3. The testing arrangement is shown in Figure 2.5.1.

Test series V6 - single 'v' beams 5-FV3 and 5aFV3 with slab thicknesses 3/8" and top plates attached - Beams 5-FV3 failed in tension under a load of 1.555 kips, whereas beam 5aFV3 failed under a slightly higher load of 2.035 kips. Failure of both beams was caused by the cracking in tension of the bottom side of the v-section at midspan while the top plate broke at approximately one foot on each of the centre, as shown in Figure 3.4.10. The addition of epoxy spots to beam 5aFV3 resulted in a slight increase in strength as compared to beam 5FV3. The load-deflection curves are shown in Figure 3.4.4.

Test series V7 - single 'v' beams 6-FV3 and 6aFV4 with slab thicknesses 4/8" = 1/2" and top plates attached - As in the previous test series, failure of beams 6-FV4 and 6aFV4 was also caused by the cracking in tension of the bottom side of the v-section at midspan followed by the breaking of the top

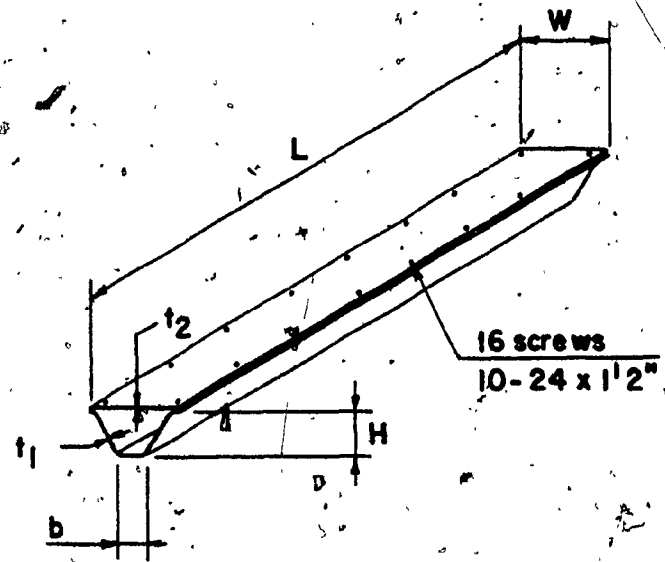
plates on each side of the centerline. Beam 6-FV4 failed under a load of 2.27 kips as indicated in Table 3.4.1. Beam 6aFV4 failed under a higher load of 3.12 kips because of the contribution of the epoxy to its overall strength. Comparing this test series to series V2 shows that with the addition of a top plate, the beam was able to sustain a larger load. The load capacity increased from 1.555 kips to 2.27 kips, or an increase in strength of 46%. Figure 3.4.5 shows the load-deflection curves of both beams.

Test series V8 - single 'v' beams 7-FV4 and 7aFV4 with top plates and steel bars at the bottom - The behaviour of both beams 7-FV4 and 7aFV4 under tensile loading was similar to beam 3-FV3a. In both cases, the beam failed due to the cracking of the v-section at the bottom and yield of the steel. The ultimate load for beam 7-FV4 was 4.15 kips and that of beam 7aFV4 was 3.905 kips. The epoxy spots were again responsible for the difference in strength. The load-deflection curves of both beams are shown in Figure 3.4.6.

Test series V9 - double 'v' beam 12aFV3 with top plate attached - The left v-section of beam 12aFV3 cracked in tension under a load of 3.7825 kips, but was still capable of carrying some load until complete failure occurred at a lower load than initially applied. Total failure of the beam was caused by the tearing of the two v-sections at midspan and subsequent crashing of the top plate at two locations as shown in Figure 3.4.18. Beam 12aFV3 failed in a similar way to beams 5-FV3 and 5aFV3 of test series V6. It is also

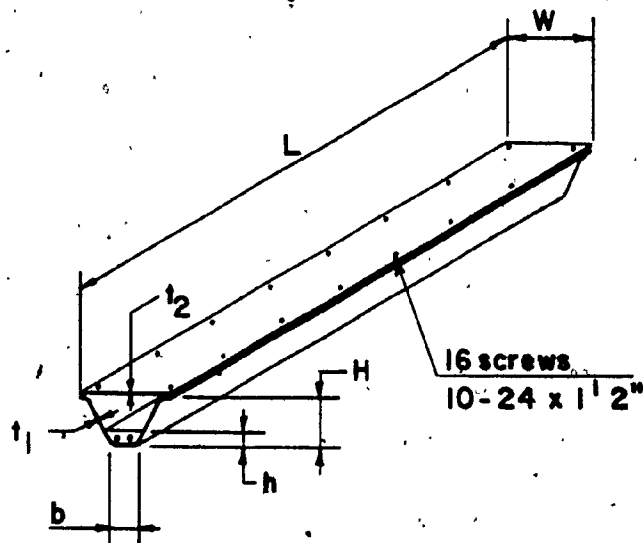
noteworthy that beam 12aFV3 and the comparable double 'v' beams without top plates of test series V5 failed under almost similar loads. This indicates that the top plates does improve significantly the strength of double 'v' beams. The load-deflection curve is shown in Figure 3.4.7.

Test series V10 - double 'v' beam 13aFV4 with top plate attached - The sequence of failure of beam 13aFV4 was identical to beam 12aFV3 in the previous test series. The right v-section was the first to crack under a load of 4.40 kips and was still able to carry more load. Beam 13aFV4 failed thereafter under a relatively small load, as shown in Figure 3.4.20. The comparison between beam 13aFV4 and double 'v' beams without top plates of test series V5 proved that the beam capacity is governed by tension. The load-deflection curve is given in Figure 3.4.8.



Test Series	Sample No.	L	W	b	H	t ₁	t ₂
V6	5FV3	12'-0"	15 3/4"	4 1/2"	8"	3/8"	1/2"
V6	5aFV3	12'-0"	15 3/4"	4 1/2"	8"	3/8"	1/2"
V7	6FV4	12'-0"	15 3/4"	4 1/2"	8"	1/2"	1/2"
V7	6aFV4	12'-0"	15 3/4"	4 1/2"	8"	1/2"	1/2"

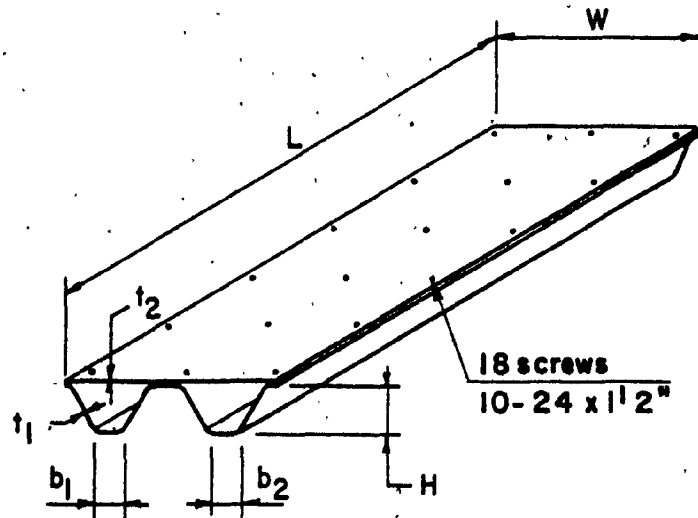
Figure 3.4.1. Dimensions of single 'V' beams with top plates.



Test Series	Sample No.	L	W	H	b	h	t ₁	t ₂
V8	7FV4	12'-0"	15 $\frac{3}{4}$ "	8"	4 $\frac{1}{2}$ "	1 $\frac{3}{4}$ "	1/2"	1/2"
V8	7aFV4*	12'-0"	15 $\frac{3}{4}$ "	8"	4 $\frac{1}{2}$ "	1 $\frac{3}{4}$ "	1/2"	1/2"

* With spots of epoxy

Figure 3.4.2. Dimensions of single V beams with top plates and steel reinforcement: (2# 3 bars - area = 22 in²)



Test Series	Sample No.	L	W	H	b ₁	b ₂	t ₁	t ₂
V9	12aFV3	12'-0"	32"	8"	4 1/2"	4 1/2"	3/8"	1/2"
V10	13aFV4	12'-0"	32"	8"	4 1/2"	4 1/2"	1/2"	1/2"

Figure 3.4.3. Dimensions of double 'v' beams with top plates.

Table 3.4.1. Comparative results and equivalent uniform distributed loads. (4th. stage)

Sample No.	Failure load P (kips)	Calculated load P (kips)	Equivalent uniform distributed load for 12'-0" span (tested)		k/f_f	Equiv. uniform load for 10'-0" span(calculated)
			k/ft	kN/m		
5FV3	1.555	1.77	0.266	3.89	0.388	5.662
5aFV3	1.80	1.77	0.308	4.50	0.449	6.553
6FV4	2.27	2.27	0.389	5.68	0.567	8.275
6aFV4	3.12	2.27	0.535	7.80	0.779	11.368
7FV4	4.15	2.934	0.711	10.38	1.036	13.119
7aFV4	3.905	2.934	0.669	9.77	0.973	14.229
12aFV3	3.7825	3.525	0.648	9.463	0.944	13.777
13aFV4	4.40	4.50	0.754	11.00	1.098	16.024

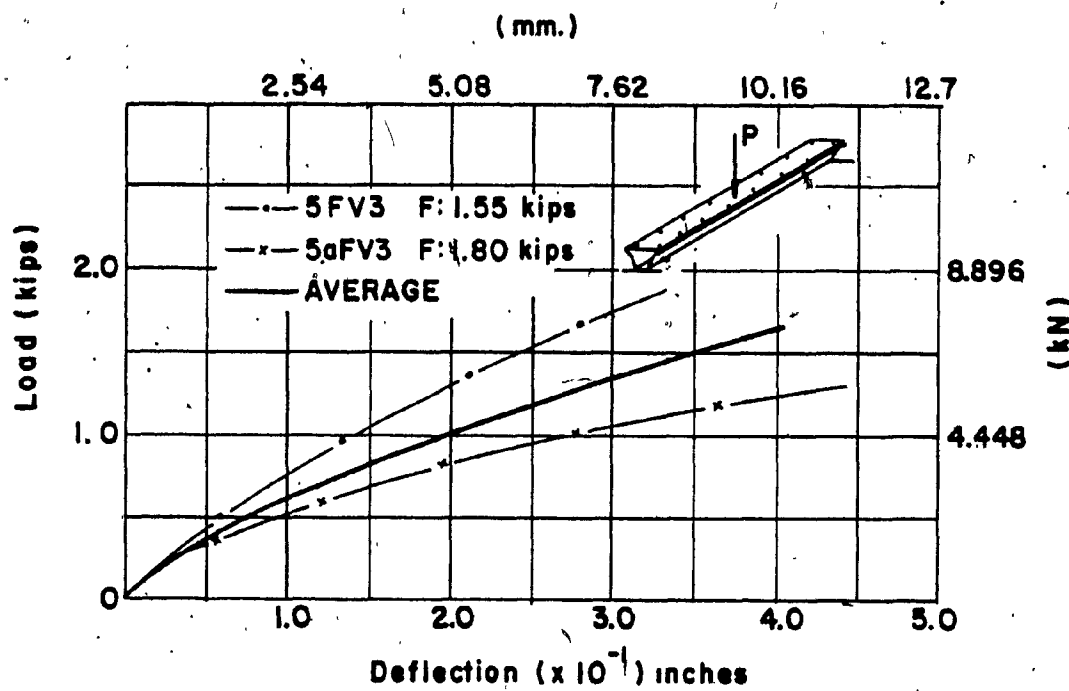


Figure 3.4.4 Load-Deflection curve

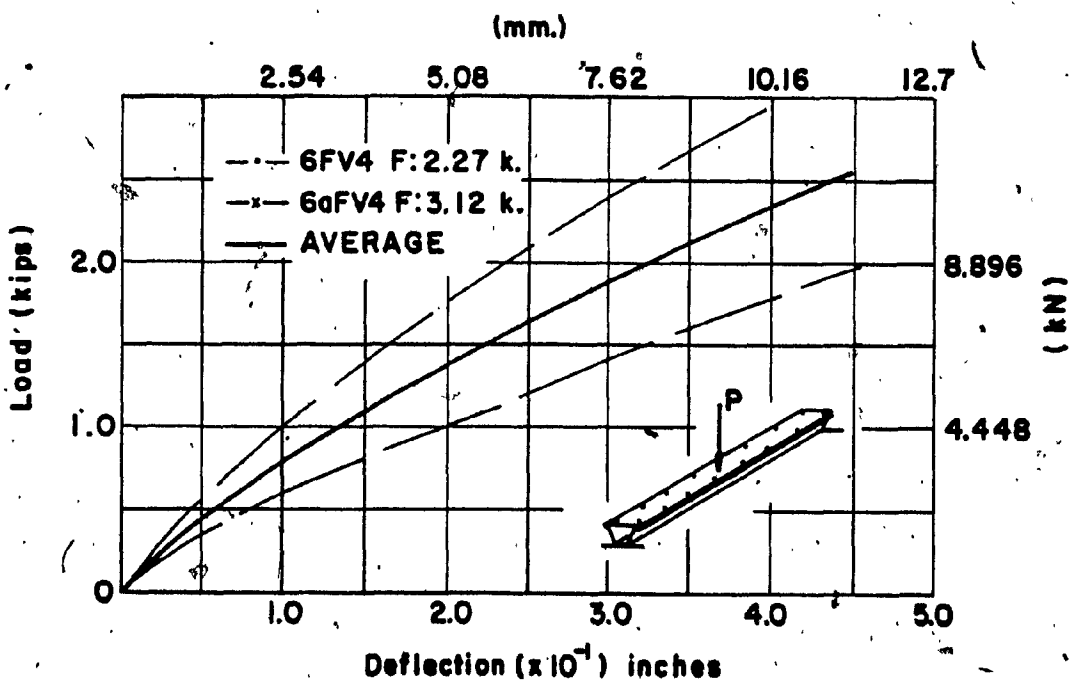


Figure 3.4.5 Load-Deflection curve.

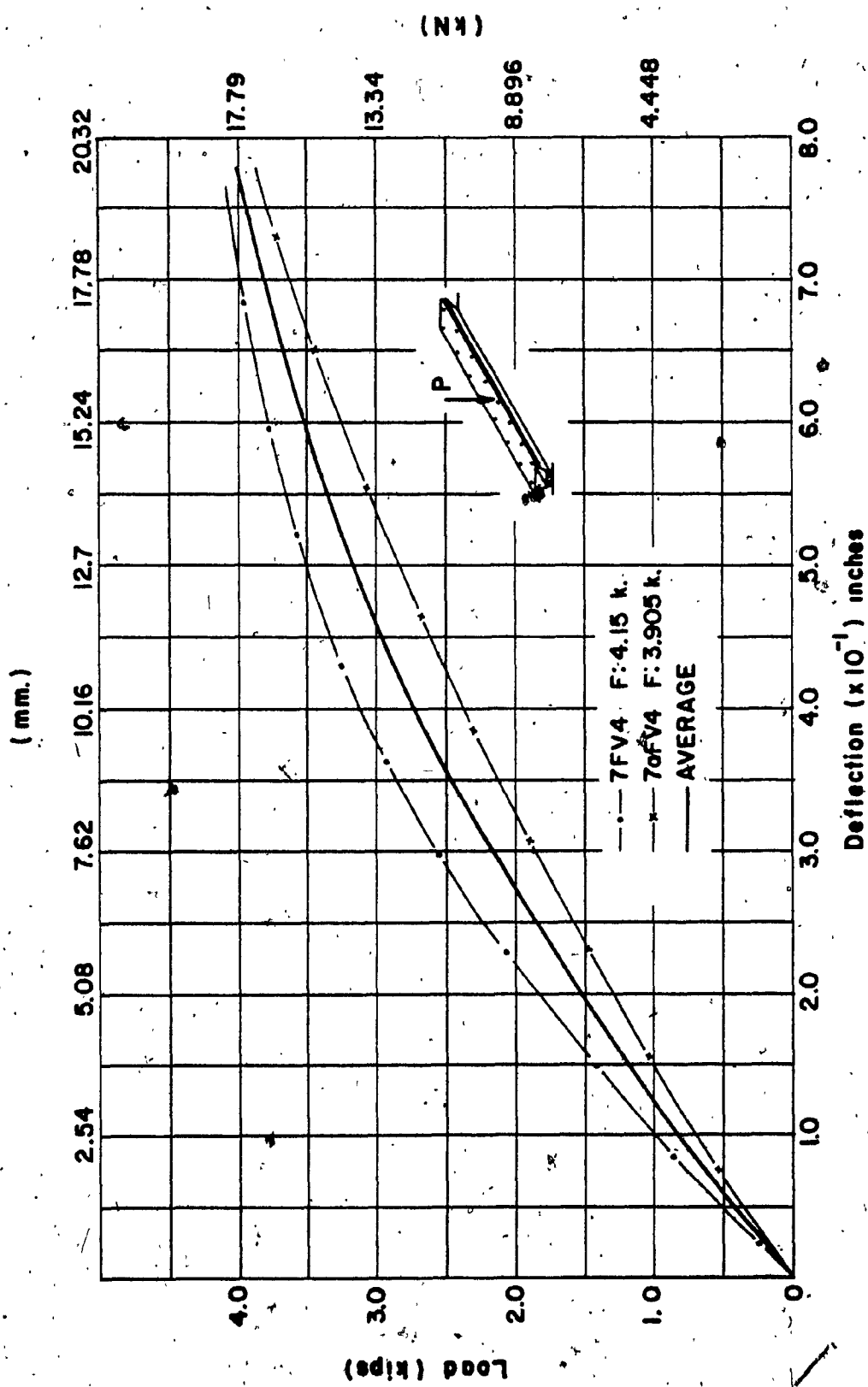


Figure 3.4.6. Load-Deflection curve.

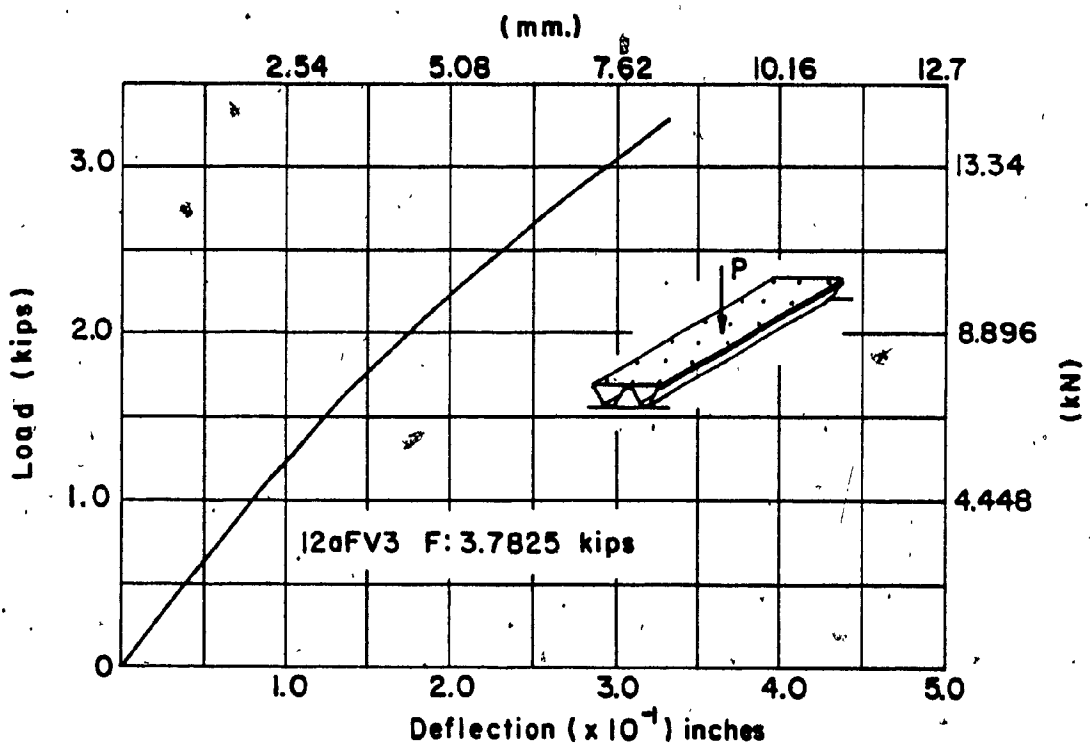


Figure 3.4.7 Load-Deflection curve

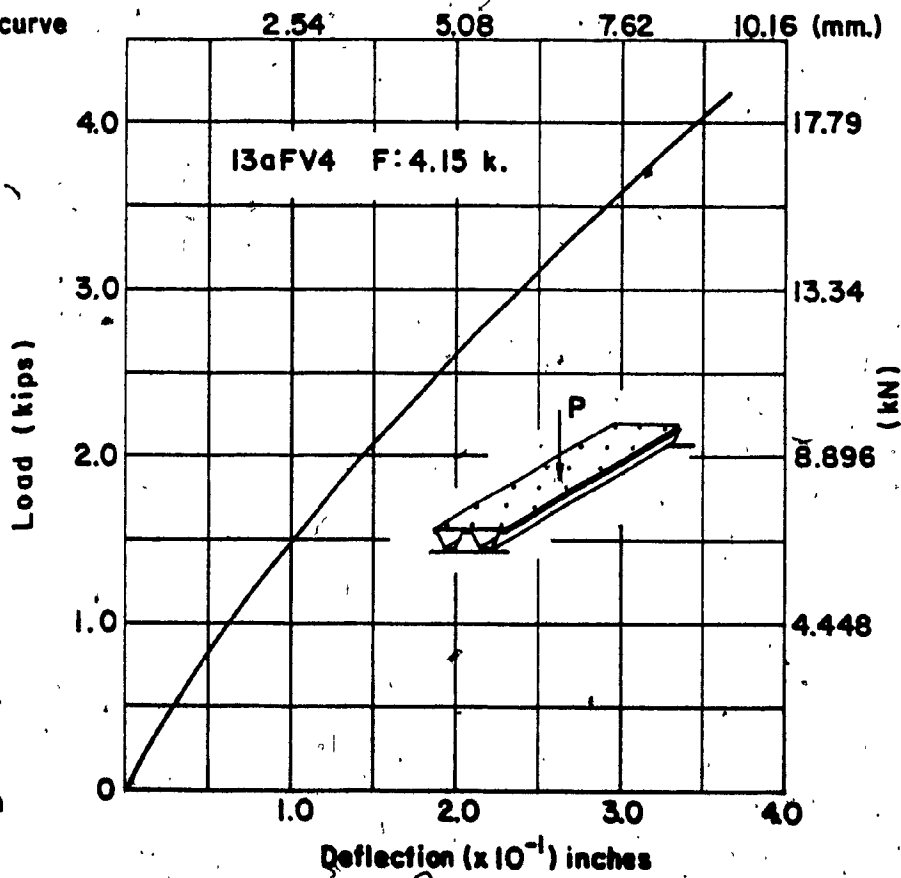


Figure 3.4.8.
Load-Deflection
curve.

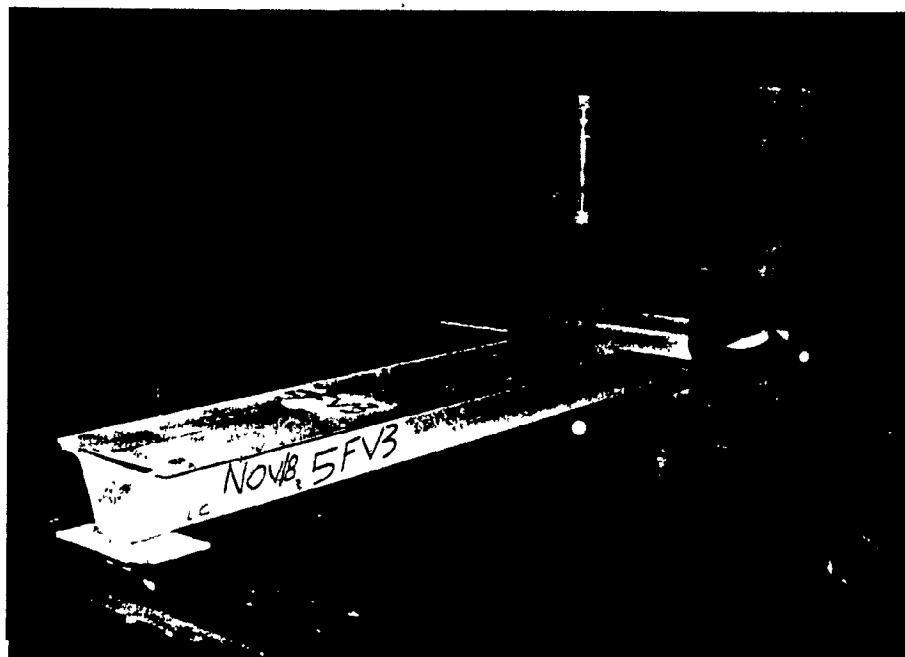


Figure 3.4.9. View of testing set-up of Beam 5FV3.



Figure 3.4.10. View of Beam 5FV3 (At failure)

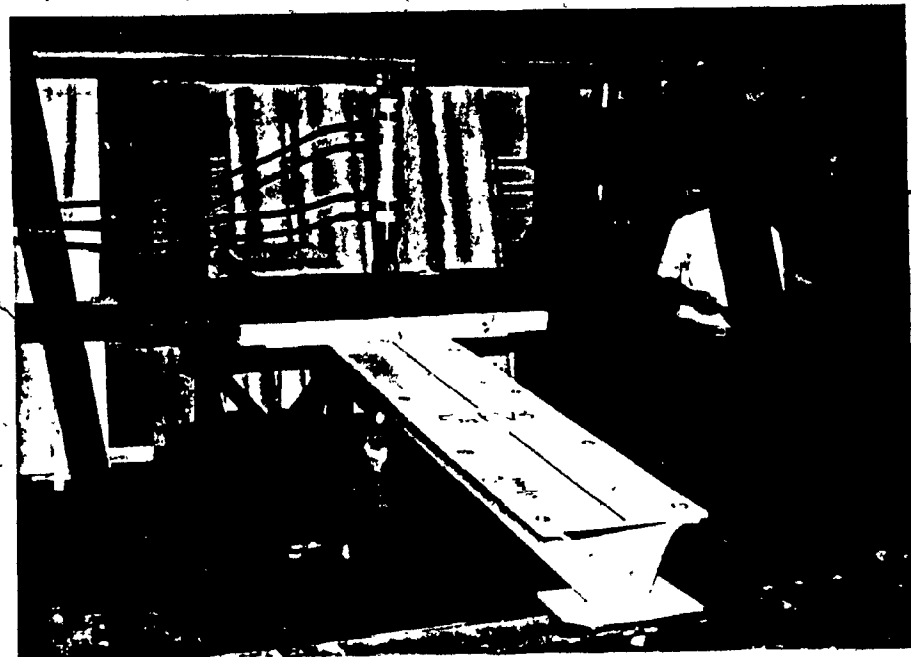


Figure 3.4.11. View of testing set-up of Beam 5aFV3

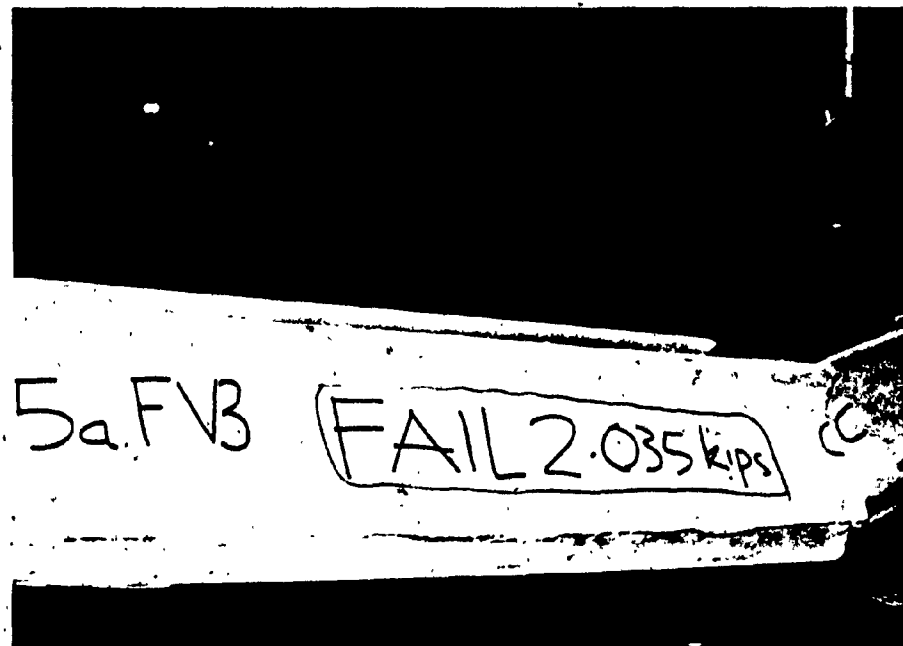


Figure 3.4.12. View of Beam 5aFV3 (At failure.)

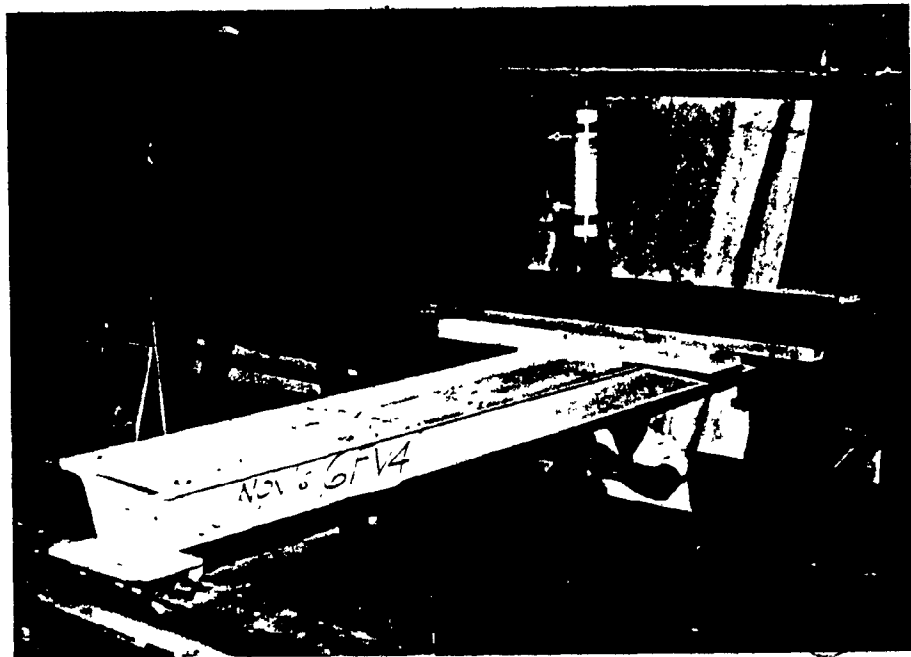


Figure 3.4.13. View of testing set-up of Beam 6FV4



Figure 3.4.14. View of Beam 6FV4 (At failure)

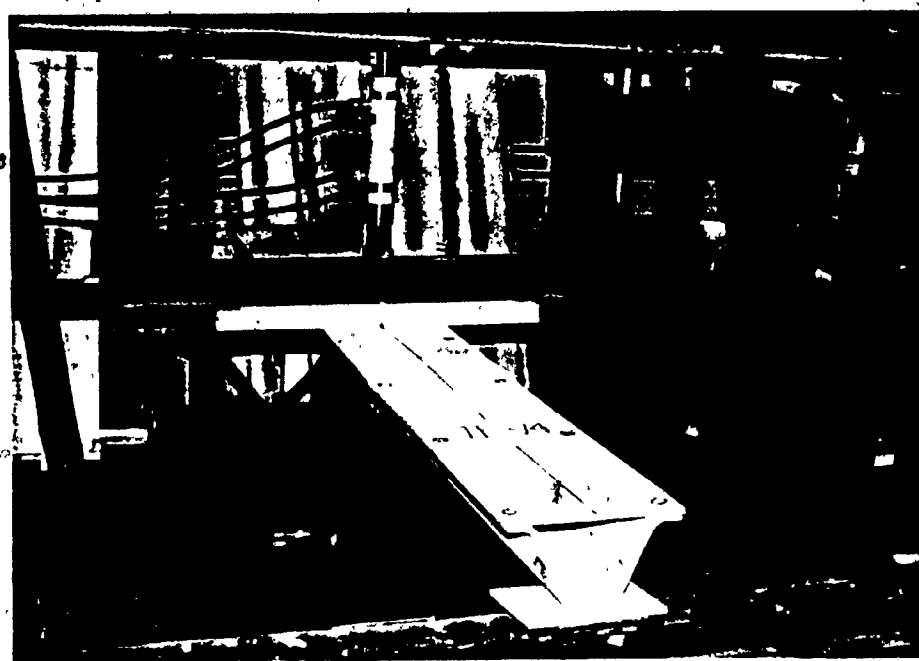


Figure 3.4.15. View of testing set-up of Beam 7FV4

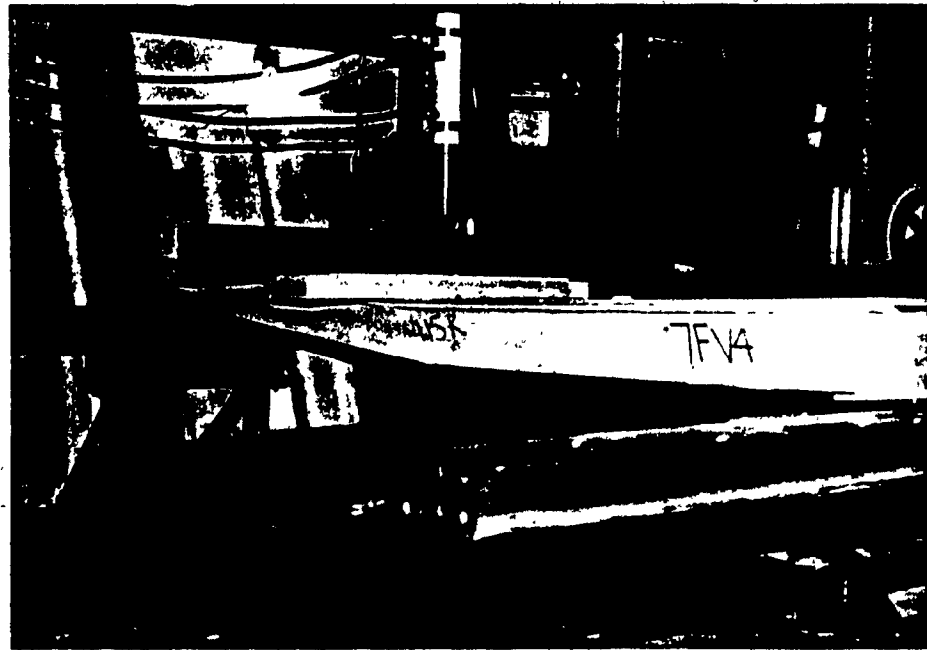


Figure 3.4.16 View of Beam 7FV4 (At failure)

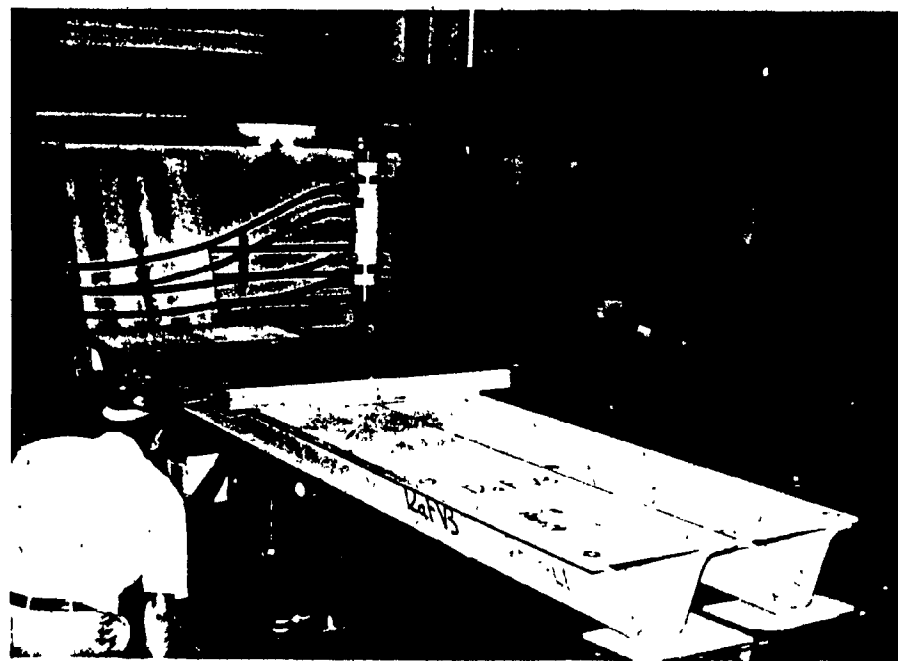


Figure 3.4.17. View of testing set-up of Beam I2aFV3



Figure 3.4.18. View of Beam I2aFV3 (At failure).

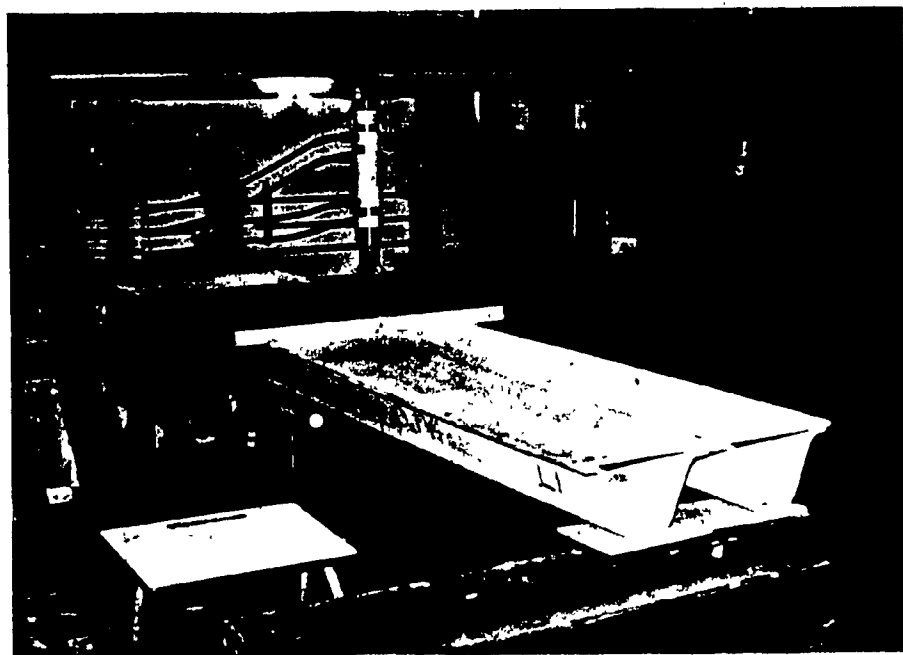


Figure 3.4.19. View of testing set-up of Beam 13aFV4

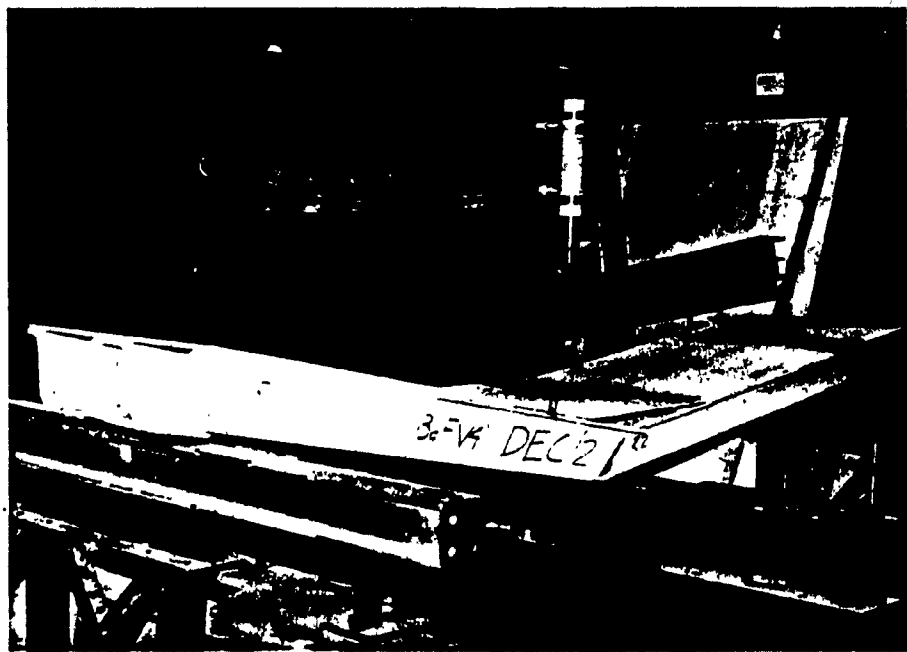


Figure 3.4.20. View of Beam 13aFV4.(At failure).

3.5 Fifth Stage - Beams Made of Single 'v' Elements and Double 'v' Elements Loaded in Floor Plane

In the fifth stage, single 'v' beams and double 'v' beams were tested as beams in horizontal plane as shown in Figures 3.5.3 and 3.5.4. The purpose of this test series was to establish horizontal carrying capacity as it may be required to supporting wall between shear walls under horizontal forces due to wind, earthquake or flood.

Test series V11, V12, V13 and V14 were performed in this stage. Test series V11 represented the testing of single 'v' beam 8-FV3(a). It measured 10'-0" long and 7 $\frac{1}{4}$ " deep as shown in Figure 3.5.1. Single 'v' beams 9-FV3(a) and 9-FV4(b) were tested in series V12. Each beam was 12'-0" long and 7 $\frac{1}{4}$ " deep as indicated in Figure 3.5.1. A test was also performed on double 'v' beam 14-FV3 in test series V13 which had a length of 12'-0" and depth of 7 $\frac{1}{4}$ " as given in Figure 3.5.2. Test series V14 was carried out on double 'v' beams 15-FV3(a) and 15-FV3(b). They both measured 12'-0" long and 7 $\frac{1}{4}$ " deep as shown in Figure 3.5.2.

All the beam samples in this stage were tested as simply supported. Each beam was held firmly in between timber formers as shown in Figures 3.5.3 and 3.5.4. Load was applied on the top of the middle former. In addition, some samples were restrained at the centre against sidesway and torsion by means of horizontal ties.

Test series V11 - single 'v' beam 8-FV3a with timber formers -

Beam 8-FV3a failed under a load of 0.89 kips. Failure occurred when the beam split at midspan, flush with the middle timber former. Twisting of the beam started under a 0.45 kip load and increased with load until failure occurred.

The beam failed under both tension and torsion and as a result, larger deflections were obtained under small loads as indicated by the load-deflection curve of Figure 3.5.5.

Test series V12-single 'v' beams 9-FV4a and 9-FV4b with timber formers - As in the previous test series, beam 9-FV4a failed under a combination of tension and torsion under a load of 0.94 kips. Beam 9-FV4b and subsequent panels were tested with horizontal ties to prevent twisting of the beams.

The failure of beam 9-FV4b was caused by the tearing of the asbestos at the bottom (midspan) under a load of 1.55 kips.

The load-deflection curves of both beams are shown in Figure 3.5.6.

Test series V13-double 'v' beam 14-FV3 with timber formers -

Beam 14-FV4 failed at midspan and was caused by the cracking in tension of the lower part of the two v-sections. Prior to failure, the joint between the two sections opened to approximately $\frac{1}{2}$ of an inch. The failure load was 2.27 kips.

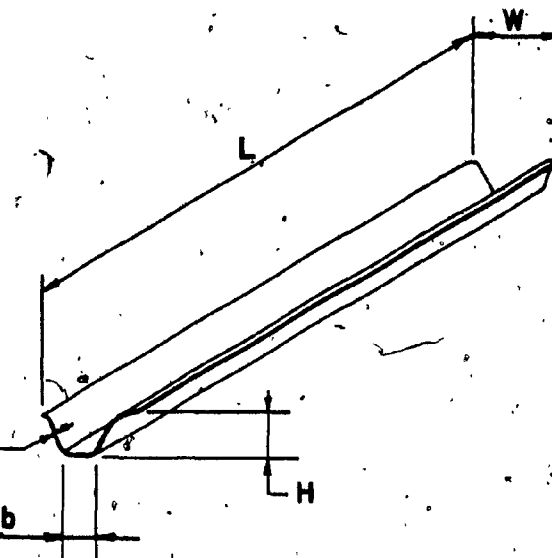
Figure 3.5.7 shows the load-deflection curve of beam 14-FV3.

Test series V14-double beams 15-FV4(a) and 15-FV4(b) with timber formers -

The sequence of failure was identical for both beams. Main cracks on the lower part of the top

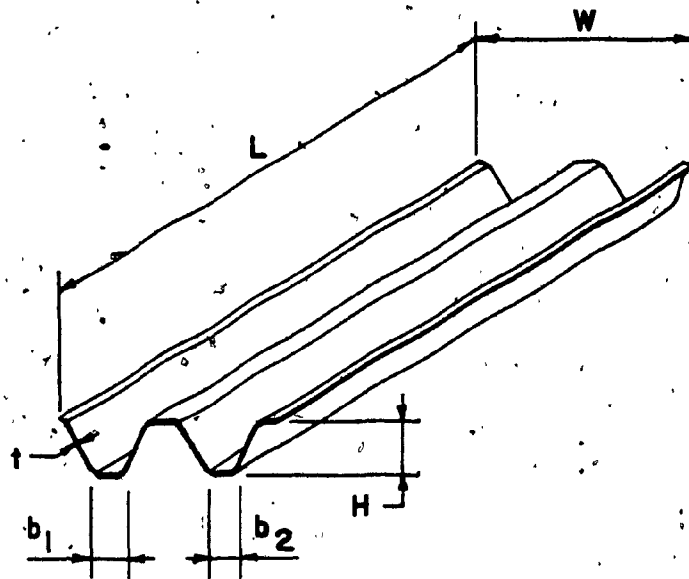
v-section were first observed, and at the same time the joint between the two sections started to open. Under increment of load, the joint continued to open until the failure of the lower part of both sections.

After the separation of the joint, each panel was working separately under the load, resulting in the failure in tension of both sections. The failure load for beam 15-FV4(a) was 3.21 kips while beam 15-EV4(b) failed under a lower load of 2.975 kips. The load-deflection curves of both beams are shown in Figure 3.5.8.



Test Series	Sample No.	L	W	b	H	t
VII	8FV3a	10'-0"	14 1/2"	4 1/2"	7 3/4"	3/8"
VI2	9FV4a	12'-0"	14 1/2"	4 1/2"	7 3/4"	1/2"
VI2	9FV4b	12'-0"	14 1/2"	4 1/2"	7 3/4"	1/2"

Figure 3.5.1. Dimensions of single 'v' beams



Test Series	Sample No.	L	W	H	b ₁	b ₂	t
VI3	14FV3	10'-0"	30 $\frac{1}{2}$ "	7 $\frac{3}{4}$ "	4 $\frac{1}{2}$ "	4 $\frac{1}{2}$ "	$\frac{3}{8}$ "
VI4	15FV4a	12'-0"	31 $\frac{1}{2}$ "	7 $\frac{3}{4}$ "	4 $\frac{1}{2}$ "	4 $\frac{1}{2}$ "	$\frac{1}{2}$ "
VI4	15FV4b	12'-0"	31 $\frac{1}{2}$ "	7 $\frac{3}{4}$ "	4 $\frac{1}{2}$ "	4 $\frac{1}{2}$ "	$\frac{1}{2}$ "

Figure 3.5.2. Dimensions of double 'v' beams

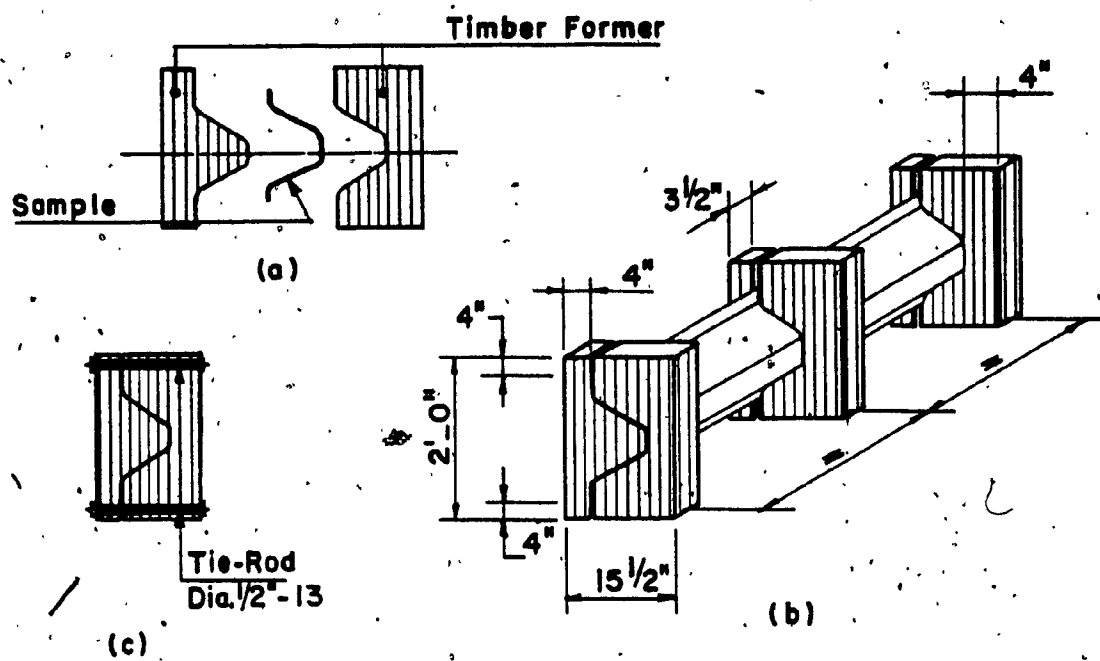


Figure 3.5.3. Horizontal loading arrangement for single 'V' element

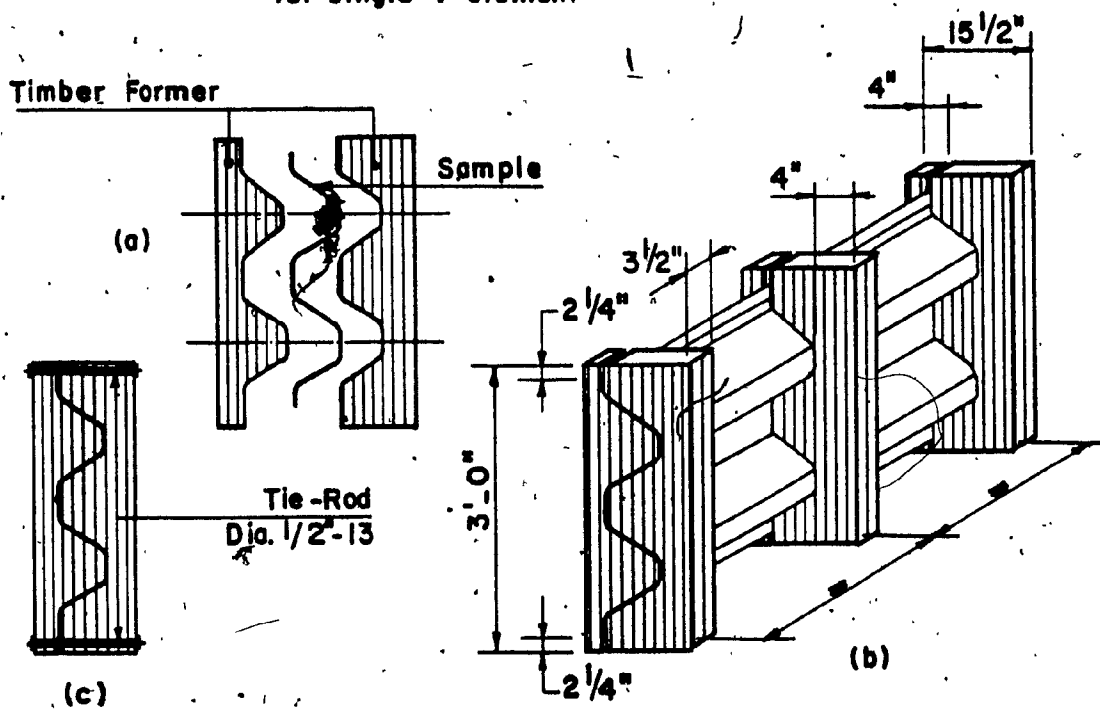


Figure 3.5.4. Horizontal loading arrangement for double 'V' element.

Table 3.5.1 Comparative results and equivalent uniform distributed loads. (5th stage)

Sample No.	Failure load P (kips)	Calculated load P (kips)	Equivalent uniform distributed load for 10'-0" span (tested)	
			k/ft	kN/m
8FV3a	0.89	2.96	0.164	2.685
14FV3			0.469	6.847

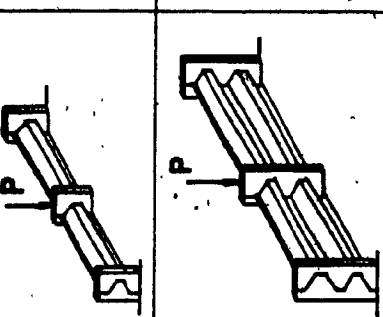
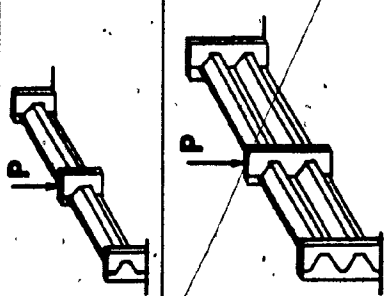


Table. 3.5.2. Comparative results and equivalent uniform distributed loads. (5th. stage)

Sample No.	Failure load P (kips)	Calculated load P (kips)	Equivalent uniform distributed load for 12' - 0" span (tested)		Equiv. uniform load for 10' - 0" span(calculated)	
			k/ft	kN/m	k/ft	kN/m
9FV4a	0.94	2.453	0.161	2.35	0.235	3.429
9FV4b	1.35	2.453	0.266	3.878	0.387	5.648
15FV4a	3.21	0.550		8.03	0.801	11.698
15FV4b	2.975		0.510	7.443	0.743	10.841



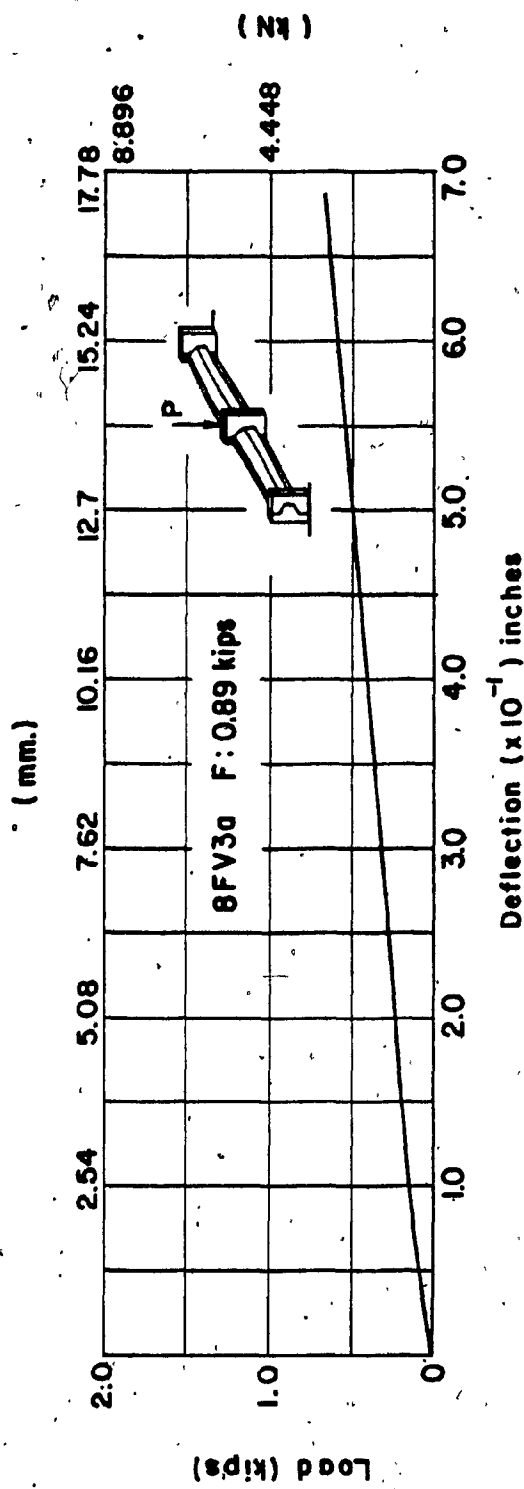


Figure 3.5.5 Load-Deflection curve

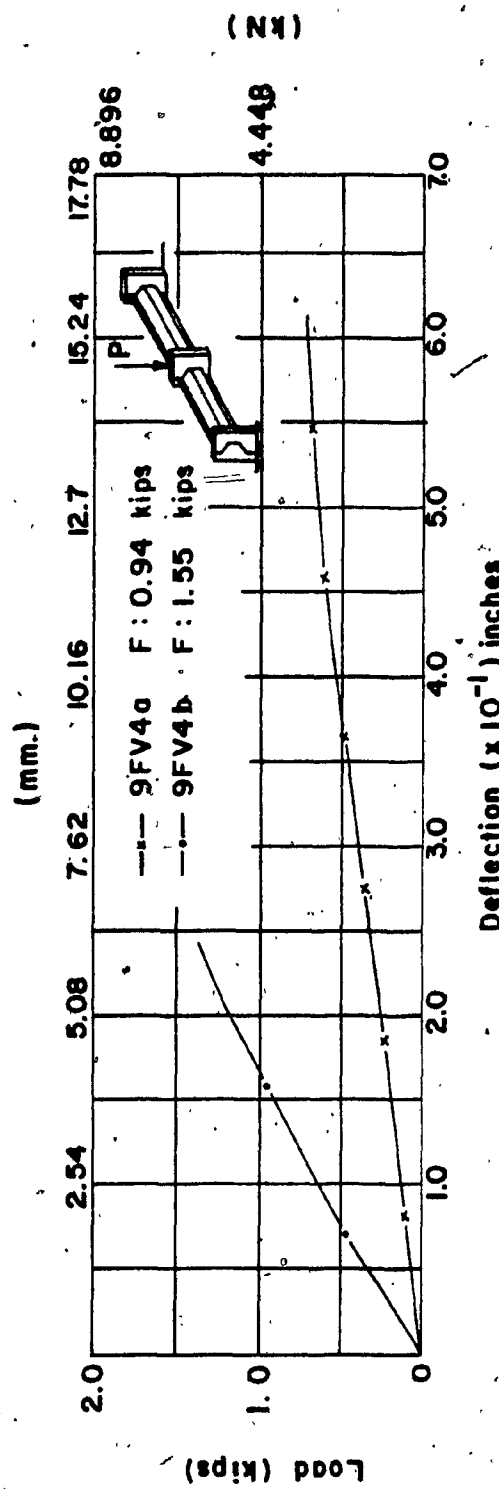


Figure 3.5.6 Load-Deflection curve

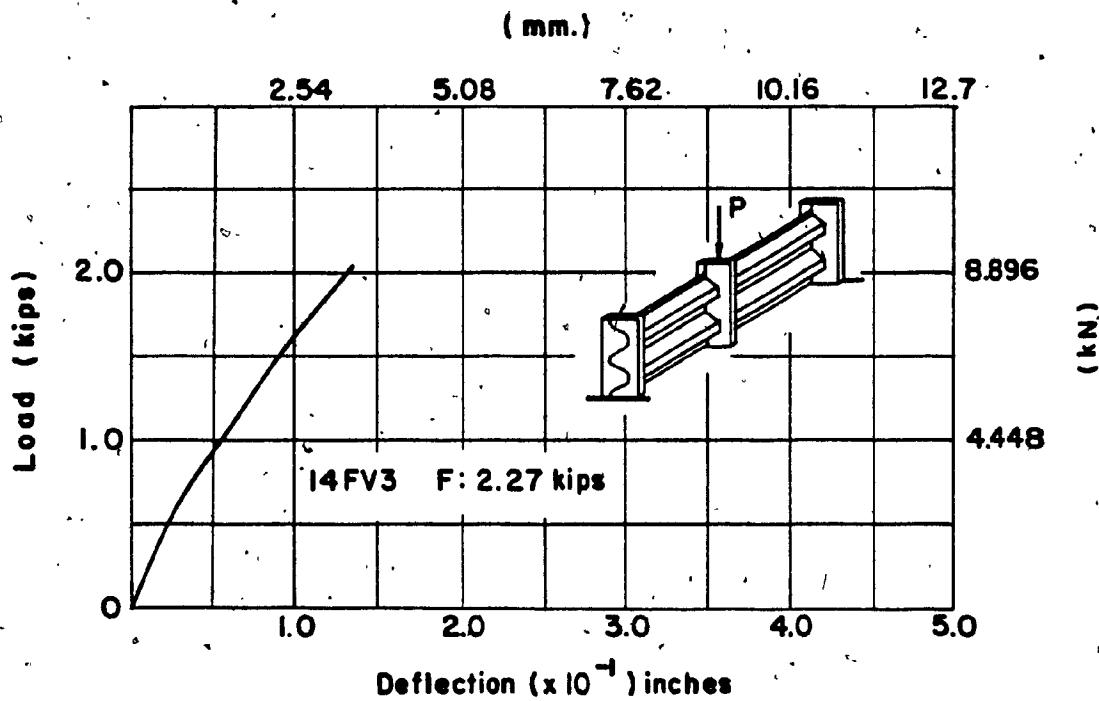


Figure 3.5.7 Load-Deflection curve

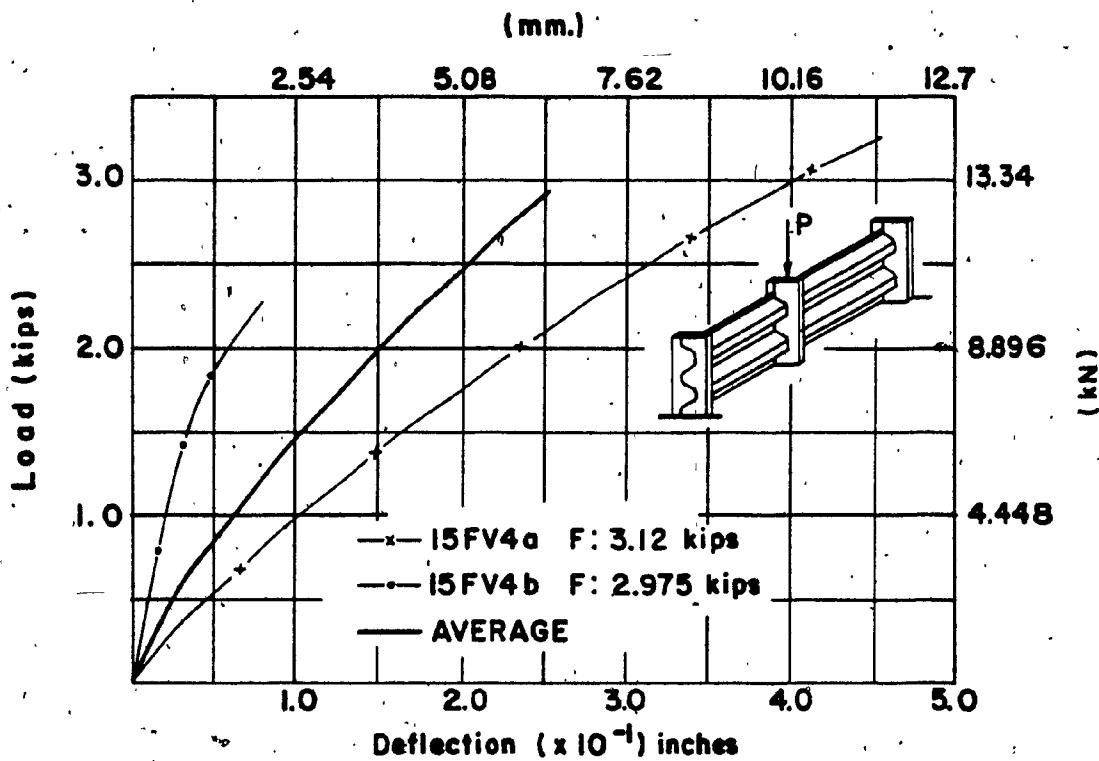


Figure 3.5.8 Load-Deflection curve

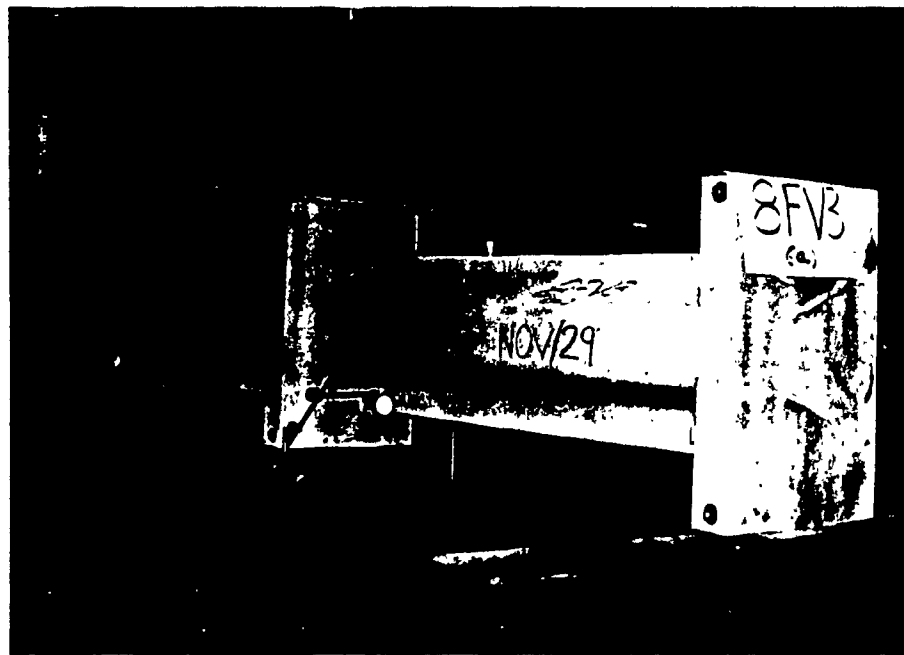


Figure 3.5.9. View of testing set-up of Beam 8FV3a.



Figure 3.5.10. View of Beam 8FV3a (At failure).

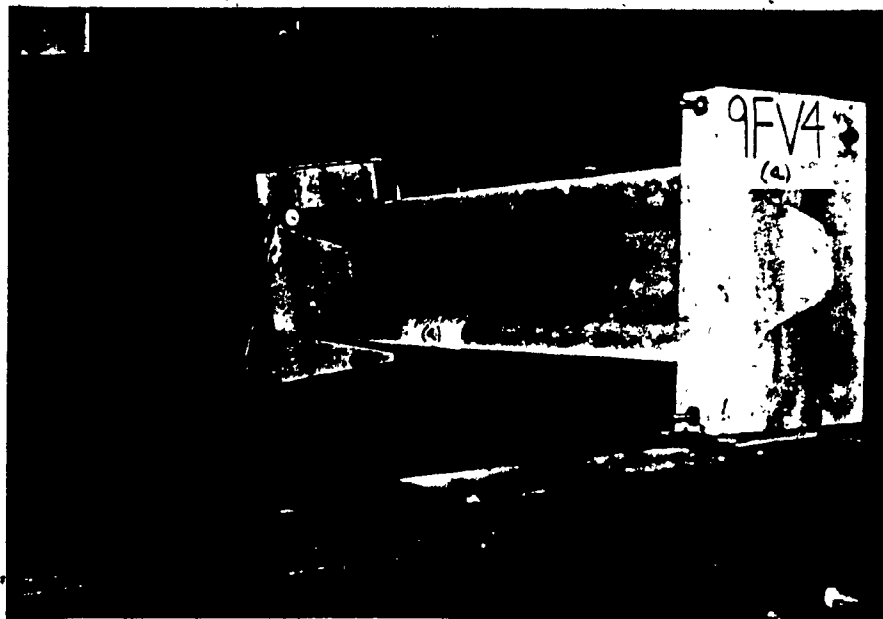


Figure 3.5.11. View of Beam 9FV4a (Twisting under load)



Figure 3.5.12. View of Beam 9FV4a (At failure)

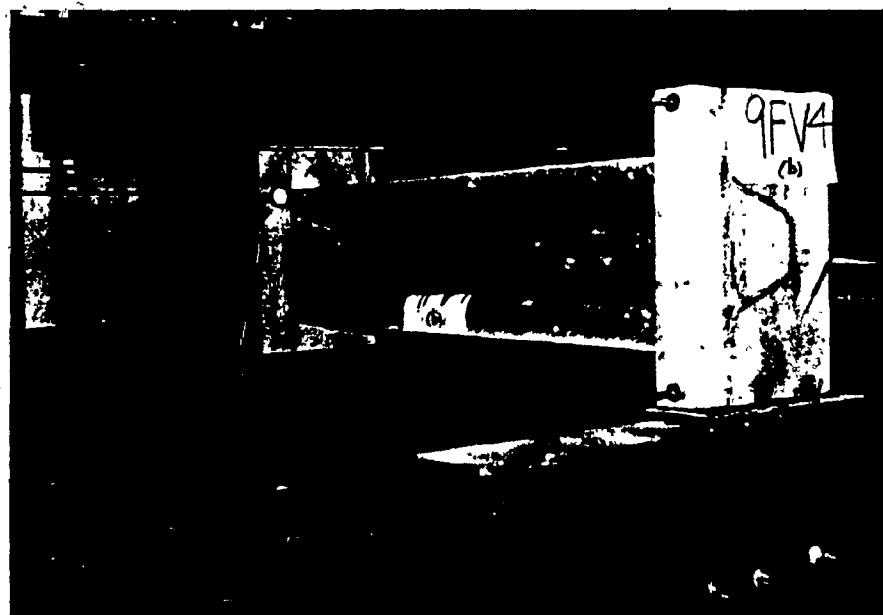


Figure 3.5.13. View of testing set-up of Beam 9FV4b

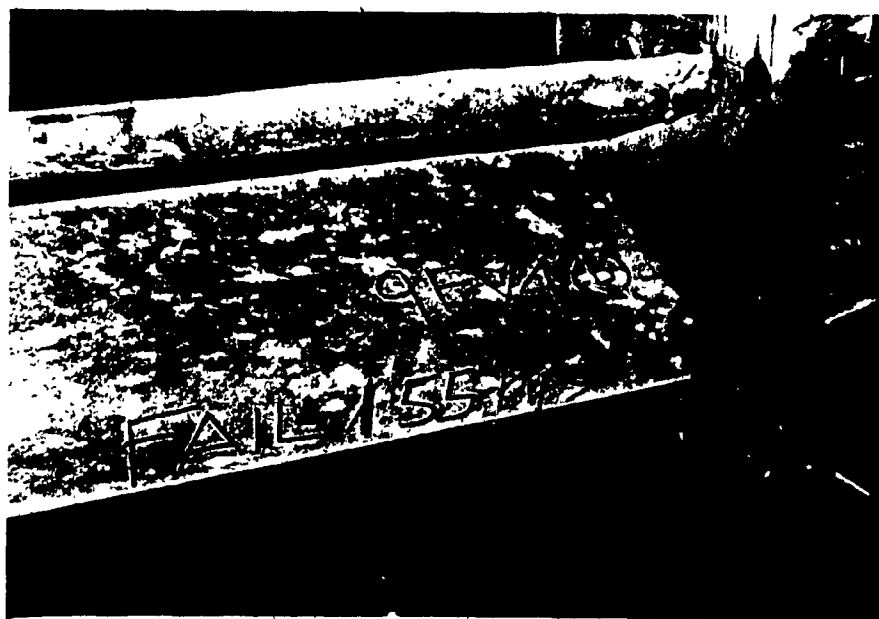


Figure 3.5.14. View of Beam 9FV4b (At failure)

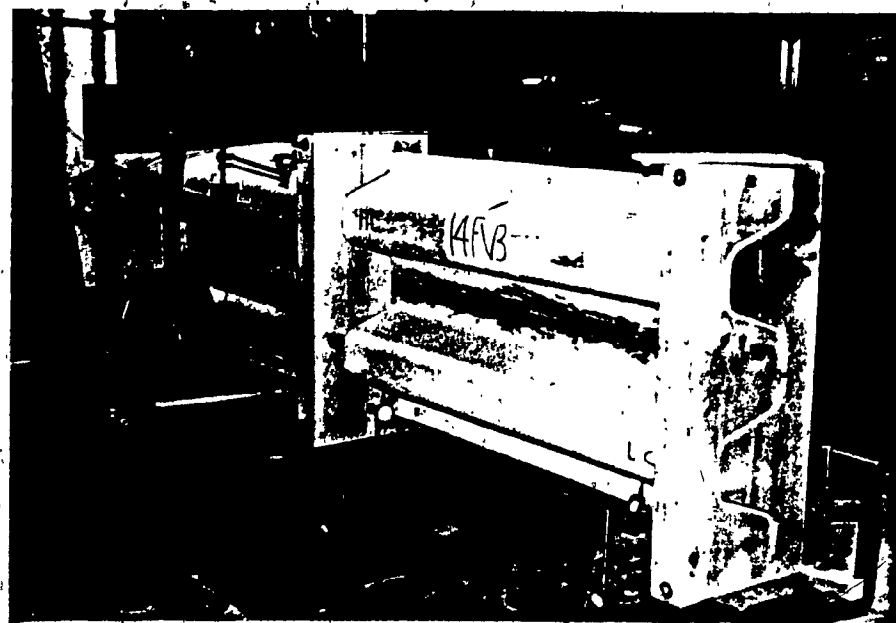


Figure 3.5.15. View of testing set-up of Beam 14FV3



Figure 3.5.16. View of Beam 14FV3 (At failure)

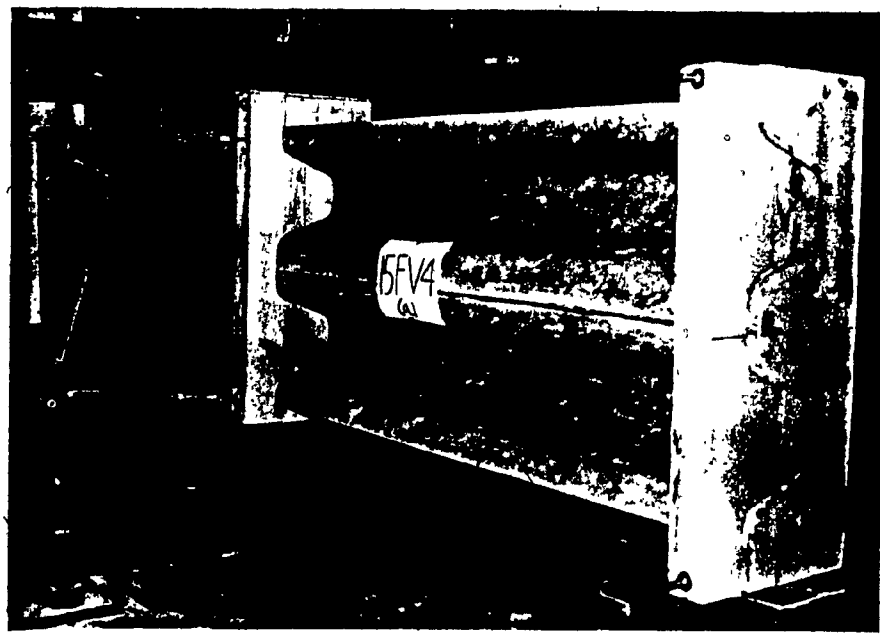
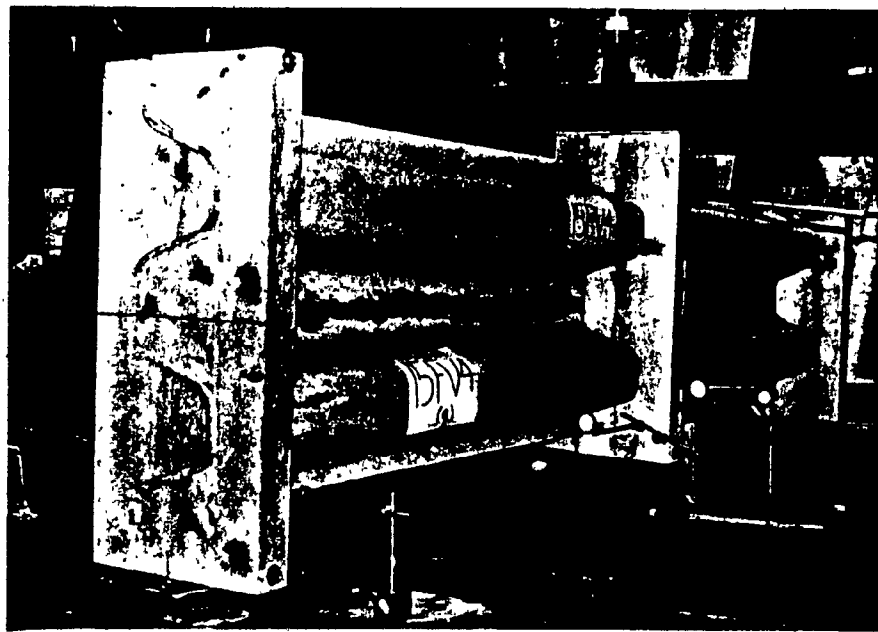


Figure 3.5.17. Views of testing set-up of Beam 15FV4a.



Figure 3.5.18 Views of Beam 15FV4 a (At failure)

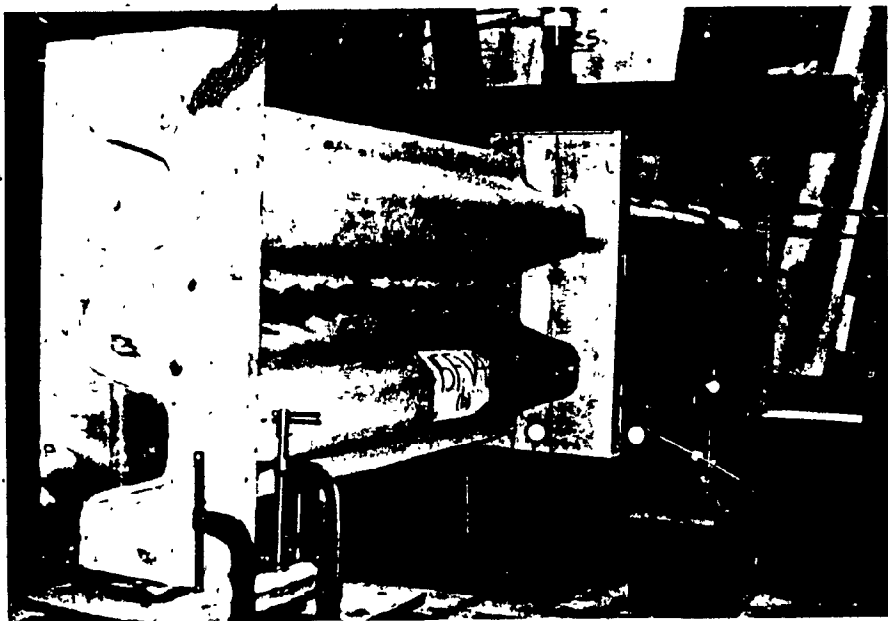


Figure 3.5.19. View of testing set-up of Beam 15FV4 b.



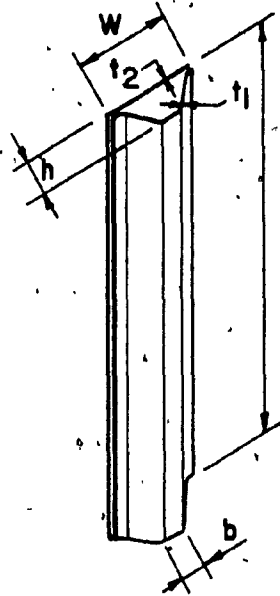
Figure 3.5.20. View of Beam 15FV4 b (At failure).

3.6 Sixth Stage - Columns Made of 'v' Element

In the sixth stage, the capacity of assemblies working as columns or walls was established and the advantages of epoxy connections were checked.

This stage consisted of one test series V15. It represented the testing of two columns denoted by 4WV4 and 4WV4a. Each column was made of a single 'v' element and attached to a $\frac{1}{2}$ " thick densite plate as shown in Figure 3.6.1. To column 4WV4a spots of epoxy were laid in between the v-section and the plate. The dimensions of both columns are shown in Figure 3.6.1. The testing arrangement is shown in Figure 2.5.2.

Test series V15-single 'v' columns 4WV4 and 4WV4a in compression - Columns 4WV4 and 4WV4a failed under compressive loads of 63 kips and 55.685 kips respectively. The failure of 4WV4 was caused by the splitting of asbestos at approximately 3'-3" up from the bottom. Column 4WV4a failed under a lower load because the top of the v-section was not flush with the plate and as a result, the vertical load was taken only by the v-section. The column failed at the top of the section.



Test Series	Sample No.	H	W	b	h	t ₁	t ₂
VI5	4WV4	10'-0"	15 $\frac{3}{4}$ "	4 $\frac{1}{2}$ "	8"	1/2"	1/2"
VI5	4WV4a*	10'-0"	15 $\frac{3}{4}$ "	4 $\frac{1}{2}$ "	8"	1/2"	1/2"

* with spots of epoxy

Figure 3.6.1 Dimensions of columns

Table 3.6.1. Comparison of tested and calculated results

	Sample No.	Failure load 'P'	f _c ' (psi)	Calculated load 'P'
	4WV4	63,185 k.	10,000	54.06
	4WV4a.	55,685 k.	8,858	54.06

3.7 Supplemental Tests - Properties of Asbestos-Cement

The properties of asbestos-cement as specified by Atlas Turner Inc., were verified. Tests were performed on small samples on a Tinus Olsen machine at room temperature and under normal laboratory conditions.

Tensile Test - The test specimen had a "dog bone" configuration which usually fails at the central portion where the stresses are not affected by the gripping device. Electric strain gauges were placed on both sides of the narrow portion of the sample. The load was applied in equal increments until failure of the specimen. The resulting stress-strain diagram is shown in Figure 3.7.1. The modulus of elasticity and the tensile strength along the fibers were found to be 1.75×10^6 psi and 1900 psi respectively, both values are comparable to those specified by Atlas Turner Inc.

Rupture Strength Evaluation - In order to eliminate the influence of strength variability, tests were carried out on cut-out sections from roof panels 1-SR5 and 2-SR5. Three samples from each roof panel were used for testing and each sample had dimensions 6" x 6" x 3/8" thick. The results are shown in Table 3.7.1 and the average rupture strength was found to be 4.69 kips/in².

Compressive Strength Evaluation - Three small samples were cut-out from each wall panel of test series S5, S6, S7 and S8 and compression tests were conducted on each of them. Each sample was 6" long by 6" wide by 3/8" thick. The test results are tabulated in Tables 3.7.2a and 3.7.2b.

Strength of Angle Connector - Tests were performed on three small samples of angle connectors as shown in Table 3.7.3, in order to evaluate the rupture strength. The overall dimensions of each sample were 6" x 3 $\frac{1}{2}$ " x 3/8" thick. Table 3.7.3 also shows the tests results and the average rupture strength.

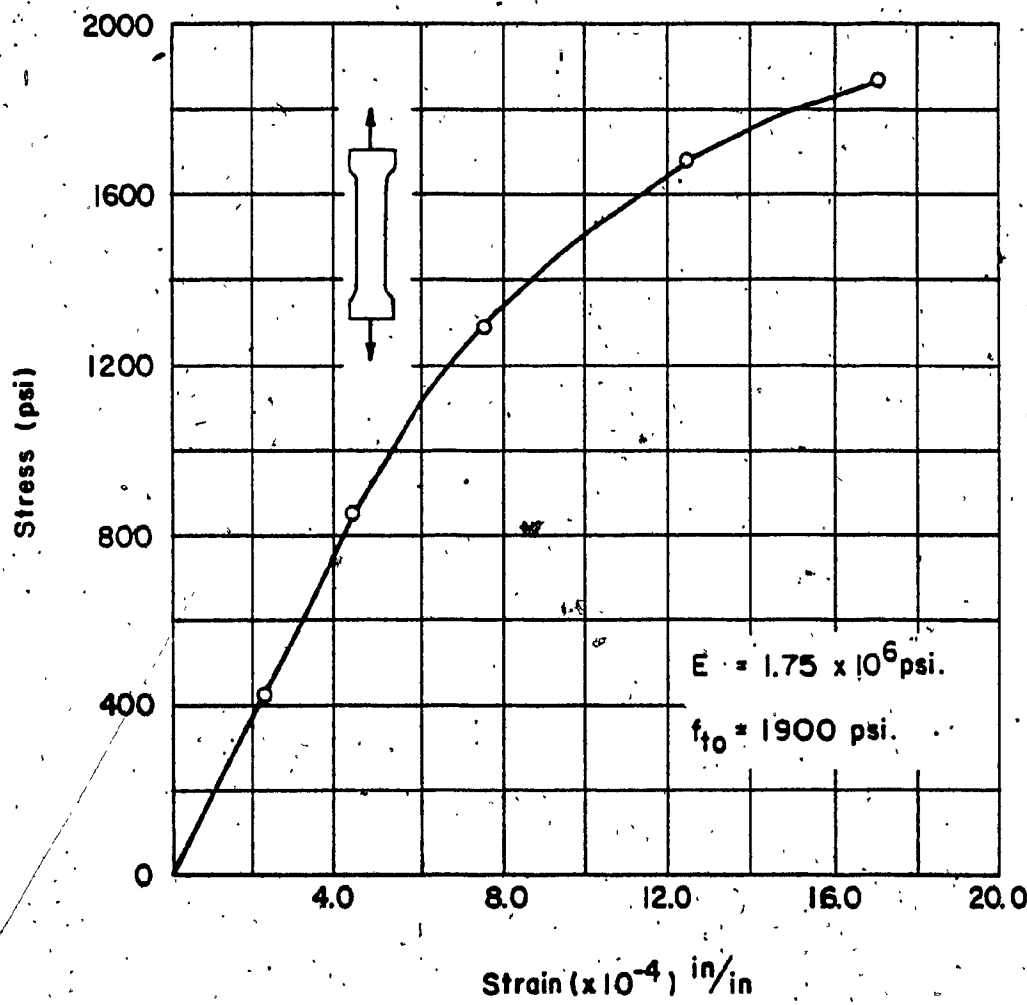
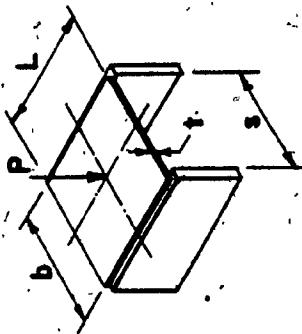


Figure 3.7.1. Stress-Strain curve for asbestos-cement in tension along the fibers.

Note: Circles indicate readings on electric strain gauges.

Table 3.7.1. Rupture strength evaluation

	Sample No.	Cut-out section No.	L	b	s	t	Failure load 'P' (lb.)	Average (lb.)	Rupture strength kips/in ²
I-SR5	1	6"	6"	5½"	3/8"	513			
	2	6"	6"	5½"	3/8"	436	487	4.76	
	3	6"	6"	5½"	3/8"	512			
2-SR5	1	6"	6"	5½"	3/8"	454			
	2	6"	6"	5½"	3/8"	431	456	4.459	
	3	6"	6"	5½"	3/8"	482			



Rupture strength = 4.64 kips/in² (Average)

Table 3.7.2.a. Compressive strength evaluation

	Sample No.	cut-out section No.	h	b	t	Failure load 'P' (kips)	Average (kips)	Compressive strength (psi)
5SW6	1	6"	6"	3/8"	11.35			
	2	6"	6"	3/8"	10.40	10.43	7884	
	3	6"	6"	3/8"	9.55			
6SW6	1	6"	6"	3/8"	13.25			
	2	6"	6"	3/8"	12.55	12.60	9524	
	3	6"	6"	3/8"	12.00			

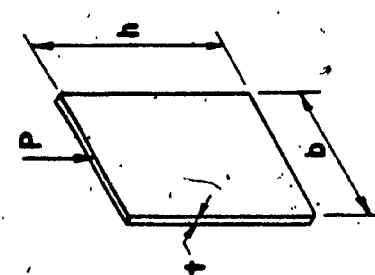
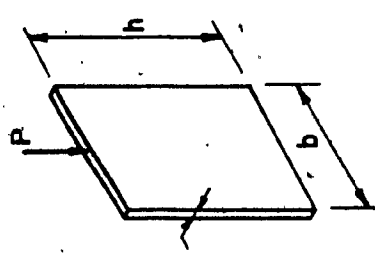


Table 3.7.2.b. Compressive strength evaluation

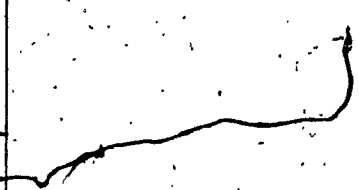
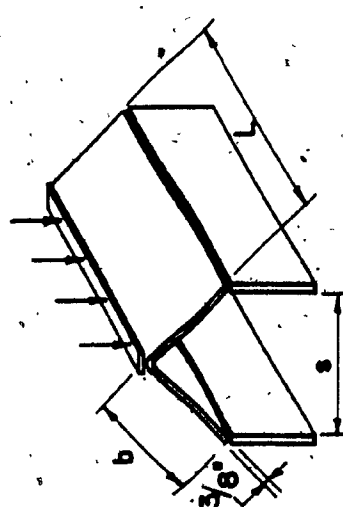
	Sample No.	Cut-out section No.	<i>h</i>	<i>b</i>	<i>t</i>	Failure load ' <i>P</i> ' (kips)	Average (kips)	Compressive strength (psi)
7SW5	1	6"	6"	3/8"	7.25			
	2	6"	6"	3/8"	12.15	12.65		
	3	6"	6"	3/8"	13.25			
8SW5	1	6"	6"	3/8"	5.75			
	2	6"	6"	3/8"	13.825	13.04		
	3	6"	6"	3/8"	12.25			



Compressive strength = 9200 psi (Average)

Table 3.7.3. Strength of angle connector

Sample No.	L	b	s	Failure load (lb.)	Average (lb.)	Rupture strength kips/in ²
1	6"	3 1/2"	4 1/4"	200	182	1.375
2	6"	3 1/2"	4 1/4"	99		
3	6"	3 1/2"	4 1/4"	246		



CHAPTER 4

CONCLUSIONS

CHAPTER 4

CONCLUSIONS

4.1. Safe Loading Definition

Asbestos-cement structures, like any other structures, must be designed to carry load with sufficient safety. Because asbestos-cement elements normally have thin walls, the dead weight is insignificant as compared to the live load, and therefore, one load factor $S = 1.7$ can be taken for the total loading. However, a sudden collapse mode should be considered and an additional factor of safety of 1.35 is recommended, thus making the safety of asbestos-cement structures comparable to other structures. Therefore an overall factor of safety of $(1.7 \times 1.35) = 2.25$ is recommended for a controlled condition of erection (factory) and a higher factor of safety of 2.5 should be considered for structures erected on site. Additional load factor should be considered for screws and structures which are exposed to humidity and increased water content. Calculated values of safe load capacity for structures tested in this project are shown in Tables 4.1 and 4.2.

4.2 Proposed Design Procedure

4.2.1 Flexural Members

Test results demonstrate that the flexural strength may be calculated using the proposed new method of designing

asbestos-cement structures. Comparison of tested and calculated results are shown in Table 4.1. As it can be seen, the panels tested have almost the same strength as calculated, except for some exceptions. Results of beams tested in a horizontal plane are not included in the comparisons.

4.2.2 Compression Members

Panels tested in compression revealed strengths close to the calculated values according to present ACI practice for wall design (ACI 381-83). The results are compared in Table 4.2 and safe loading values for tested compression members are also included.

Table 4.1. Comparison of tested and calculated results and allowable loads

Type	Test series	Sample No.	Failure load 'P' (kips)	Calculated load 'P' (kips)	$\frac{P_{\text{tested}}}{P_{\text{cal.}}}$	Allowable load k/ft	Allowable load k/ft ²
FLEXURAL Beam elements	S1	I-SR6	4.150	3.98	1.04	0.24	0.060
	S2	2-SR6	2.975	3.98	0.75		
	S3	I-SR5	2.880	3.32	0.87	0.21	0.054
	S4	2-SR5	3.120	3.35	0.93		
	V1	IFV3a	1.550	1.68	0.92		
		IFV3b	1.310	1.68	0.78	0.118	
	V2	2FV4a	1.555	1.79	0.87	0.106	
		2FV4b	1.555	1.79	0.87		
	V3	3FV3a	2.740	2.414	1.14	0.227	
	V4	10FV3a	3.7825	3.40	1.11		
		10FV3b	3.750	3.40	1.10	0.311	
	V5	11FV4a	4.680	3.414	1.37		
		11FV4b	4.150	3.414	1.22	0.303	
	V6	5FV3	1.555	1.77	0.88		
		5aFV3	1.800	1.77	1.01	0.115	
	V7	6FV4	2.270	2.27	1.0		
		6aFV4	3.120	2.27	1.40	0.185	
	V8	7FV4	4.150	2.934	1.40		
		7aFV4	3.905	2.934	1.33	0.276	
	V9	12aFV3	3.7825	3.525	1.07	0.260	
	V10	13aFV4	4.400	4.50	0.98	0.300	

Table 4.2. Comparison of tested and calculated results and allowable loads

Type	Test series	Sample No.	Failure load 'P' (kips)	Calculated load 'P' (kips)	$\frac{P_{\text{tested}}}{P_{\text{cal.}}}$	Allowable load (kips)
COMPRESSION Wall Panels	S6	6SW6	63.00	54.48	1.16	25
	S7	7SW5	35.00	31.00	1.13	
	S8	8SW5	37.50	31.00	1.21	15
Columns	V15	4WV4	63.185	54.06	1.17	
		4WV4a	55.685	54.06	1.03	24

CHAPTER 5

PROPOSED DESIGN PROCEDURE FOR ASBESTOS-CEMENT STRUCTURES

CHAPTER 5

PROPOSED DESIGN PROCEDURE FOR ASBESTOS-CEMENT STRUCTURES

5.1 Flexural Strength

Present practice of calculating flexural strength of asbestos-cement beams is based on an assumption of stress distribution as shown in Figure 5.1. It is assumed that the concentrated compressive force acts at the top of the beam and that the tensile stresses are assumed to follow a triangular distribution. The section fails when the maximum tensile stress f_r is reached at the bottom, also called the rupture strength. (1) (5).

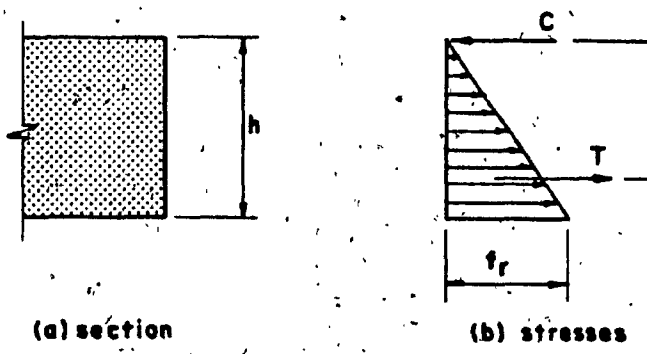


Figure 5.1. Stresses at failure.

In spite of the fact that such calculation gives for some sections, as indicated in Appendix A, results comparable with tests, it does not confirm the true behaviour of asbestos-cement which under higher stress demonstrates plastic deformations as can be seen from the stress-strain curve in Figure 3.7.1.

A new method has been adopted here, similar to that used for reinforced concrete (2). This method is based on assumption of a simplified rectangular stress block in the tension zone as shown in Figure 5.2. This assumption is based on observation that prior to failure the bottom extreme fibers of the section are under elastoplastic stress-strain behavior. The stress diagram in the tension zone can be approximated by a rectangular distribution at the final stage as it is done in the analysis of concrete structures.

Generalized I - shaped section is shown in Figure 5.2(a). The strain distribution is shown in Figure 5.2(b) and the stress block at cracking failure can be considered as shown in Figure 5.2(c).

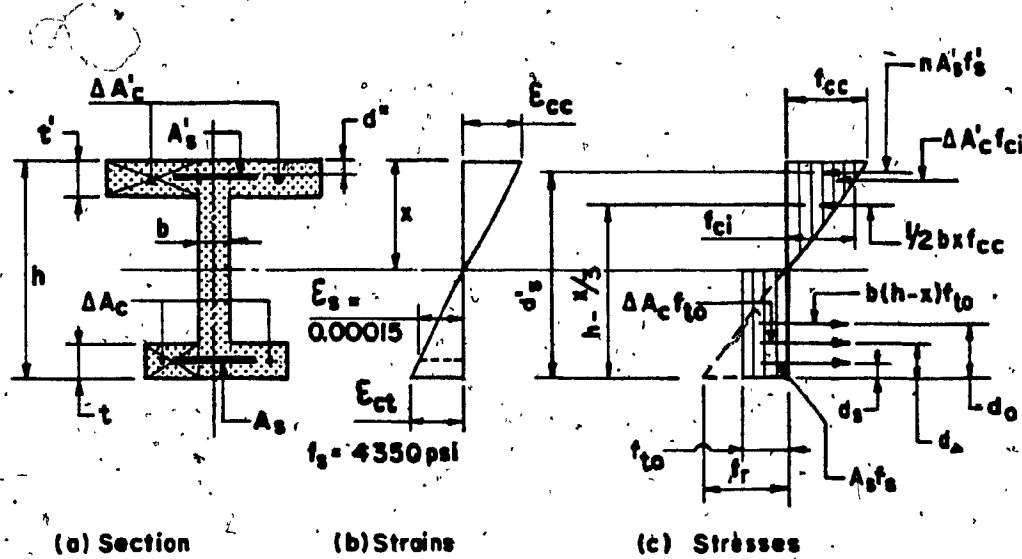


Figure 5.2. Strains and Stresses at failure.

where

f_{cc} : compressive stress of top fibers

f'_s : strength in steel in the compression zone

E_{cc} : modulus of elasticity of asbestos-cement
in compression

E_{ct} : modulus of elasticity of asbestos-cement
in tension

f_r : approximate rupture strength

n : modular ratio (E_s/E_c)

Location of neutral axis can be established from the
equilibrium of tension and compression forces

$$C - T = 0$$

$$nA'_s f'_s + \Delta A'_c f_{ci} + \frac{bx}{2} f_{cc} - b(h-x) f_{to} - \Delta A_c f_{to} - A_s f_s = 0 \quad (1)$$

where

x : height of compression zone

h : total height of section

f_{to} : ultimate tensile uniaxial strength of
asbestos-cement

f_s : 4350 psi, assuming that strain in tension
is 0.00015

$\Delta A'_c$: area of concrete in compression in excess
of basic rectangular bh

ΔA_c : area of concrete in tension in excess of
basic rectangular bh

A'_s : area of steel in compression zone

A_s : area of steel in tension zone.

Stresses in the compression zone can be calculated as:

$$f_{cc} = 2f_{to} \left(\frac{x}{h-x} \right) \quad (2)$$

$$f'_s = 2nf_{to} \left(\frac{x-d''}{h-x} \right) \quad (3)$$

Substituting equations (2) and (3) in equation (1) gives the value of x .

The flexural cracking moment can be expressed as:

$$M_{cr} = \phi f_{to} b h^2 (A + B\psi_t - \sum \psi_{ti} \delta_i) \quad (4)$$

where

$$A = \frac{1}{2} - \frac{\gamma \psi_c}{1+2\psi_c} - \frac{1-2\psi_c}{6(1+2\psi_c)} - \frac{1}{6} \left(\frac{1+2\psi_c}{2+2\psi_c} \right)^2$$

$$B = 1 - \frac{\gamma \psi_c}{1+2\psi_c} - \frac{1}{3(1+2\psi_c)}$$

ϕ : capacity reduction factor - should be taken as 0.9, as for flexural concrete elements.

$$\psi_c = \frac{\Delta A' c + n A' s}{b h}$$

= coefficient of strengthening of section in compression in excess of basic rectangular bh .

$$\psi_t = \frac{A_c f_{to} + A_s f_s}{b h f_{to}}$$

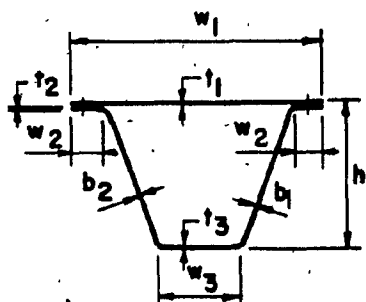
= coefficient of strengthening of section in tension in excess of basic rectangular bh .

$$\sum \psi_{ti} \delta_i = \psi_c \frac{d_A}{h} + \psi_s \frac{d_s}{h} = \frac{\Delta A_c d_A}{bh^2} + \frac{4350 A_s d_s}{bh^2 f_{to}}$$

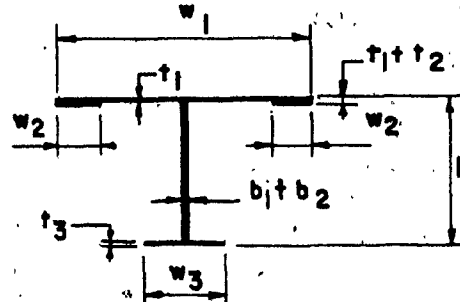
Values of coefficients A and B can also be taken from Table 5.1. For beam with no steel reinforcement,

$$\psi_c = \frac{\Delta A_c}{bh} \quad \text{and} \quad \psi_t = \frac{\Delta A_c}{bh}$$

This method may be used to calculate the flexural cracking strength of any section. The flexural cracking strengths of panels made of S-shape and V-shaped sections tested were calculated using equation (4). The panels cross-sections were replaced by equivalent cross-section of I-beams with same heights. The widths and thicknesses of flanges of I-beams were taken as equal to panels' widths and thicknesses respectively. The widths of webs were taken as the sum of all panels webs as shown in Figure 5.3.



(a) True section



(b) Equivalent section

Figure 5.3. Equivalent section.

Table 5.1. Coefficients A and B

χ_{th}	ψ_c	A			B		
		0	0.5	1.0	0	0.5	1.0
0	0.290	0.425	0.450	0.490	0.670	0.835	0.890
0.1	0.290	0.400	0.430	0.440	0.670	0.810	0.860
0.2	0.290	0.375	0.395	0.405	0.670	0.780	0.825
0.3	0.290	0.350	0.360	0.365	0.670	0.760	0.790

Equation (4) was used to calculate the flexural strengths of asbestos-cement samples with and without reinforcement. The computed values as can be seen in Tables of Results are very close to test results. Therefore, the method described may be safely recommended to design practice, for asbestos-cement section of any shape. Detailed calculations are shown in Appendix A.

5.2 Compressive Strength

Test results demonstrate that strength of asbestos-cement structures such as walls or columns subjected to compression can be calculated using American Concrete Institute (ACI) practice for walls and the Empirical Equation (14-1) of Section 14.2.3 of ACI-1983 Code of Practice (3).

$$P_u = 0.55 \cdot \phi f'_c A_g \cdot \left[1 - \left(\frac{l_c}{32h} \right)^2 \right] \quad (5)$$

P_u : factored vertical load on wall

f'_c : specified compressive strength of asbestos-cement

A_g : cross-sectional area

$\frac{l_c}{h}$: height to thickness ratio of the wall.

$\frac{l_c}{32h}$ should be considered for overall column strength taking l_c as described and local strength between screws.

Equation (5) was used to calculate the capacity of asbestos-cement walls tested. Detailed calculations are also shown in Appendix A.

5.3 Determination of Safe Service Load

The previous sections elaborated on a design procedure which estimated ultimate or failure capacities of structural elements made of asbestos-cement. These elements when working in flexure are known as beams and floors, whereas those under compression are known as columns or walls.

The determination of the factor of safety, also known as the load factor, comes prior to the establishment of safe service load levels. Building codes normally prescribe different load factors for dead and live loads, together with various load combinations. For example, concrete structures usually have a 1.4 factor attributed to the dead load whereas for live loads, a 1.7 factor is used. In consequence, when we consider that in the case of asbestos-cement elements which normally have thin walls, the structural element dead weight is insignificant compared with the imposed live load and therefore it is proposed to assume one constant load factor labelled S_1 with a value of 1.7 for all loads (dead and live).

However, asbestos-cement structures are subject to sudden cracking and simultaneous collapse. Unlike asbestos-cement, cracking of normal reinforced concrete structure is a consequence of the steel having yielded and even though full collapse has not yet occurred and the steel not yet ruptured, the structure may be considered as non-serviceable.

In order to put safety-wise asbestos-cement structures into parity with other structures made of materials demonstrating large plastic deformations before failure, it is proposed to consider additional factor of safety $S_2 = 1.35$. Thus it is proposed to consider overall factor of safety for asbestos-cement.

$$S = (S_1 \times S_2) = (1.7 \times 1.35) = 2.25$$

or more conservatively $S = 2.5$ for structure erected on site in condition where adequate technical supervision is not available.

Consequently, the following design procedure is proposed:

1. Establish design loads.
2. Multiply design load by factor $S = 2.25$ for structures produced in control condition or $S = 2.5$ for structures erected on site in order to establish ultimate loads.
3. Design structure using formulae for ultimate capacity.

The above procedure is valid for structures working in dry conditions and additional load factor should be considered for structures which are exposed to humidity and increased water content. Information in this respect should be obtained from asbestos-cement producer. An additional factor of safety should be considered for connections as recommended by PCI (Prestressed Concrete Institute) (4).

REFERENCES.

REFERENCES

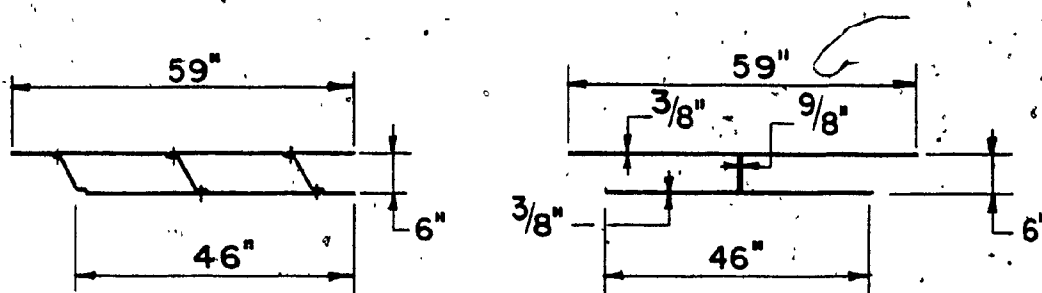
1. de Mahieu, L., "La Theorie de l'Asbeste-Ciment"
S.A. Eternit N.V., Kapell-Op-Den-Bos, Belgium,
1973.
2. Zielinski, Z.A., CE600 Course Script Advanced
Reinforced Concrete Design, Concordia University,
Montreal, Quebec, 1982.
3. ACI Committee 318, "Building Code Requirements for
Reinforced Concrete (ACI 318-83)", American
Concrete Institute, 1983.
4. PCI Committee on Connection Details, "PCI Manual
on Design of Connections for Precast Prestressed
Concrete", PCI 1973.
5. Godbout, P. and A. Brais, "A Study for the
Establishment of Test Procedures of Atlas Sheets
with Regards to 'T' and 'Cavity' Decks", Atlas
Asbestos Company, Montreal, Quebec, Canada,
April 1977.

APPENDIX A
DESIGN CALCULATIONS

APPENDIX A

A-1 ROOF PANEL STRENGTH

Roof Panels 1-SR6 & 2-SR6



$$M_{cr} = f_{t0} b h^2 \left[A + B \psi_t - \sum \psi_{ti} \delta_i \right]$$

$$\psi_c = \frac{\Delta A_c}{bh} = \left[\frac{2 \times 28.94 \times 3/8}{9/8 \times 6} \right] = 3.215 ; t'/h = 3/8 / 6 = 0.0625$$

$$A = \frac{1}{2} - \left[\frac{0.0625 \times 3.215}{1 + (2 \times 3.215)} \right] - \left[\frac{1 - (2 \times 3.215)}{6(1 + 2 \times 3.215)} \right] - \frac{1}{6} \left[\frac{1 + (2 \times 3.215)}{2 + (2 \times 3.215)} \right]^2 \\ = 0.463$$

$$B = 1 - \left[\frac{0.0625 \times 3.215}{1 + (2 \times 3.215)} \right] - \left[\frac{1}{3(1 + 2 \times 3.215)} \right] = 0.9281$$

$$\psi_t = \frac{\Delta A_c}{bh} = \left[\frac{2 \times 22.4375 \times 3/8}{9/8 \times 6} \right] = 2.493$$

$$\sum \psi_{ti} \delta_i = \frac{\Delta A_c d_A}{bh^2} = \left[\frac{2 \times 22.4375 \times 3/8 \times 3/16}{9/8 \times (6)^2} \right] = 0.0779$$

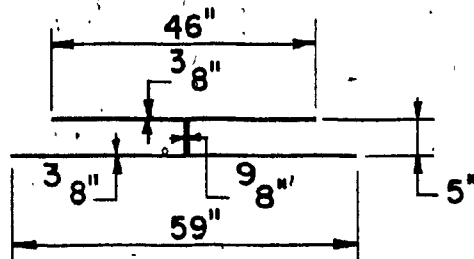
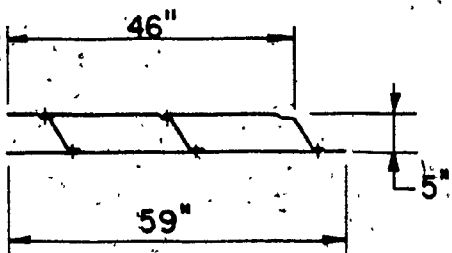
$$S_v = \frac{9/8}{8} (6)^2 \left[0.4653 + 0.9281 (2.493) - 0.0779 \right] = 109.3967$$

$$S_H = [0.29 bh^2] = [(0.29)(3/8)(26)^2] + [(0.29)(3/8)(40)^2] = 321.03$$

$$M_{cr} = \frac{f_{t0}}{\frac{1}{109.3967} + \frac{\sin 60^\circ}{321.03}} = \frac{1650}{0.0118387} = 139,373.41$$

$$P = \frac{4 \times M_{cr}}{L} = \frac{4 \times 11.61}{11.67} = 3.98 \text{ kips}$$

Roof Panel 1-SR5



$$M_{cr} = f_{t0} b h^2 \left[A + B \psi_t - \sum \psi_i \delta_i \right]$$

$$\psi_c = \frac{\Delta A'_c}{bh} = \left[\frac{2 \times 22.4375 \times 3/8}{9/8 \times 5} \right] = 2.9917$$

$$\psi_t = \frac{\Delta A'_t}{bh} = \left[\frac{2 \times 22.4375 \times 3/8}{9/8 \times 5} \right] = 2.9917$$

$$\gamma = \frac{t'}{h} = 0.075$$

$$\sum \psi_i \delta_i = \frac{\Delta A'_i \delta_i}{bh^2} = \left[\frac{2 \times 22.4375 \times 3/8 \times 3/16}{(9/8)(5)^2} \right] = 0.1122$$

$$A = \frac{1}{2} - \left[\frac{0.075 \times 2.9917}{1 + (2 \times 2.9917)} \right] - \left[\frac{1 - 2(2.9917)}{6(1 + 2 \times 2.9917)} \right] - \frac{1}{6} \left[\frac{1 + (2 \times 2.9917)}{2 + (2 \times 2.9917)} \right]^2 \\ = -0.4593$$

$$B = 1 - \left[\frac{0.075 \times 2.9917}{1 + (2 \times 2.9917)} \right] - \left[\frac{1}{3(1+2 \times 2.9917)} \right] = 0.9201$$

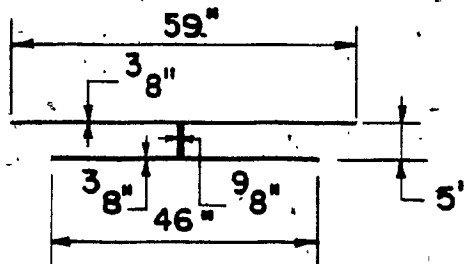
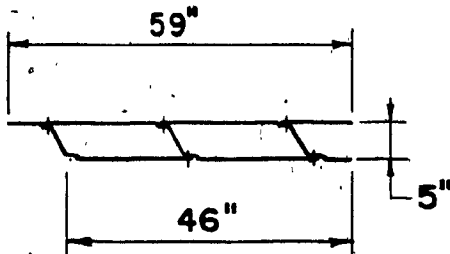
$$S_v = (9/8)(5)^2 \left[0.4593 + 0.9201(2.9917) - 0.1122 \right] = 87.18$$

$$S_H = \sum [6.29bh^2] = [(0.29)(3/8)(26^2) + (0.29)(3/8)(26^2) + (0.29)(3/8)(40)^2] \\ = 321.03$$

$$M_{cr} = \frac{f_{t0}}{\frac{1}{87.18} + \frac{\sin 60}{321.03}} = \frac{1650}{0.014168} = 116,459.2 \text{ in} = 9.70 \text{ ft-kips}$$

$$P_c = \frac{4M_{cr}}{L} = \frac{4 \times 9.70}{11.67} = 3.32 \text{ kips}$$

Roof Panel 2-SR5



$$M_{cr} = f_{t0} bh^2 \left[A + B\psi_t - \sum \psi_i \delta_i \right]$$

$$\psi_c = \frac{\Delta A'_c}{bh} = \frac{2 \times 28.94 \times 3/8}{9/8 \times 5} = 3.8587$$

$$\gamma = \frac{t'}{h} = \frac{3/8}{5} = 0.075$$

$$\psi_t = \frac{\Delta A_c}{bh} = \frac{2 \times 22.4375 \times 3/8}{9/8 \times 5} = 2.9917$$

$$\sum \psi_i \delta_i = \frac{\Delta A_c d_4}{bh^2} = \frac{2 \times 22.4375 \times 3/8 \times 3/16}{9/8 \times (5)^2} = 0.1121$$

$$A = \frac{1}{2} - \left[\frac{0.075 \times 3.8587}{1 + (2 \times 3.8587)} \right] - \left[\frac{1 - (2 \times 3.8587)}{6(1 + 2 \times 3.8587)} \right] - \frac{1}{6} \times \left[\frac{1 + (2 \times 3.8587)}{2 + (2 \times 3.8587)} \right]^2 \\ = 0.4611$$

$$B = 1 - \left[\frac{0.075 \times 3.8587}{1 + (2 \times 3.8587)} \right] - \left[\frac{1}{3(1+2 \times 3.8587)} \right] = 0.9286$$

$$S_v = \frac{9}{8}(5)^2 \left[0.4611 + 0.9286(2.9917) - 0.1122 \right] = 87.9467$$

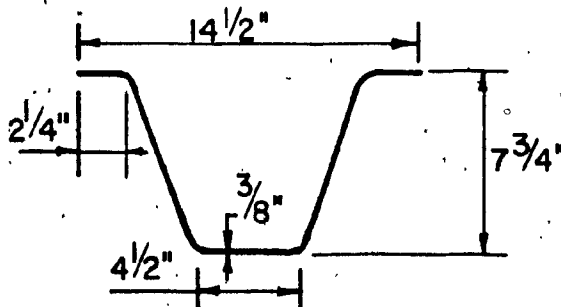
$$S_H = \sum [0.29bh^2] = [(0.29)(3/8)(26)^2 + (0.29)(3/8)(26)^2 + (0.29)(3/8)(40)^2] \\ = 321.03$$

$$M_{cr} = \frac{f_{t0}}{\left[\frac{1}{87.9467} + \frac{\sin 60^\circ}{321.03} \right]} = \frac{1650}{0.014068} = 117,287.46 \text{ lb-in} = 9.77 \text{ k-ft}$$

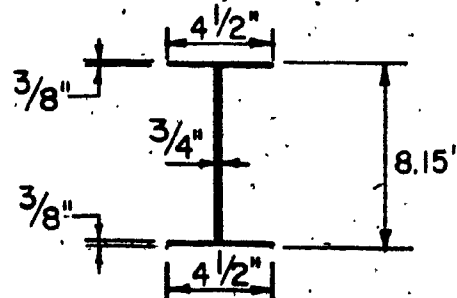
$$P = \frac{M_{cr} \cdot 4}{L} = \left[\frac{9.77 \times 4}{11.67} \right] = 3.35 \text{ kips}$$

A-2 BEAM STRENGTH

Beam Panels 1FV3 (a & b)



$$h = 7.75 / \sin 72^\circ = 8.15"$$



$$M_{cr} = f_{t0} bh^2 \left[A + B \psi_t - \sum \psi_{ti} \delta_i \right]$$

$$\psi_c = \frac{\Delta A' c}{bh} = \left[\frac{2 \times 1.875 \times 3/8}{3/4(8.15)} \right] = 0.2301$$

$$\gamma = t/h = \left[\frac{3/8}{8.15} \right] = 0.046$$

$$A = \frac{1}{2} - \left[\frac{0.046 \times 0.2301}{1+(2 \times 0.2301)} \right] - \left[\frac{1-(2 \times 0.2301)}{6(1+2 \times 0.2301)} \right] - \frac{1}{6} \left[\frac{1+(2 \times 0.2301)}{2+(2 \times 0.2301)} \right]^2 \\ = 0.3724$$

$$B = 1 - \left[\frac{0.046 \times 0.2301}{1+(2 \times 0.2301)} \right] - \left[\frac{1}{3(1+2 \times 0.3201)} \right] = 0.7645$$

$$\psi_t = 0.2301$$

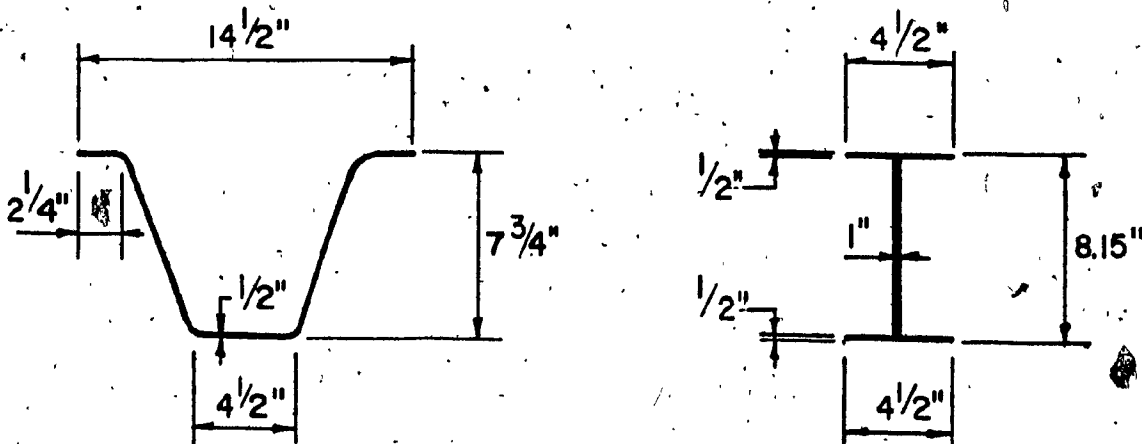
$$\psi_{ti}\delta_i = \frac{\Delta A_C d_A}{bh^2} = \left[\frac{2 \times 1.875 \times 3/8 \times 3/16}{\frac{1}{4}(8.15)^2} \right] = 0.00529$$

$$M_{cr} = 1800 \times 0.75 \times (8.15)^2 \left[0.3724 + 0.7645(0.2301) - 0.00529 \right] \\ = 48.69 \text{ in kips}$$

$$M_{cr} = \frac{PL}{4}; P = 1.68 \text{ kips}$$

Failure load = 1.68 kips

Beams 2-FV4 (a & b)



$$M_{cr} = f_{t0} b h^2 \left[A + B \psi_t - \sum \psi_{ti} \delta_i \right]$$

$$\psi_c = \frac{\Delta A'_c}{bh} = \left[\frac{2 \times 1.75 \times \frac{1}{4}}{1 \times 8.15} \right] = 0.2147$$

$$\gamma = t'/h = \frac{1}{8.15} = 0.06135$$

$$A = \frac{1}{2} - \left[\frac{0.06135 \times 0.2147}{1 + (2 \times 0.2147)} \right] - \left[\frac{1 - (2 \times 0.2147)}{6(1 + 2 \times 0.2147)} \right] - \frac{1}{6} \left[\frac{1 + (2 \times 0.2147)}{2 + (2 \times 0.2147)} \right]^2$$

$$= 0.3666$$

$$B = 1 - \left[\frac{0.06135 \times 0.2147}{1 + (2 \times 0.2147)} \right] - \left[\frac{1}{3(1 + 2 \times 0.2147)} \right] = 0.7576$$

$$\psi_t = \frac{\Delta A_c}{bh} = 0.2147$$

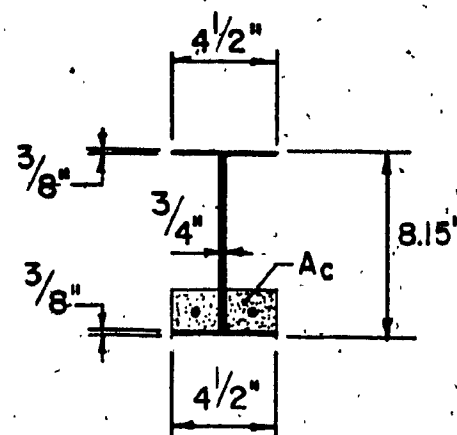
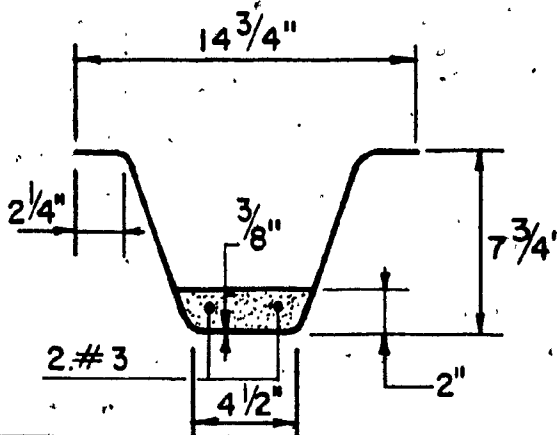
$$\sum \psi_{ti} \delta_i = \frac{\Delta A_c d}{bh^2} = \left[\frac{2 \times 1.75 \times \frac{1}{4} \times \frac{1}{4}}{1 \times (8.15)^2} \right] = 0.00659$$

$$M_{cr} = 1800 \times 1 \times (8.15)^2 \left[0.3666 + 0.7576(0.2147) - 0.00659 \right]$$

$$= 62.49 \text{ in kips}$$

$$\text{Failure Load } P = \left[\frac{62.49 \times 4}{140} \right] = 1.79 \text{ kips}$$

Beam 3-FV3a



$$M_{cr} = f_{to} bh^2 \left[A + B \psi_t - \sum \psi_{ti} \delta_i \right]$$

$$\psi_c = \frac{\Delta A' c}{bh} = \left[\frac{2 \times 1.875 \times 3/8}{\frac{3}{4} \times 8.15} \right] = 0.2301$$

$$\gamma = t'/h = \left[\frac{3/8}{8.15} \right] = 0.046$$

$$A = \frac{1}{2} - \left[\frac{0.046 \times 0.2301}{1 + (2 \times 0.2301)} \right] - \left[\frac{1 - (2 \times 0.2301)}{6(1 + 2 \times 0.2301)} \right] - \frac{1}{6} \left[\frac{1 + (2 \times 0.2301)}{2 + (2 \times 0.2301)} \right]^2 \\ = 0.3724$$

$$B = 1 - \left[\frac{0.046 \times 0.2301}{1 + (2 \times 0.2301)} \right] - \left[\frac{1}{3(1+2 \times 0.2301)} \right] = 0.7645$$

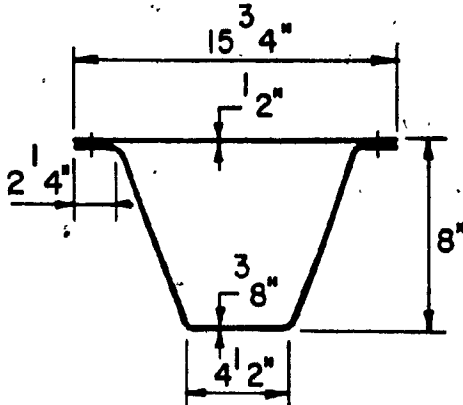
$$\psi_t = \left[\frac{\Delta A_c}{bh} + \frac{A_c f_c}{bh f_{to}} + \frac{A_s f_s}{bh f_{to}} \right] = \left[\frac{2 \times 1.875 \times 3/8}{\frac{3}{4} \times 8.15} \right] + \left[\frac{10 \times 300}{\frac{3}{4} \times 8.15 \times 1800} \right] \\ + \left[\frac{0.22 \times 4350}{\frac{3}{4} \times 8.15 \times 1800} \right] = 0.5897$$

$$\sum \psi_{ti} \delta_i = \left[\frac{\Delta A_c d_A}{bh^2} + \frac{A_s (4350) d_s}{bh^2 f_{to}} + \frac{A_c (300) d_c}{bh^2 f_{to}} \right] \\ = \left[\frac{2 \times 1.875 \times 3/8 \times 3/16}{\frac{3}{4} \times (8.15)^2} \right] + \left[\frac{0.22 \times 4350 \times 1}{\frac{3}{4} \times (8.15)^2 \times 1800} \right] + \left[\frac{10 \times 300 \times 1}{\frac{3}{4} \times (8.15)^2 \times 1800} \right] \\ = 0.04942$$

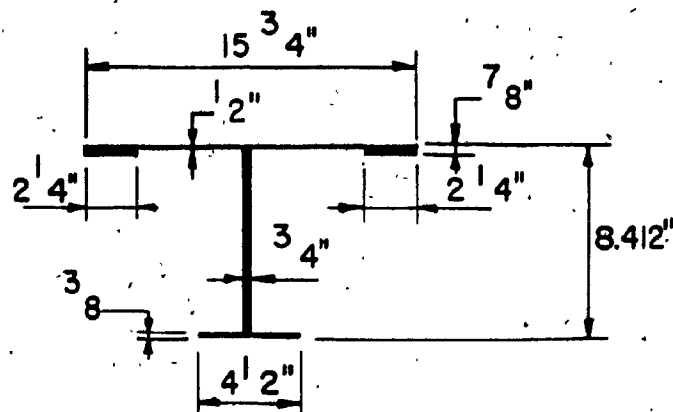
$$M_{cr} = 1800 \times \frac{3}{4} \times (8.15)^2 \left[0.3724 + 0.7645(0.5897) - 0.04942 \right] = 70 \text{ in kips}$$

$$\text{Failure load } P = \frac{70 \times 4}{116} = 2.414 \text{ kips}$$

Beams 5FV3 & 5aFV3



$$h = \frac{8}{\sin 72} = 8.412"$$



$$M_{cr} = f_{to} b h^2 \left[A + B \psi_t - \sum \psi_{ti} \delta_i \right]$$

$$\psi_c = \frac{\Delta A'_c}{bh} = \left[\frac{(2 \times 7.375 \times \frac{1}{4}) + (2 \times 2.25 \times 3/8)}{\frac{1}{4} \times 8.412} \right] = 1.436$$

$$\gamma = t'/h = \left[\frac{1}{4}/8.412 \right] = 0.0594$$

$$A = \frac{1}{2} - \left[\frac{0.0594 \times 1.436}{1+(2 \times 1.436)} \right] - \left[\frac{1-(2 \times 1.436)}{6(1+2 \times 1.436)} \right] - \frac{1}{6} \left[\frac{1+(2 \times 1.436)}{2+(2 \times 1.436)} \right]^2 \\ = 0.4533$$

$$B = 1 - \left[\frac{0.0594 \times 1.436}{1+(2 \times 1.436)} \right] - \left[\frac{1}{3(1+2 \times 1.436)} \right] = 0.8919$$

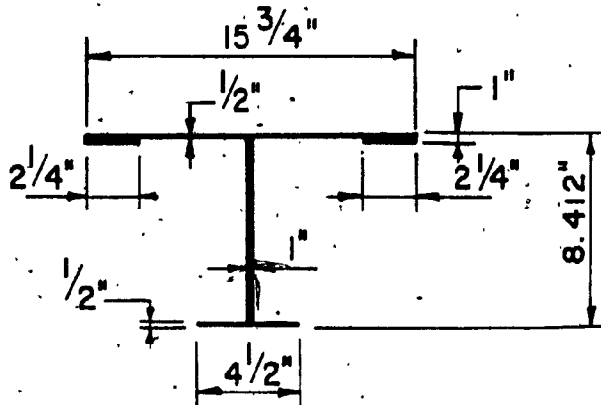
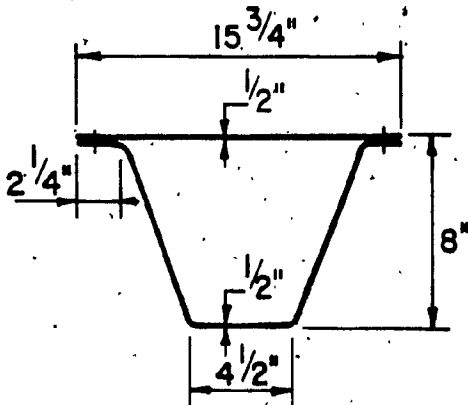
$$\psi_t = \frac{\Delta A_c}{bh} = \left[\frac{2 \times 1.875 \times 3/8}{\frac{1}{4} \times 8.412} \right] = 0.2229$$

$$\sum \psi_{ti} \delta_i = \frac{\Delta A_c d_A}{bh^2} = \left[\frac{2 \times 1.875 \times 3/8 \times 3/16}{\frac{1}{4} \times (8.412)^2} \right] = 0.00497$$

$$M_{cr} = 1800 \times \frac{1}{4} \times (8.412)^2 \left[0.5433 + 0.8919(0.2229) - 0.00497 \right] = 61.82 \text{ in kips}$$

$$\text{Failure load } P = \frac{61.82 \times 4}{140} = 1.77 \text{ kips}$$

Beams 6FV4 & 6aFV4



$$M_{cr} = f_{to} b h^2 \left[A + B \psi_t - \sum \psi_{ti} \delta_i \right]$$

$$\psi_c = \frac{\Delta A_c}{bh} = \left[\frac{(2 \times 7.375 \times \frac{1}{2}) + (2 \times 2.25 \times \frac{1}{2})}{(1 \times 8.413)} \right] = 1.144$$

$$\gamma = t'/h = \left[\frac{1}{8.412} \right] = 0.0594$$

$$A = \frac{1}{3} - \left[\frac{0.0594 \times 1.144}{1 + (2 \times 1.144)} \right] - \left[\frac{1 - (2 \times 1.144)}{6 \times (1+2 \times 1.144)} \right] - \frac{1}{6} \left[\frac{1 + (2 \times 1.144)}{2 + (2 \times 1.144)} \right]^2 \\ = 0.4466$$

$$B = 1 - \left[\frac{0.594 \times 1.144}{1 + (2 \times 1.144)} \right] - \left[\frac{1}{3(1 + 2 \times 1.144)} \right] = 0.8779$$

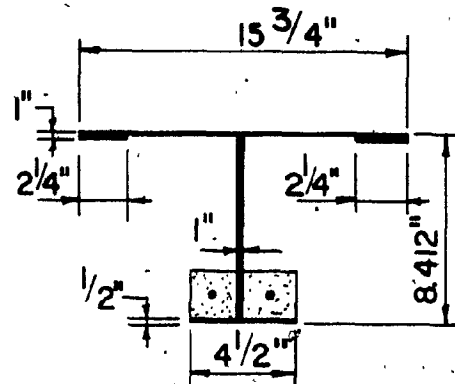
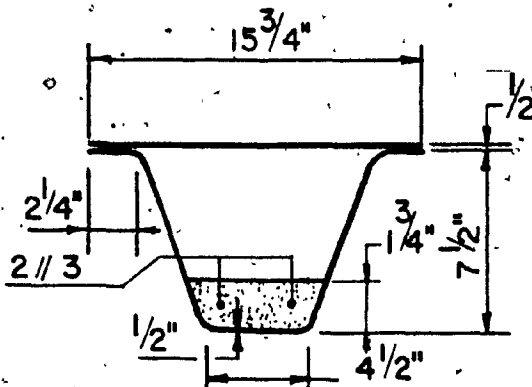
$$\psi_t = \frac{\Delta A_c}{bh} = \left[\frac{2 \times 1.75 \times \frac{1}{2}}{1 \times 8.412} \right] = 0.2080$$

$$\sum \psi_{ti} \delta_i = \frac{\Delta A_c d_A}{bh^2} = \left[\frac{2 \times 1.75 \times \frac{1}{2} \times \frac{1}{2}}{1 \times (8.412)^2} \right] = 0.00619$$

$$M_{cr} = 1800 \times 1 \times (8.412)^2 \left[0.4466 + 0.8779(0.2080) - 0.00619 \right] = 79.35 \text{ in kips}$$

$$\text{Failure load} = \frac{79.35 \times 4}{140} = 2.27 \text{ kips}$$

Beams 7FV4 & 7aFV4



$$M_{cr} = f_{t0} b h^2 [A + B \psi_t - \sum \psi_{ti} \delta_i]$$

$$\psi_c = \frac{\Delta A' c}{bh} = \left[\frac{(2 \times 7.375 \times \frac{1}{2}) + (2 \times 2.25 \times \frac{1}{2})}{(1 \times 8.412)} \right] = 1.144$$

$$\gamma = t'/h = \frac{1}{8.412} = 0.059$$

$$A = \frac{1}{2} - \left[\frac{0.059 \times 1.144}{1 + (2 \times 1.144)} \right] - \left[\frac{1 - (2 \times 1.144)}{6(1 + 2 \times 1.144)} \right] - \frac{1}{6} \left[\frac{1 + (2 \times 1.144)}{2 + (2 \times 1.144)} \right]^2 \\ = 0.4466$$

$$B = 1 - \left[\frac{0.059 \times 1.144}{1 + (2 \times 1.144)} \right] - \left[\frac{1}{3(1 + 2 \times 1.144)} \right] = 0.8779$$

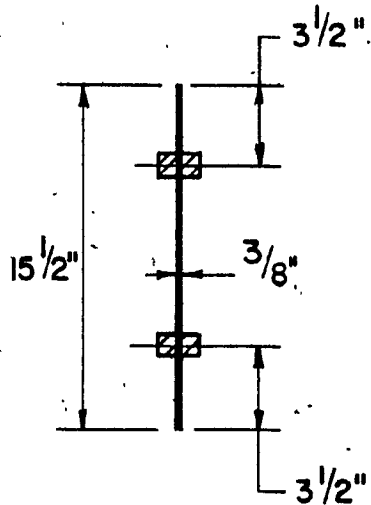
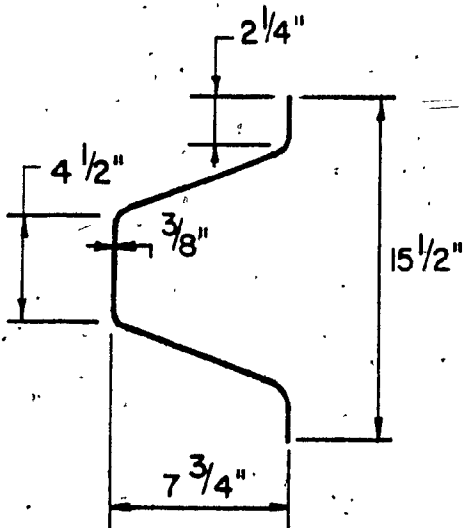
$$\psi_t = \left[\frac{\Delta A_c}{bh} + \frac{A_e f_c}{bhf_{t0}} + \frac{A_s f_s}{bhf_{t0}} \right] \\ = \left[\frac{2 \times 1.75 \times \frac{1}{2}}{1 \times 8.412} \right] + \left[\frac{0.22 \times 4350}{1 \times 8.412 \times 1800} \right] + \left[\frac{8.75 \times 300}{1 \times 8.412 \times 1800} \right] = 0.4446$$

$$\sum \psi_{ti} \delta_i = \left[\frac{\Delta A_c d_A}{bh^2} + \frac{A_s (4350) d_s}{bh^2 f_{t0}} + \frac{A_c (300) d_c}{bh^2 f_{t0}} \right] \\ = \left[\frac{2 \times 1.75 \times \frac{1}{2} \times \frac{1}{2}}{1 \times (8.412)^2} \right] + \left[\frac{0.22 \times 4350 \times 0.875}{1 \times (8.412)^2 \times 1800} \right] + \left[\frac{8.75 (300) 0.875}{1 \times (8.412)^2 \times 1800} \right] = 0.0308$$

$$M_{rc} = 1800 \times 1 \times (8.412)^2 \left[0.4466 + 0.8779(0.4466) - 0.0308 \right] = 102.68 \text{ in kips}$$

$$\text{Failure load } P = \frac{102.68 \times 4}{140} = 2.934 \text{ kips}$$

Beam 8FV3a



length = 116", P [failure] = 0.89 kips

$$M_{cr} = \frac{PL}{4} = \frac{(0.89)(9.67)}{4} = 2.151 \text{ ft-kips}$$

$$\Delta A_C' = \Delta A_C = \left[\frac{3}{8} \times 8.25 \right] - \left[\frac{3}{8} \times 3\frac{1}{4} \right] = 1.875 \text{ in}^2$$

$$\psi_c = \frac{\Delta A_C'}{bh} = \frac{1.875}{(3/8)(15\frac{1}{4})} = 0.32258$$

$$\psi_t = \frac{\Delta A_C}{bh} = 0.32258$$

$$\sum \psi_{ti} \delta_i = \left[\frac{(1.875)(3.5)}{(15\frac{1}{4})^2(3/8)} \right] = 0.07284$$

$$\gamma = \frac{t'}{h} = \frac{3/8}{15\frac{1}{4}} = 0.02419$$

$$A = \frac{1}{2} - \left[\frac{(0.02419)(0.32258)}{1 + 2(0.32258)} \right] - \left[\frac{1-2(0.32258)}{6(1+(0.32258)^2)} \right] - \frac{1}{6} \left[\frac{1+(0.32258)2}{2+(0.32258)2} \right]^2 \\ = 0.39484$$

$$B = 1 - \left[\frac{(0.02419)(0.32258)}{1 + 2(0.32258)} \right] - \left[\frac{1}{3 + 6(0.32258)} \right] = 0.79264$$

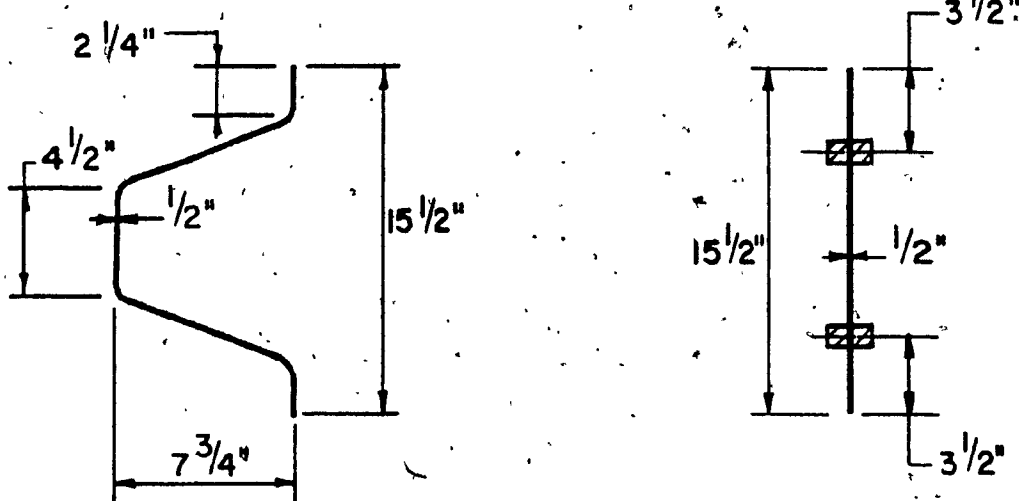
$$2.151' \times 12 = f_{to} (3/8) (15\frac{1}{2})^2 [(0.39484 + 0.32258(0.79264) - 0.07284)]$$

$$f_{to} = \frac{2.151 \times 12}{52.046} = 496 \text{ ksi} = 496 \text{ psi}$$

For: $f_{to} = 1650 \text{ psi}$

$$M_{cr} = 1650(52.046) = 85,875.9 \text{ lb-in} = 7.156 \text{ ft-kips} = P = \left[\frac{4 \times 7.156}{9.67} \right] = 2.96 \text{ k}$$

Beams 9FV4 (a & b)



Length = 140" = 11.67'; $P[\text{failure}] = 0.94 \text{ k}$

$$M_{cr} = \frac{PL}{4} = \frac{(0.94)(11.67)}{4} = 2.742 \text{ ft-kips}$$

$$\Delta A_c' = \Delta A_c = 1.875 \text{ in}^2$$

$$\psi_c = \frac{\Delta A_c'}{bh} = 0.32258$$

$$\psi_t = \frac{\Delta A_c}{bh} = 0.32258$$

$$\sum \psi_{ti} \delta_i = 0.07284$$

$$\gamma = \frac{t'}{h} = 0.02419$$

$$A = 0.39484; B = 0.79264$$

$$2.742 \times 12 = f_{to} (3/8) (15\frac{1}{2})^2 [0.39484 + 0.32258(0.79264) - 0.07284]$$

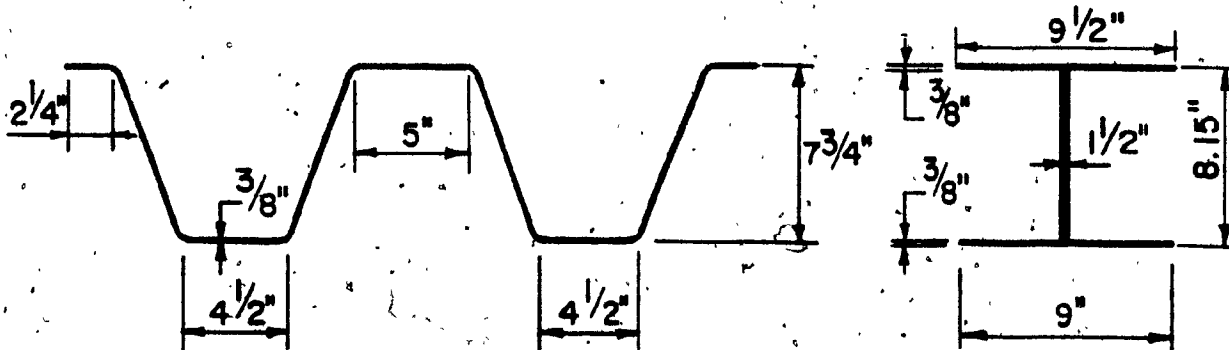
$$f_{to} = \left[\frac{2.742 \times 12}{52.046} \right] = 0.632 \text{ ksi} = 632 \text{ psi}$$

And for $f_{to} = 1650 \text{ psi}$.

$$M_{cr} = (1650)(52.046) = 85,875.9 \text{ lb-in} = 7.1563 \text{ ft-kips}$$

$$P = \frac{4M_{cr}}{L} = \left[\frac{4 \times 7.1563}{11.67} \right] = 2.453 \text{ k}$$

Beams 10FV3 (a & b)



$$M_{cr} = f_{to} bh^2 [A + B \psi_t - \sum \psi_{ti} \delta_i]$$

$$\psi_c = \frac{\Delta A_c}{bh} = \left[\frac{2 \times 4 \times 3/8}{1\frac{1}{2} \times 8.15} \right] = 0.2454$$

$$\gamma = \frac{t'}{h} = \frac{3/8}{8.15} = 0.046$$

$$A = \frac{1}{2} - \left[\frac{0.046 \times 0.2454}{1 + (2 \times 0.2454)} \right] - \left[\frac{1 - (2 \times 0.2454)}{6(1 + 2 \times 0.2454)} \right] - \left[\frac{1 + (2 \times 0.2454)}{2 + (2 \times 0.2454)} \right]^2 \\ = 0.3758$$

$$B = 1 - \left[\frac{0.046 \times 0.2454}{1 + (2 \times 0.2454)} \right] - \left[\frac{1}{3(1 + 2 \times 0.2454)} \right] = 0.7688$$

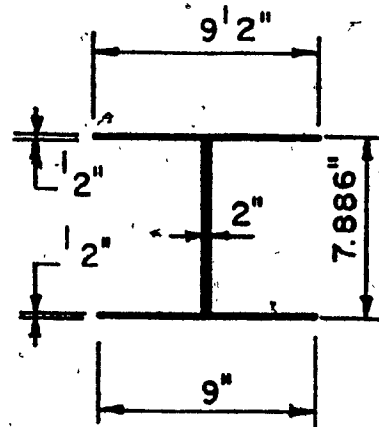
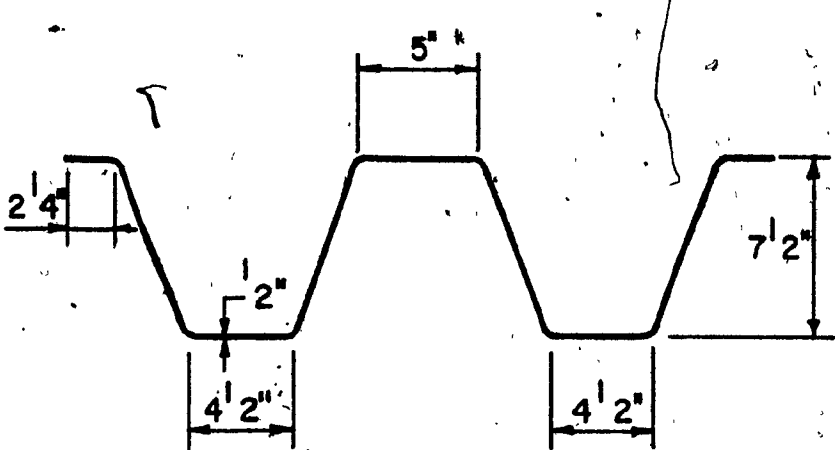
$$\psi_t = \frac{\Delta A_c}{bh} = \left[\frac{2 \times 3.75 \times 3/8}{1\frac{1}{2} \times 8.15} \right] = 0.2301$$

$$\sum \psi_{ti} \delta_i = \frac{\Delta A_c d_A}{bh^2} = \left[\frac{2 \times 3.75 \times 3/8 \times 3/16}{1\frac{1}{2} \times (8.15)^2} \right] = 0.00529$$

$$M_{cr} = 1800 \times 1\frac{1}{2} \times (8.15)^2 [0.3758 + 0.7688(0.2301) - 0.00529] = 98.2 \text{ in-kips}$$

$$\text{Failure load} = \left[\frac{98.2 \times 4}{116} \right] = 3.4 \text{ kips}$$

Beams 11FV4 (a & b)



$$M_{cr} = f_{to} bh^2 \left[A + B \psi_t - \sum \psi_{ti} \delta_i \right]$$

$$\psi_c = \frac{\Delta A' c}{bh} = \frac{2 \times 3.75 \times \frac{1}{2}''}{2 \times 7.886} = 0.2378$$

$$\gamma = \frac{t'}{h} = \frac{1}{7.886} = 0.0634$$

$$A = \frac{1}{2} - \frac{0.0634 \times 0.2378}{1 + (2 \times 0.2378)} - \frac{1 - (2 \times 0.2378)}{6(1 + 2 \times 0.2378)} - \frac{1}{6} \frac{1+2 \times 0.2378}{24(2 \times 0.2378)}^2 \\ = 0.3713$$

$$B = 1 - \frac{0.0634 \times 0.2378}{1 + (2 \times 0.2378)} - \frac{1}{3(1 + 2 \times 0.2378)} = 0.7634$$

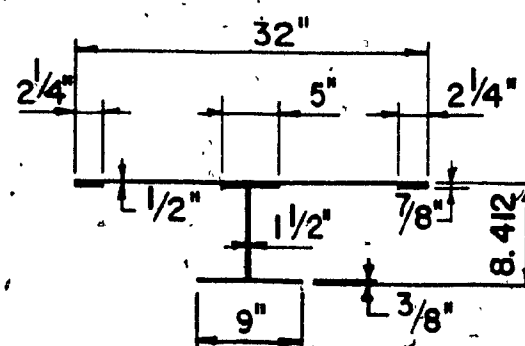
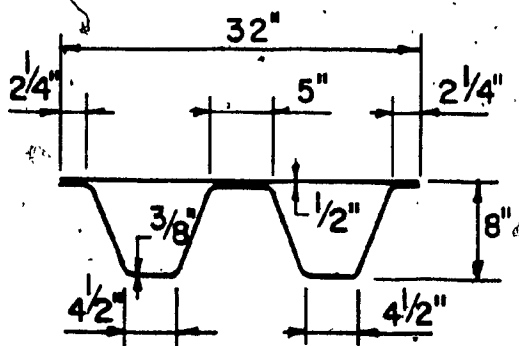
$$\psi_t = \frac{\Delta A_c}{bh} = \frac{2 \times 3.5 \times \frac{1}{2}}{2 \times 7.886} = 0.2219$$

$$\sum \psi_{ti} \delta_i = \frac{\Delta A_c d_A}{bh^2} = \frac{2 \times 3.5 \times \frac{1}{2} \times \frac{1}{4}}{2 \times (7.886)^2} = 0.00704$$

$$M_{cr} = 1800 \times 2 \times (7.886)^2 [0.3713 + 0.7634(0.2219) - 0.00704] \\ = 119.475 \text{ in-kips.}$$

$$\text{Failure load} = \frac{119.475 \times 4}{140} = 3.414 \text{ kips.}$$

Beam 12aFV3



$$M_{cr} = f_{to} b h^2 \left[A + B \psi_t - \sum \psi_{ti} \delta_i \right]$$

$$\psi_c = \frac{\Delta A' c}{bh} = \left[\frac{(2 \times 14.50 \times 3) + (2 \times 2.25 \times 3/8) + (2 \times 1.75 \times 3/8)}{1\frac{1}{2} \times 8.412} \right]$$

$$\gamma = \frac{t'}{h} = \frac{1}{8.412} = 0.0594$$

$$A = \frac{1}{2} - \left[\frac{0.0594 \times 1.387}{1+(2 \times 1.387)} \right] + \left[\frac{1 - (2 \times 1.387)}{6(1+2 \times 1.387)} \right] - \frac{1}{6} \left[\frac{1+2 \times 1.387}{2+(2 \times 1.387)} \right]^2$$

$$= 0.4524$$

$$B = 1 - \left[\frac{0.0594 \times 1.387}{1+(2 \times 1.387)} \right] - \left[\frac{1}{3(1+2 \times 1.387)} \right] = 0.8898$$

$$\psi_t = \frac{\Delta A_c}{bh} = \left[\frac{2 \times 3.75 \times 3/8}{1\frac{1}{2} \times 8.412} \right] = 0.2229$$

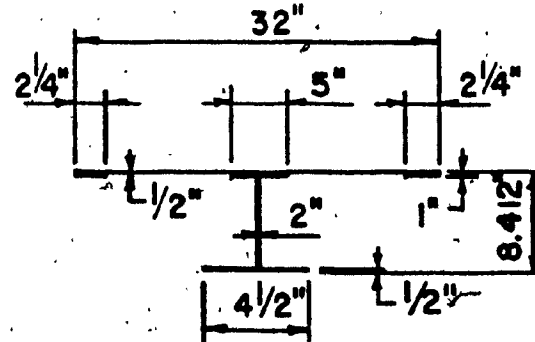
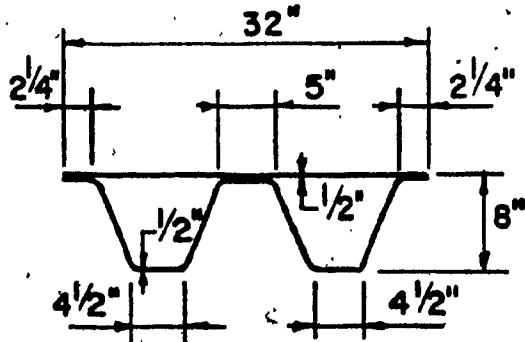
$$\sum \psi_{ti} \delta_i = \frac{\Delta A_c d_A}{bh^2} = \left[\frac{2 \times 3.75 \times 3/8 \times 3/16}{1\frac{1}{2} \times (8.412)^2} \right] = 0.00497$$

$$M_{cr} = 1800 \times 1\frac{1}{2} \times (8.412)^2 [0.4524 + 0.8898(0.2229) - 0.00497]$$

$$= 123.38 \text{ in-kips}$$

$$\text{Failure load} = \frac{123.38 \times 4}{140} = 3.525 \text{ kips.}$$

Beam 13aFV4



$$M_{cr} = f_{to} \frac{bh^2}{4} [A + B \psi_t - \sum \psi_{ti} \delta_i]$$

$$\psi_c = \frac{\Delta A' c}{bh} = \frac{(2 \times 14 \times \frac{1}{2}) + (2 \times 2.25 \times \frac{1}{2}) + (2 \times 1.5 \times \frac{1}{2})}{(2 \times 8.412)} = 1.055$$

$$\gamma = \frac{t'}{h} = \frac{1}{8.412} = 0.0594$$

$$A = \frac{1}{2} - \left[\frac{0.0594 \times 1.055}{1 + (2 \times 1.055)} \right] - \left[\frac{1 - (2 \times 1.055)}{6(1+2 \times 1.055)} \right] - \frac{1}{6} \left[\frac{1 + (2 \times 1.055)}{2 + (2 \times 1.055)} \right]^2 \\ = 0.4439$$

$$B = 1 - \left[\frac{0.059 \times 1.055}{1 + (2 \times 1.055)} \right] - \left[\frac{1}{3(1+2 \times 1.055)} \right] = 0.8727$$

$$\psi_t = \frac{\Delta A_c}{bh} = \left[\frac{2 \times 3.5 \times \frac{1}{2}}{2 \times 8.412} \right] = 0.2080$$

$$\sum \psi_{ti} \delta_i = \frac{\Delta A_c d_A}{bh^2} = \left[\frac{2 \times 3.5 \times \frac{1}{2} \times \frac{1}{2}}{2 \times (8.412)^2} \right] = 0.00618$$

$$M_{cr} = 1800 \times 2 \times (8.412)^2 [0.4439 + 0.8727(0.2080) - 0.00618]$$

$$= 157.75 \text{ in-kips}$$

$$\text{Failure load} = \frac{157.75 \times 4}{140} = 4.5 \text{ kips.}$$

A-3 WALL AND COLUMN STRENGTHS

Wall 5SW6

(a) Overall stability

$$A_g = 27 \text{ in}^2$$

$$\begin{aligned} P_u &= 0.55 \phi A_g f'c \left[1 - \left(\frac{k_{lc}}{32h} \right)^2 \right] \\ &= 0.55 \times 0.7 \times 27 \times 8600 \left[1 - \left(\frac{120}{32 \times 6} \right)^2 \right] \\ &= 54.48 \text{ kips} \end{aligned}$$

(b) Local buckling

Distance between screws = 24"

$$\begin{aligned} P_u &= 0.55 \phi A_g f'c \left[1 - \left(\frac{k_{lc}}{32h} \right)^2 \right] \\ &= 0.55 \times 0.7 \times 27 \times 8600 \left[1 - \left(\frac{0.8 \times 12}{32 \times 3/8} \right)^2 \right] \\ &= 32.18 \text{ kips (governs)} \end{aligned}$$

Wall 6SW6

(a) Overall stability

$$A_g = 27 \text{ in}^2$$

$$\begin{aligned} P_u &= 0.55 \phi A_g f'c \left[1 - \left(\frac{k_{lc}}{32h} \right)^2 \right] \\ &= 0.55 \times 0.7 \times 27 \times 8600 \left[1 - \left(\frac{120}{32 \times 6} \right)^2 \right] \\ &= 54.48 \text{ kips (governs)} \end{aligned}$$

(b) Local buckling

Distance between screws = 12"

$$\begin{aligned} P_u &= 0.55 \times 0.7 \times 27 \times 8600 \left[1 - \left(\frac{0.8 \times 6}{32 \times 3/8} \right)^2 \right] \\ &= 75.09 \text{ kips} \end{aligned}$$

Walls 7SW5 and 8SW5

(a) Overall stability

$$A_g = 26 \text{ in}^2$$

$$P_u = 0.55 \phi A_g f'c \left[1 - \left(\frac{k_{lc}}{32h} \right)^2 \right]$$
$$= 0.55 \times 0.7 \times 26 \times 8600 \left[1 - \left(\frac{120}{32 \times 5} \right)^2 \right]$$
$$= 37.66 \text{ kips}$$

(b) Local buckling

Distance between screws = 24"

$$P_u = 0.55 \times 0.7 \times 26 \times 8600 \left[1 - \left(\frac{0.8 \times 12}{32 \times 3/8} \right)^2 \right]$$
$$= 31 \text{ kips (governs)}$$

Columns 4WV4 and 4WV4a

$$A_g = 19 \text{ in}^2$$

$$P_u = 0.55 \phi A_g f'c \left[1 - \left(\frac{k_{lc}}{32h} \right)^2 \right]$$
$$= 0.55 \times 0.7 \times 19 \times 8600 \left[1 - \left(\frac{120 \times 0.8}{32 \times 8} \right)^2 \right]$$
$$= 54.06 \text{ kips.}$$

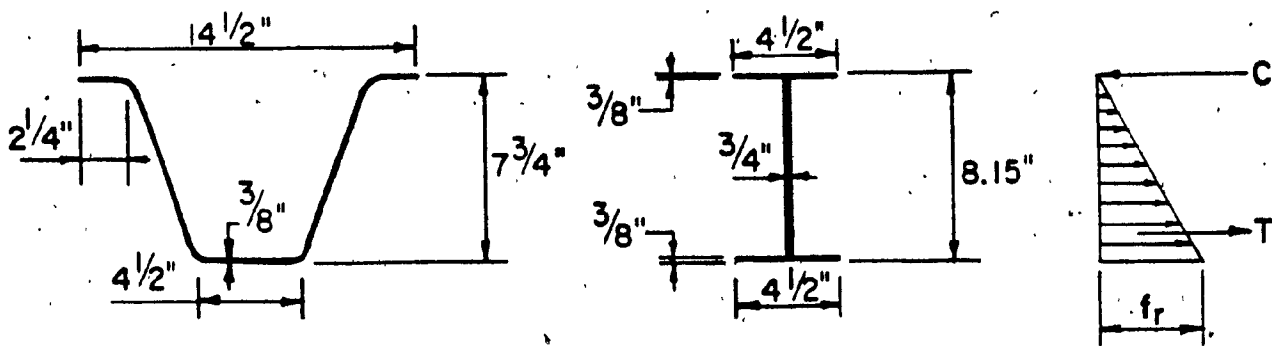
Sample	Failure Load (kips)	Present practice f_r (psi)	Proposed method f_{rg} (psi)	SPECIFIED TENSILE STRENGTH = (1800 - 2000) psi	SPECIFIED RUPTURE STRENGTH = 3100 psi
IFV3a	1.555	1500	1670		
IFV3b	1.555	1500	1670		
3FV3a	2.74	1597	1968		
5FV3	1.555	1697	1585		
5aFV3	1.80	1966	1830		
10FV3a	3.7825	1826	1975		
10FV3b	3.75	1810	1958		
12aFV3	3.7825	2577	1931		
13aFV4	4.40	2229	1757		
	0.487	2381	2720		

Note. Proposed method gives results close to tested values.

Comment: Results calculated according to present practice deviate significantly in the case of unsymmetrical sections such as 12aEV3 and 13aEV4.

PRESENT PRACTICE

Sample Problem:



Panel 1FV3a

Failure load = 1.555 kips

$$M = PL/4 = (1.555 \times 116)/4 = 45.095 \text{ in-kips}$$

$$45.095 = (\frac{1}{2} \times (2 \times 8.15)/3 \times f_r \times \frac{3}{4} \times 8.15) + (3/8 \times f_r \times 4.5 \times (8.15 - 3/16))$$

$$f_r = 1500 \text{ psi.}$$